

CRISPR3 Regulates Exopolysaccharide Production in *Myxococcus xanthus*

Regina Ann Wallace

Thesis submitted to the faculty of the Virginia Polytechnic Institute and State University in
partial fulfillment of the requirements for the degree of

Master of Science
In
Biological Sciences

Zhaomin Yang, Chair
Daniel G. S. Capelluto
Birgit Scharf
Brenda S. J. Winkel

September 20th, 2013

Blacksburg, VA

Keywords: *Myxococcus xanthus*, exopolysaccharide (EPS), *pilA*, CRISPR, RAMP

Copyright 2013, Regina Ann Wallace

CRISPR3 Regulates Exopolysaccharide Production in *Myxococcus xanthus*

Regina Ann Wallace

Department of Biological Sciences

ABSTRACT

Myxococcus xanthus, a model organism for studying development and Type IV pili (T4P), harbors three Clustered Regularly Interspaced Short Palindromic Repeats (CRISPR) on its chromosome. CRISPR systems, which function as an adaptive immune system in prokaryotes, are classified into three types based on CRISPR-associated genes. Evidence suggests that these three types mediate immunity slightly differently. *M. xanthus* CRISPR1 and CRISPR2 are Type I systems while CRISPR3 is a Type III-B system. In a genetic screen, a *mariner* transposon insertion in the 13th spacer of CRISPR3 (3SP13) was found to restore exopolysaccharide (EPS) production to a *pilA* mutant. Since the deletion of CRISPR3 failed to suppress a *pilA* mutation and expression of CRISPR3 from a heterologous promoter led to *pilA* suppression, it was concluded that the 3SP13 transposon insertion is a gain-of-function mutation. Deletion of the adjacent Repeat Associated Mysterious Proteins (RAMP) genes indicated that they are essential for the 3SP13 transposon insertion to suppress *pilA*, providing evidence that Type III-B systems may be involved in the regulation of chromosomal genes. We suggest that one of the spacers, once expressed and processed, may inhibit the expression of a negative regulator of EPS production in *M. xanthus*.

ATTRIBUTION

Dr. Wesley Black, who was a Research Assistant Professor in Dr. Zhaomin Yang's lab, created some of the strains and plasmids utilized in experiments in my thesis research. Most importantly, he isolated BY802 ($\Delta pilA$ CRISPR3*), which was the starting point of the study described in Chapter 2. Chengyun Li, who was a visiting scholar in Dr. Yang's lab, is the first author of the manuscript that is included in Chapter 3. Chengyun created plasmids and strains used in this manuscript and carried out a majority of the experiments outlined in the manuscript.

DEDICATION

I dedicate this thesis to my family and my fiancé; with out your love and support, I never would have accomplished so much. Mom and Dad, Ruth and Corneilus Wallace, thank you for always being there when I needed you and always encouraging me. Eric Wiggins, my fiancé, thank you for putting up with me all of these years and being that one person who can always make me smile.

ACKNOWLEDGEMENTS

I would like to thank Dr. Zhaomin Yang for being my advisor the past few years. Thank you for giving me the opportunity to work in your lab and helping me get into Graduate School here at Virginia Tech. I would also like to thank my committee members, Dr. Daniel Capelluto, Dr. Birgit Scharf, and Dr. Brenda Winkel. There were times that I didn't think that I would be able to finish, and with out your support and advice I probably wouldn't have.

To past and present members of the Yang Lab, especially Dr. Wesley Black, thank you for all the help that you provided, without which I would have been lost. To the VT-PREP and MAOP family, thank you for your constant support and encouragement. To the Stevens Lab and the Scharf Lab, especially Alison Kernell, Revathy Ramachandran, Benjamin Webb, and Hardik Zatakia, thanks for all of the great conversations.

This work was partially supported by the National Institutes of Health grant GM071601 and the National Science Foundation grant MCB-0135434 to Dr. Zhaomin Yang.

TABLE OF CONTENTS

Chapter 1: Literature Review	1
I. Structure and function of CRISPR in Prokaryotes	2
A. Discovery and Prevalence of CRISPR	2
B. Structural features of CRISPR	2
C. CRISPR can function as a prokaryotic immune system	5
D. Proposed mechanisms of CRISPR mediated immunity	8
E. The role of Type III-B CRISPR-RAMP module in CRISPR mediated immunity	12
F. CRISPR systems may regulate cellular processes other than immunity	13
II. <i>Myxococcus xanthus</i> : The experimental system	15
A. <i>Myxococcus xanthus</i> undergoes a complex life cycle that requires S motility	15
B. Type IV pilus is a bacterial motility apparatus	17
C. The interplays of T4P and EPS in <i>M. xanthus</i> S motility	21
References Cited	23
Chapter 2: Restoration of Exopolysaccharide Production to a <i>pilA</i> Mutant by CRISPR Mutations in <i>Myxococcus xanthus</i>	32
Abstract	33
Introduction	34
Materials and Methods	36
Results	43
Discussion	55

Rational and Future Direction	60
References Cited	62
Chapter 3: Type IV Pilus Form an Integrated Structure Extending from the Cytoplasm to the Outer Membrane	67
Abstract	68
Introduction	69
Materials and Methods	72
Results and Discussion	79
Concluding Remarks	94
References Cited	97
Chapter 4: Summary of Other Experiments	103
CRISPR3 Related Experiments	104
<i>M. xanthus</i> Pil Related Experiments	116
References Cited	125

TABLE OF CONTENTS- FIGURES

Chapter 1:

Figure 1-1: A typical CRISPR locus has four conserved features	3
Figure 1-2: The three types of CRISPR-Cas systems and their subtypes	6
Figure 1-3: Proposed mechanism of CRISPR mediated immunity	9
Figure 1-4: Life cycles of <i>M. xanthus</i>	16
Figure 1-5: A and S motility in <i>M. xanthus</i>	18
Figure 1-6: Type IV Pili model	20
Figure 1-7: Model for the regulation of EPS production	22

Chapter 2:

Figure 2-1: CRISPR3* is a gain-of-function mutation that suppresses $\Delta pilA$, $\Delta pilB$ and $\Delta sglK$ in EPS production	44
Figure 2-2: Structure of the <i>M. xanthus</i> CRISPR3 locus	46
Figure 2-3: RAMP genes but not MXAN_7275-7270 are required for CRISPR3* to suppress $\Delta pilA$	49
Figure 2-4: Detrimental effect of CRISPR3* on development and its dependence on RAMP genes	51
Figure 2-5: CRISPR3* may affect processing of CRISPR3 RNA transcripts upstream of the transposon insertion	53
Figure 2-6: CRISPR2 and CRISPR3 Cas6 and repeat alignment	59

Chapter 3:

Figure 3-1: <i>pil</i> deletions can be complemented in <i>trans</i>	80
Figure 3-2: <i>pilB</i> ^{WA} suppresses some but not all T4P ⁻ <i>pil</i> deletions in	

EPS production	82
Figure 3-3: Conserved domains of PilQ	87
Figure 3-4: Pairwise interactions among Pil proteins in Y2H system	89
Figure 3-5: Quantification of β -galactosidase in Y2H experiment	90
Figure 3-6: An integrated T4P structure	95
Chapter 4:	
Figure 4-1: CRISPR3 regions for various expression constructs	109
Figure 4-2: Plasmid map of over expression vector pNC107	121

TABLE OF CONTENTS-TABLES

Chapter 2:

Table 2-1: Strains and Plasmids	37
---------------------------------	----

Chapter 3:

Table 3-1: <i>Myxococcus xanthus</i> strains used in this study	73
---	----

Table 3-2: Plasmids used in this study	75
--	----

Table 3-3: Interactions among <i>M. xanthus</i> Pil proteins detected by Y2H mating protocol	85
--	----

Chapter 4:

Table 4-1: Strains and plasmids used in CRISPR3 related experiments	112
---	-----

Table 4-2: Primers used to examine CRISPR	114
---	-----

Table 4-3: Strains and plasmids used in <i>M. xanthus</i> Pil related experiments	122
---	-----

Table 4-4: Primers used for <i>M. xanthus</i> Pil experiments	124
---	-----

List of Abbreviations

Cas	CRISPR-associated
CASCADE	CRISPR-associated complex for antiviral defense
CRISPR	Clustered Regularly Interspaced Short Palindromic Repeats
crRNA	CRISPR RNA
CW	Calcofluor White
CYE	Casitone Yeast Extract
EPS	Exopolysaccharide
GOF	Gain-of-function
IM	Inner Membrane
LOF	Loss-of-function
OM	Outer Membrane
PAM	Protospacer Adjacent Motif
Pre-crRNA	Pre-CRISPR RNA
RAMP	Repeat Associated Mysterious Proteins
TracrRNA	Trans-encoded CRISPR RNA
T4P	Type IV pilus

Chapter 1
Literature Review

I. Structure and Function of CRISPR in Prokaryotes

A. Discovery and Prevalence of CRISPR

In 1987, a mysterious repetitive region was discovered on the chromosome of *Escherichia coli* K12 (45). This repetitive region consisted of five direct repeats with each separated by 32 nucleotides (45). Such repetitive regions have now been identified in half of bacterial genomes and almost all archaeal genomes (33, 57). The number of repetitive regions is highly variable among organisms, with *Methanococcus jannaschii* having the most with 20 independent repetitive loci (14, 59). Despite the high variability, archaeal genomes typically possess five repetitive regions with bacterial genomes possessing about three (34). These repetitive regions were assigned many different names in the early literature including Direct Variable Repeats, Tandem Repeats (TREPs), Short Regularly Spaced Repeats (SRSRs), Spacer Interspersed and Direct Repeats (SPIDRs), and Long Clustered Tandem Repeats (LCTRs) (35, 59, 71, 72, 84). In 2002, Jansen and colleagues introduced the acronym CRISPR, for Clustered Regularly Interspaced Short Palindromic Repeats, which has been used since (47).

B. Structural features of CRISPR

There are four key conserved elements in a CRISPR locus (Figure 1-1). The first is a leader sequence, the second is the numerous identical direct repeats, the third is the non-repetitive spacers of similar size between the repeats, and the fourth is a set of CRISPR-associated (*cas*) genes adjacent to the CRISPR array (47, 63). These four elements can be classified into two groups, non-protein coding and protein coding elements. The non-protein coding elements include the leader sequence, direct repeats and non-repetitive spacers. The protein coding elements are the *cas* genes. These conserved features of CRISPR are discussed below in more detail.

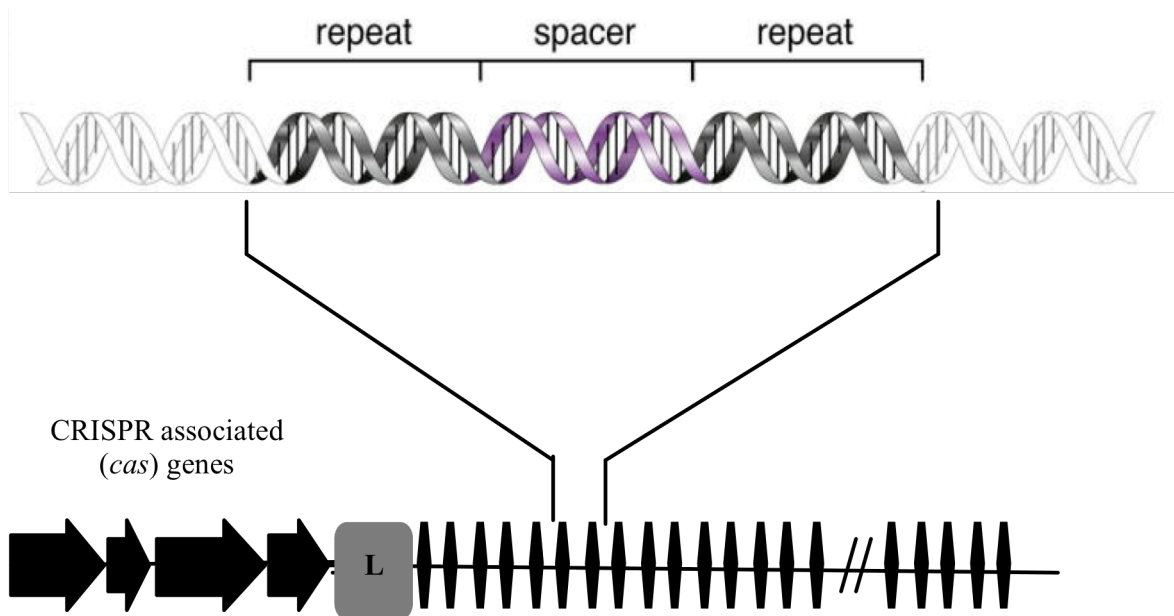


Figure 1-1: A typical CRISPR locus has four conserved features

A CRISPR array consists of identical direct repeats (black diamonds) interspaced by variable sequences termed spacers (black lines). Immediately upstream of a CRISPR array is the leader (L) sequence. Adjacent to the CRISPR array are CRISPR-associated (*cas*) genes depicted here by black arrows. Figure modified from Karginov & Hannon, 2010 (52). Used under fair use, 2013.

Non-Protein coding elements of CRISPR

At the 5' end of all CRISPR arrays, there is an A/T rich region termed the leader sequence (47, 59, 93). A leader sequence, is generally a few hundred base pairs long and is typically highly similar in one species, although it varies dramatically in different species (47). The leader sequence likely contains the promoter for the CRISPR array (47). The direct repeats are the identifying feature of CRISPR arrays. These repeats are short identical repetitive sequences that are interspaced by variable sequences. The direct repeats are typically 21- 48 base pairs long and can range from a few repeats to hundreds in a CRISPR locus (36, 47). An interesting characteristic of the repeats is that their RNA transcript may form hairpin structures (57). Repeats have been demonstrated to possess conserved sequences leading to the hypothesis that repeats are involved in the recognition of CRISPR arrays by Cas proteins and promote the interaction between the RNA transcript of the CRISPR array and the Cas proteins (57). The direct repeats are separated by non-repetitive sequences termed spacers. These spacers vary in both sequence and length in a single CRISPR array. The lengths of spacers range from 26 -72 base pairs, with spacers in a single array typically being similar in length (59). Spacer sequences have been found to be homologous to mobile genetic elements, as well as, chromosomal genes, which will be discussed in more detail later (12, 22, 70, 78).

Protein coding elements of CRISPR

The protein coding elements of CRISPR are the CRISPR-associated (*cas*) genes (47). Forty-five *cas* genes have been identified in numerous organisms (36, 47). These Cas proteins were initially divided into eight subtypes. These subtypes are based on the organism they were initially identified in: Ecoli (*Esherichia coli*), Ypest (*Yersenia pestis*), Nmeni (*Neisseria meningitidis*), Dvulg (*Desulfovibrio vulgaris*), Tneap (*Themotoga neapolitana*), Hmari

(*Haloarcula marismortui*), *Apern* (*Aeropyrum pernix*), and *Mtube* (*Mycobacterium tuberculosis*) (36). There is an additional subtype known as RAMP proteins, for Repeat Associated Mysterious Proteins (36, 62, 63). Recently, multiple research groups proposed a new unified classification for CRISPR-Cas systems. The new classification divides the CRISPRs into three types, Type I, II and III (Figure 1-2) (64). The three types are distinguished by the presence of one key Cas protein (64). Type I is defined by the presence of Cas3, which has a nuclease and a helicase domain. Type II is defined by Cas9, which contains two nuclease domains. Type III is defined by Cas10, which contains a nuclease and a polymerase domain. The three CRISPR-Cas systems are further divided into subtypes based on *cas* genes other than the defining *cas* gene. Type I consists of six subtypes, I-A through I-F, while Type II and III consist of two subtypes, II-A, II-B and III-A, III-B, respectively (64). The function of these different types of CRISPR-Cas systems will be discussed further throughout this thesis.

C. CRISPR can function as a prokaryotic immune system

CRISPRs were proposed to function in various different processes early on, including replicon partitioning, DNA repair, and developmental regulation (62, 72, 96). In 1995, Mojica and colleagues identified long CRISPR arrays in the genomes of *Haloferax mediterranei* and *Haloferax volcanii* (72). These arrays were present in the chromosome and in megaplasmids, but not on smaller plasmids, leading to the hypothesis that these regions may be important since they are present in the largest and probably most essential replicons of the cell. Because the direct repeats are common in genes encoding proteins involved in replicon partitioning, it was inferred that CRISPR was likely involved in replicon partitioning (72). In 2002, Makarova and colleagues noticed a conserved gene neighborhood containing *cas* genes predicted to encode DNA helicases and RecB family nucleases (62). They suggested that these genes, as well as

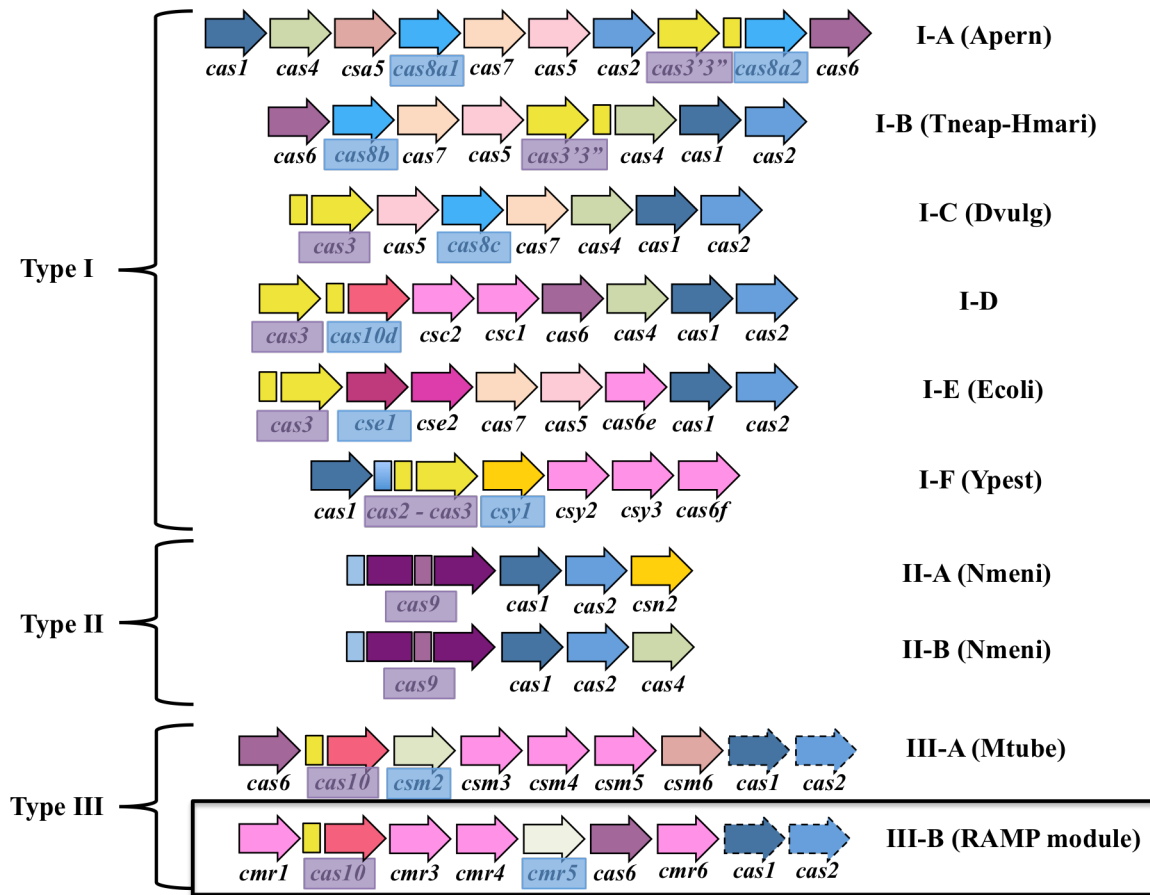


Figure 1-2: The three types of CRISPR-Cas systems and their subtypes

Depicted are the three major types of CRISPR-Cas systems: Type I, II, and III and their subtypes. Highlighted in purple are the defining *cas* genes for the three types and those in blue distinguish the subtypes. *cas1* and *cas2* in the Type III systems are indicated by dotted arrows since these genes may be associated with other CRISPR systems in the same organism. The CRISPR system that is of focus throughout this this is Type III-B CRISPR-RAMP system, which is distinguished by a box around it. Figure modified from Makarova *et al.*, 2011 (64). Used under fair use, 2013.

surrounding genes, may have a role in DNA repair (62). In 1993, two CRISPR-associated genes in *Myxococcus xanthus*, *devR* and *devS*, were found to eliminate fruiting body development when mutated (96). These findings led to the hypothesis that Cas proteins and CRISPR may regulate developmental processes. The notion that CRISPRs may be involved in replicon partitioning, DNA repair, and developmental regulation persisted for many years without a unified view.

CRISPRs were proposed to function as a novel adaptive immune system against invading genetic elements in prokaryotes analogous to the RNAi pathway in eukaryotes first in 2005 (12, 63, 70, 78). This hypothesis arose because many spacers were found to be homologous to mobile genetic elements like bacteriophages and plasmids. In 2007, Barrangou and colleagues were the first to demonstrate experimentally that CRISPR could indeed function as an adaptive immune system in prokaryotes (6). They first challenged *Streptococcus thermophilus* with a phage. The survivors were found to have incorporated one or more novel spacers into their CRISPR array adjacent to the leader sequence. More importantly, these spacers were found to be homologous to the phage DNA. They further demonstrated that the cells engineered to possess CRISPR spacers homologous to the phage DNA were resistant to the phage. When these spacers were removed from the CRISPR array, *S. thermophilus* was again sensitive to the phage (6). It was later demonstrated that CRISPR spacers could also interfere with plasmid conjugation and transformation in *Staphylococcus epidermidis* (98). These groundbreaking discoveries provide unequivocal evidence that CRISPR can function as an adaptive immune system in prokaryotes.

D. Proposed mechanisms of CRISPR mediated immunity

CRISPR-mediated immunity is proposed to function in three stages (Figure 1-3) (97). The first is the Adaptation stage, which involves the detection of foreign DNA in the cell and the integration of a novel spacer homologous to the foreign DNA into the CRISPR array. The second stage is CRISPR Expression, which involves the transcription of the CRISPR array into one long pre-CRISPR RNA (pre-crRNA), and the processing of the pre-crRNA into its mature form, CRISPR RNA (crRNA). The last stage is the Interference stage where the crRNA is used as a guide by the Cas proteins to target any invading DNA or RNA homologous to the crRNA. These stages are discussed in more detail below.

Stage 1: Adaptation

The Adaptation stage can be further divided into two steps (Figure 1-3). The first step is the recognition of invading foreign elements. During this step, a multiple Cas protein complex is proposed to recognize invading foreign genetic elements and cleave it into fragments known as protospacers (25). In the second step, the protospacer(s) is incorporated into the CRISPR array as a novel spacer proximal to the leader sequence. A new repeat sequence is incorporated at the 5' end of the novel spacer so that the CRISPR array always begins with a repeat. Protospacer adjacent motifs (PAMs) or CRISPR motifs are required in the Adaptation stage in some CRISPR-Cas systems (26). PAMs are a very short stretch of 2-5 conserved nucleotides that occur within 1 to 4 base pairs of either side of the protospacer sequence on the foreign DNA or RNA (69). PAMs are proposed to be the recognition motif that are required for the acquisition of new spacers for most CRISPR-Cas Types, excluding some Type III systems (26). The recognition of invading elements and the integration of a spacer identical to the invading elements by CRISPR proteins has proven necessary for the success of the CRISPR Expression

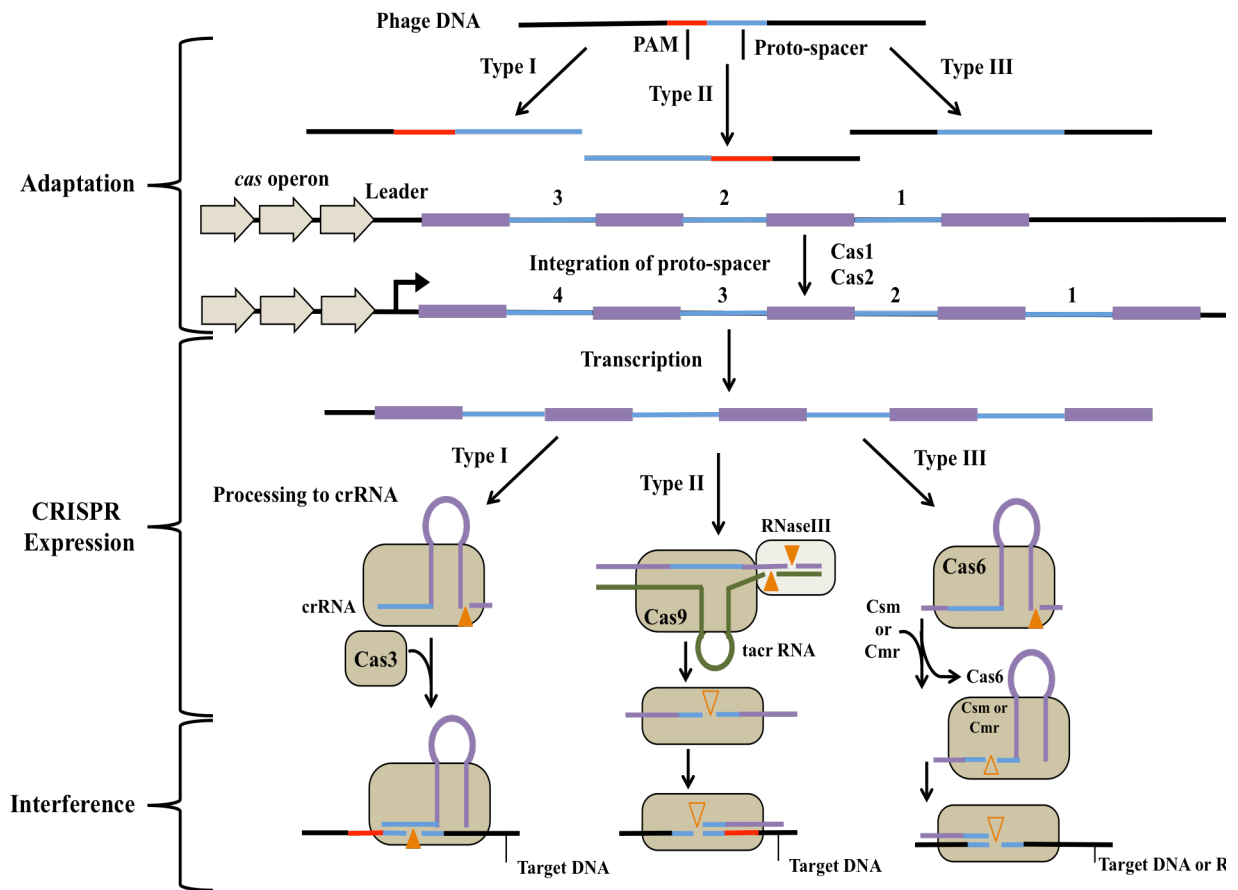


Figure 1-3: Proposed mechanism of CRISPR mediated immunity

In the Adaptation stage, Cas proteins recognize invading genetic elements cleaving the DNA into short fragments known as protospacers. The protospacer(s) is then integrated into the CRISPR array at the leader sequence end as a novel spacer. In the CRISPR Expression stage, the CRISPR array is transcribed as one long precursor, pre-crRNA. The pre-crRNA is then processed into its mature form, crRNA. The processing of pre-crRNA requires a single Cas protein or a Cas protein complex. In the Interference stage, the crRNA are used as a guide by a Cas protein or complex to target and inactivate any invading DNA the crRNA are homologous to. Each CRISPR system Type mediates immunity in a slightly different manner. Figure modified from Makarova *et al.*, 2011 (64). Used under fair use, 2013.

and Interference stage of CRISPR-mediated immunity.

Cas1, Cas2, Cas4 and Cas7 are likely required for both steps of the Adaptation stage. Cas1 and Cas2 have been found in almost all CRISPR loci and are considered “core” Cas proteins (Figure 1-2) (36, 63). Cas1 from *Pseudomonas aeruginosa*, which contains a putative integrase domain (63), has been demonstrated to have a metal-dependent endonuclease activity specific to DNA (99). Cas1 from *E. coli* was determined to be dispensable for the CRISPR Expression and Interference stages leading to the hypothesis that Cas1 is involved in one or both steps of the Adaptation stage (13). Cas4, a proposed RecB-like nuclease, is fused to Cas1 in some cases (63). Because of this, Cas4 is proposed to function alongside Cas1 in the Adaptation stage (97). *S. solfataricus* Cas2 is a metal-dependent ssRNA endonuclease with preferences for U-rich regions and has properties of an RNA-binding protein (8). Interestingly, Cas2 accumulated at the cell poles where *E. coli* is most susceptible to phage infection (29, 92). Cas2 in *E. coli* has also been demonstrated to be dispensable for the CRISPR Expression and Interference stages (13). These observations have led to the hypothesis that Cas2 may be involved in recognition and/or inactivation of phage RNA, rather than phage DNA. Cas7 was demonstrated to be unnecessary for the CRISPR Expression and Interference stages in *S. thermophilus* (6). When *S. thermophilus* was challenged with a phage none of the resistant mutants had incorporated a new spacer into the CRISPR array when *cas7* was mutated (6). These observations suggest that Cas7 is likely involved in spacer integration.

Stage 2: CRISPR Expression

The CRISPR Expression stage consists of two steps (Figure 1-3). The first step involves the transcription of the CRISPR array into one long RNA known as pre-crRNA. The second step is the processing of the pre-crRNA into its mature form known as crRNA. Evidence in

Pyrococcus furiosus found that pre-crRNA contain regions homologous to the 3' end of the leader sequence (38). This resulted in the hypothesis that transcription of CRISPR arrays begin from a promoter in the leader sequence (47). This hypothesis was later confirmed in the *E. coli* K12 strain by demonstrating that the leader sequence of CRISPRII contains a promoter active both *in vitro* and *in vivo* (79). In *Archaeoglobus fulgidus* the CRISPR arrays were shown to be transcribed as one long precursor, which was further processed into smaller crRNA (93).

All CRISPR-Cas Types have been demonstrated to process the pre-crRNA into crRNA one way or another and this processing requires a Cas protein or a set of Cas proteins (Figure 1-3). In a Type I CRISPR system in *E. coli* K12, five Cas proteins (Cse1, Cse2, Cas7, Cas5 and Cas6e, originally referred to as Cas A-E, respectively) were demonstrated to form a complex termed CASCADE for CRISPR-associated complex for antiviral defense, and this complex was shown to be responsible for the processing of the pre-crRNA to crRNA (13). A Type II CRISPR system in *S. thermophilus* was demonstrated to require a trans-encoded small CRISPR RNA (tracrRNA), RNaseIII, and Cas9 for the processing of pre-crRNA into crRNA (24). It is proposed that Cas9 binds to the pre-crRNA promoting the formation of a duplex between the tracrRNA and the repeat sequence of the pre-crRNA. This duplex between the tracrRNA and the pre-crRNA leads to the initial cleavage of the pre-crRNA in the repeat sequence by RNaseIII, resulting in an intermediate processing product (24, 32). Cas9 is then proposed to cleave the intermediate product in the spacer sequence to produce crRNA (32). In a Type III system in *P. furiosus*, a homolog of Cas6e, Cas6 was shown to have specific endonuclease activity leading to the processing of pre-crRNA (17, 18). It was further demonstrated that cleavage of the pre-crRNA occurs in the repeat 8 nucleotides from the start of the spacer (13, 18). The cleavage of the 3' end of the spacer appears less consistent, suggesting a separate activity for this processing

(18, 39, 93, 94). Despite the variations in how the processing occurs between the CRISPR Types, the processing of the pre-crRNA to crRNA appears necessary for the functioning of the CRISPR array as an adaptive immune system.

Stage 3: Interference

During the Interference stage, crRNA and selected Cas proteins are proposed to function together to confer immunity against invading foreign elements (Figure 1-3). The Cas proteins are proposed to use the crRNA as a guide to target invading DNA or RNA with homology to the crRNA. The different CRISPR-Cas Types have been shown to target different forms of invading nucleic acids. Types I, II, and III-A appear to target invading DNA, while Type III-B CRISPR-RAMP systems appear to target RNA (32, 39, 64, 86, 95). In *P. furiosus*, it has been demonstrated that the RAMP proteins in Type III-B (Cmr 1, 3-6, and Cas10) are able to form a complex that specifically targets ssRNA, but not DNA (39). In a Type I system in *E. coli*, Cas3 was shown to be required for targeting to occur (13). It was hypothesized that Cas3, which contains nuclease and helicase domains (63), inactivates foreign DNA (13). In a Type I system in *S. thermophilus*, Cas5 was also shown to contain a nuclease domain and may have similar functions as Cas3 (6). In the Type II system, Cas9, which contains two nuclease domains, has been shown to be involved in the cleavage of target DNA (48). Since Type III-B CRISPR-RAMP systems are almost always found in organisms that also have other CRISPR-Cas systems, it is possible that these two different systems work in conjunction to provide immunity against both invading DNA and RNA.

E. The role of Type III-B CRISPR-RAMP module in CRISPR mediated immunity

The Type III CRISPR system, which has been shown to mediate immunity in prokaryotes by specifically targeting ssRNA (39), has nine Cas proteins, Cmr1, Cmr3-6, Cas1, Cas2, Cas6 and Cas10 (64). Cas10 is the defining protein for Type III and Cmr5 for Type III-B (64). Like

other systems, these Cas proteins are proposed to function in the three stages (Adaptation, CRISPR Expression and Interference) to mediate immunity. Cas1 and Cas2 are proposed to function in the Adaptation stage because they were shown to be dispensable for CRISPR Expression and Interference (13). Cas1 from *P. aeruginosa* has been demonstrated to have a metal-dependent endonuclease activity specific to DNA (99), while Cas2 from *S. solfataricus* has been demonstrated to be a metal-dependent ssRNA endonuclease with preferences for U-rich regions and has properties of an RNA-binding protein (8). Cas6, an endoribonuclease, functions in the CRISPR Expression and processing stage (17, 18) as it was shown to cleave pre-crRNA in the repeat sequence (13, 18). Cmr1, Cmr3-6, and Cas10 are proposed to function in the Interference stage. Cmr1, Cmr3, Cmr4, and Cmr6 are predicted to be RNA binding proteins based on their distinct RNA recognition motifs, while Cas10 has homology suggesting nuclease and polymerase activities (36, 63). These Cmr proteins along with Cas10 and crRNA form a complex termed RAMP module that specifically targets ssRNA (39). These results indicate that the Type III-B CRISPR-RAMP system specifically function to mediate immunity in prokaryotes against foreign RNA that may enter the cell.

F. CRISPR systems may regulate cellular processes other than immunity

New evidence has recently emerged that CRISPR may regulate the function of chromosomal genes and cellular processes other than immunity. An *in silico* study of 330 organisms showed that 18% of all organisms have spacers homologous to chromosomal genes, which account for one in every 250 spacers (88). Additionally, 18% of CRISPR spacers in *Yersinia pestis* were found to originate from the genome (22). These observations led to the hypothesis that CRISPR arrays may also regulate chromosomal genes. Some groups have argued that the occurrence of self-targeting spacers is an error of the CRISPR machinery and it is

corrected by the inactivation of spacers or whole CRISPR arrays (88). However, a spacer homologous to histidyl-tRNA synthetase gene (*hisS*) from *Pelobacter carbinolicus* was shown to retard the growth of *Geobacter sulfurreducens* when both the spacer and *hisS* from *P. carbinolicus* were placed in *G. sulfurreducens* (1). These observations suggest that the spacer is active and is able to interfere with *hisS* expression (1).

The strongest evidence that CRISPR may regulate chromosomal genes or normal cellular function comes from the studies of biofilm formation in *P. aeruginosa*. The lysogenic phage, DMS3, was used to challenge *P. aeruginosa*. The lysogen was found to have lost swarming motility and biofilm formation. When the CRISPR-Cas system was disrupted in the lysogen, swarming motility and biofilm formation was restored (103). By mutating the spacers of the CRISPR array, it was found that spacer 1 of CRISPR2 was responsible for the defect in biofilm formation (16). Spacer 1 is an incomplete match for a gene on the DMS3 phage, gene 42. Nevertheless, the interaction between DMS3-42 and spacer 1 were found to be necessary for the disruption of biofilm formation in the lysogen (16). These observations suggest that spacer 1 and DMS3-42 interact to regulate both swarming motility and biofilm formation in *P. aeruginosa*. This study, along with others, uncovers a correlation between CRISPR systems and the regulation of chromosomal genes and cellular processes other than immunity.

II. *Myxococcus xanthus*: The experimental system

A. *Myxococcus xanthus* undergoes a complex life cycle that requires S motility

Myxococcus xanthus, a rod-shaped Gram-negative soil bacterium, undergoes complex life cycles (Figure 1-4) (27, 55). In the vegetative cycle, *M. xanthus*, a predatory organism, spreads out to hunt for other bacteria in its environment. When they come in contact with prey, *Escherichia coli* for example, they use what is referred to as “wolf-pack” hunting where large numbers of cells coordinate their movements and feed as a group. *M. xanthus* cells achieve this “wolf-pack” or collective hunting by secreting secondary metabolites and hydrolytic enzymes in a targeted manner in response to prey cell contact (28, 30, 41, 81, 89). Under starvation conditions, *M. xanthus* cells undergo the developmental cycle where hundreds of thousands of *M. xanthus* cells aggregate into mounds known as fruiting bodies (51, 56). In these fruiting bodies, rod-shaped *M. xanthus* vegetative cells differentiate into spherical myxospores, which are metabolically dormant and environmentally resistant (56). When *M. xanthus* cells sense limited nutrients, an intracellular signal, 3'-di-5'-(tri)diphosphate nucleotides [(p)ppGpp], accumulates in the cell initiating development (40). This intracellular signal activates the expression of early developmental genes, including the A-signaling pathway, which leads to the secretion of extracellular amino acids that are sensed by neighboring cells allowing them to coordinate their behavior (49, 50). In this dormant state, myxospores can persist for weeks to years, until nutrients are again sensed in their environment, triggering germination returning them to their vegetative state. Due to their complex life cycles, *M. xanthus* has been a model system for studying bacterial social behaviors.

M. xanthus is a non-flagellated bacterium that moves on solid surfaces by gliding motility. Gliding motility plays critical roles in the life cycles of *M. xanthus* cells (27). Motility

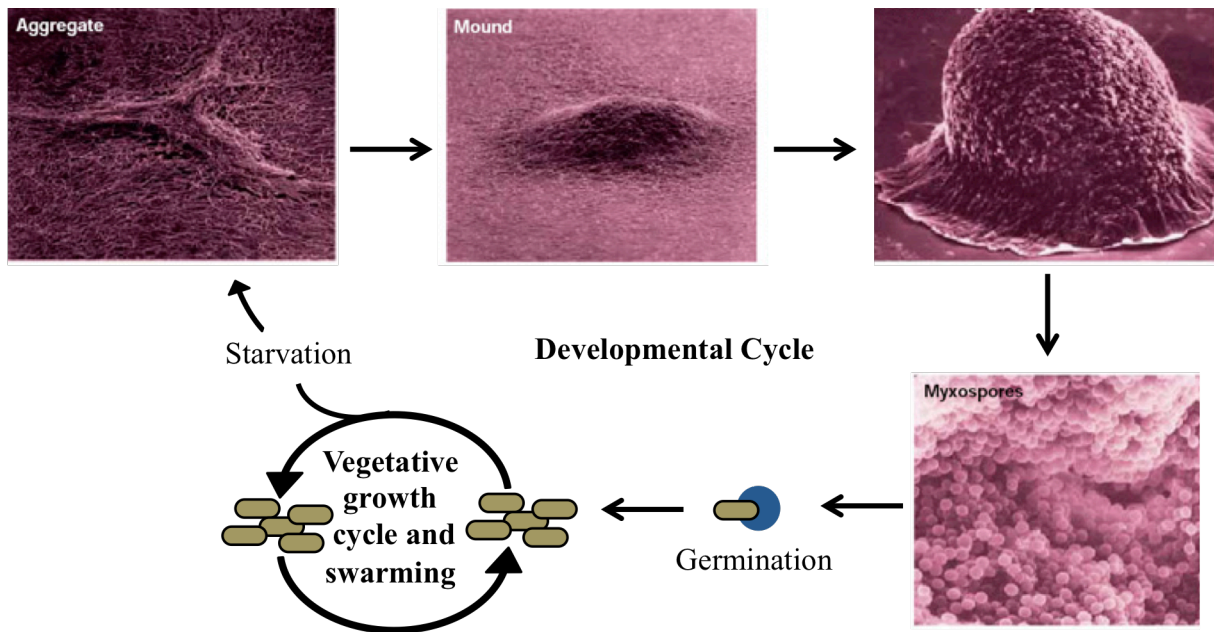


Figure 1-4: Life cycles of *M. xanthus*

Under nutrient rich conditions, *M. xanthus* cells undergo a vegetative life cycle by growth and cell division. When nutrients become limited, the vegetative cells aggregate into dome-shaped mounds, called fruiting bodies. There the vegetative cells will differentiate into environmentally resistant spherical myxospores. When the myxospores sense ample nutrients in the environment, they will germinate and return to the vegetative cycle. Figure modified from Kaiser, 2003 (49). Used under fair use, 2013.

is essential for *M. xanthus* cells to spread out and hunt as well as aggregate into fruiting bodies. *M. xanthus* cells possess two genetically distinct forms of gliding motility: Adventurous (A) motility and Social (S) motility (Figure 1-5) (43, 44, 85). A motility is responsible for the movement of single cells while S motility is only functional when cells are within close proximity to one another (43, 44). These two motility systems are genetically distinct in that under normal conditions both motility systems can be active, but if a mutation occurs in a gene involved in one motility system the other will still be functional (85). One exception to this are mutations in *mgl* (mutual gliding) genes (85). S motility has been shown to require the extension and retraction of Type IV pili (T4P) as well as the production and secretion of extracellular polysaccharides (EPS) (2, 51, 85, 100, 102). The extension and retraction of T4P together constitute the motor that powers S motility, while EPS on a neighboring cell is proposed to be the anchor and trigger for T4P retraction (10, 58, 68, 83, 87, 90, 100).

B. Type IV pilus is a bacterial motility apparatus

Genes for T4P have been identified in both Gram-negative and Gram-positive organisms and T4P have been shown to mediate a range of functions including motility, DNA uptake, and electron transport (31, 60, 68, 75). T4P have also proven essential in the virulence of many Gram-negative organisms (37). T4P are protein filaments that are 5 to 7 nm in diameter and 3 to 10 μm in length that are predominately localized to one cell pole (51, 61). Two distinct subclasses of T4P have been identified, Type IVa pili (T4aP) and Type IVb pili (T4bP). This distinction is based in part on the length and sequence of the pilin subunits (20). T4bP have been found to mediate adhesion and bacterial aggregation in enteric pathogens, including Enteropathogenic *E. coli* (EPEC) (9). These structures in EPEC are known as Bundle-forming

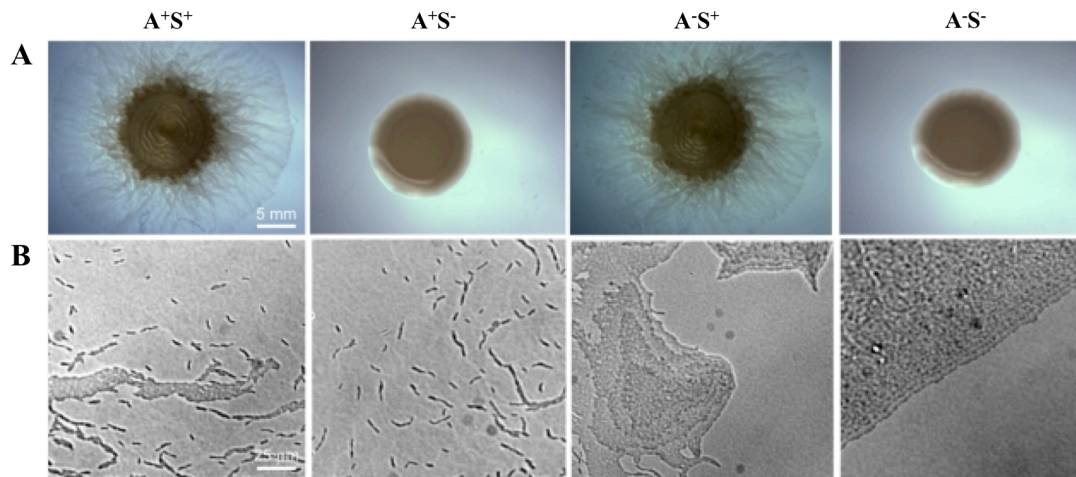


Figure 1-5: A and S motility in *M. xanthus*

A. A Colony on 0.4% agarose medium, which selects for S motility. **B.** Colony edge under magnification. A normal colony edge has cells exhibiting both A and S motility, A^+S^+ . If one of these motility systems is defective, the other system remains active, which can be seen in panel A and B for A^+S^- and A^-S^+ . If both motility systems have a defect then the cells will be non-motile, which can be seen in both panels for A^-S^- . Figure modified from Mauriello et al. (2010) (67). Used under fair use, 2013.

pili (BFP). Of the two subclasses, *M. xanthus* possesses T4aP, which mediates S motility (66, 87).

Eleven highly conserved core proteins have been shown to be essential for T4P function (3, 4, 77, 82). The nomenclature used is not consistent between all the organisms possessing T4P or BFP, but for simplicity, the nomenclature for *M. xanthus* T4P proteins will be used here. These eleven core proteins come together in a complex extending from the cytoplasm to the outer membrane (OM) to compose T4P (Figure 1-6). The T4P filament that extends from the cell is composed of mature pilin or processed PilA monomers in a three-layered helical structure (76, 100). In a *pilA* deficient strain, pilins are not produced, leading to a lack of T4P or a T4P⁻ phenotype. The signal sequence of PilA must first be cleaved off by a peptidase, PilD, which produces mature pilin that can then be assembled into the T4P filament (74). Two cytoplasmic proteins, PilB and PilT, have been shown to be involved in the assembly/extension and disassembly/retraction of T4P filament, respectively. PilB is an ATPase that provides energy for the assembly of T4P filament, while PilT is a hexameric motor ATPase that powers the retraction or disassembly of T4P filament (10, 58, 68, 83, 87, 90, 100). PilQ, a multimeric secretin, is required to form an OM pore in order for the T4P filament to be assembled and extended outside of the cell (15, 19, 42). PilQ has been proposed to interact with an OM lipoprotein, Tgl, and an inner membrane (IM) lipoprotein, PilP (5, 46, 54, 73). PilP has been proposed to also interact with two transmembrane (TM) proteins, PilN and PilO, likely acting as a bridge between the IM and the OM components (65, 80, 91). A cytoplasmic protein, PilM, likely interacts with PilN (53). Another IM protein, PilC, is a putative platform protein that likely forms a complex with other T4P IM proteins and possibly interacting with PilB and/or PilT as well (21). The coordination of these eleven proteins is essential for the function of T4P. When there is a defect

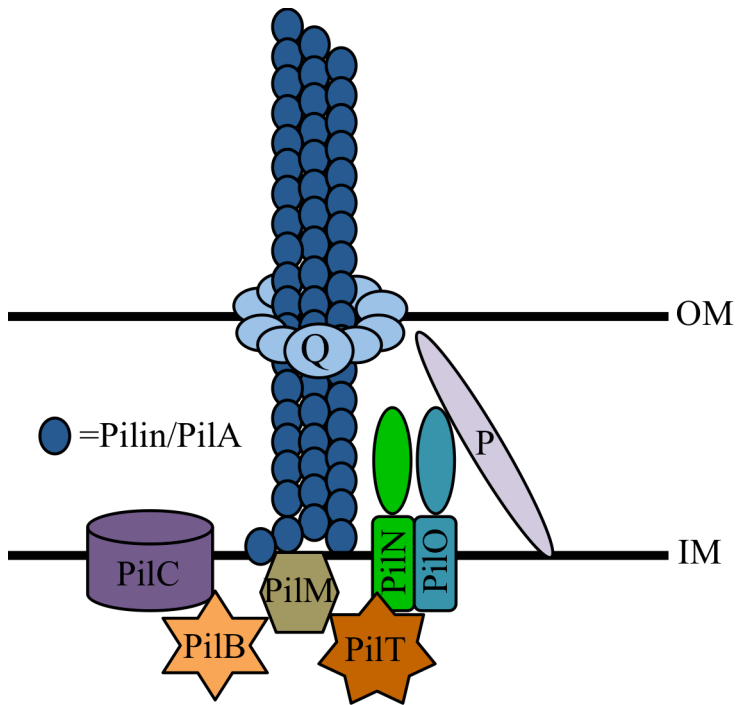


Figure 1-6: Type IV Pili model

Figure represents the proposed model of T4P. T4P consists of conserved proteins that extended from the Inner Membrane (IM) to the Outer Membrane (OM) of the cell. Not all T4P proteins are depicted here. Q and P represent PilQ and PilP, respectively. Figure based on Mattick, 2002 (66). Used under fair use, 2013.

in one of these proteins, except PilT, T4P are not assembled as well as the cell will no longer produce EPS.

C. The interplays of T4P and EPS in *M. xanthus* S motility

EPS is secreted from the cell forming a sticky matrix on the cell surface that makes up biofilms. EPS is comprised of monosaccharides, like mannose, galactose and glucose, just to name a few, that form lateral branches on the surface of the cell (2, 7). The production and secretion of EPS is regulated by a number of components, including T4P, SglK, StkA, and the Dif (Defective in fruiting) proteins (2, 7, 10, 23, 101). A model of the regulation of EPS by T4P and the Dif pathway is shown in Figure 1-7. In the EPS signal regulation pathway, T4P functions upstream of SglK, StkA, and the Dif pathway. SglK, a DnaK homologue, is required for S motility and the regulation of EPS production and has been shown to be constitutively expressed during vegetative growth and development (101). StkA, another DnaK homologue, functions downstream of SglK to negatively regulate EPS production as *stkA* mutants over produce EPS (23). The Dif pathway is a chemosensory system, which primarily functions in the regulation of EPS production in *M. xanthus* (11, 102). These proteins and many others, known or unknown, form a complex EPS regulatory network.

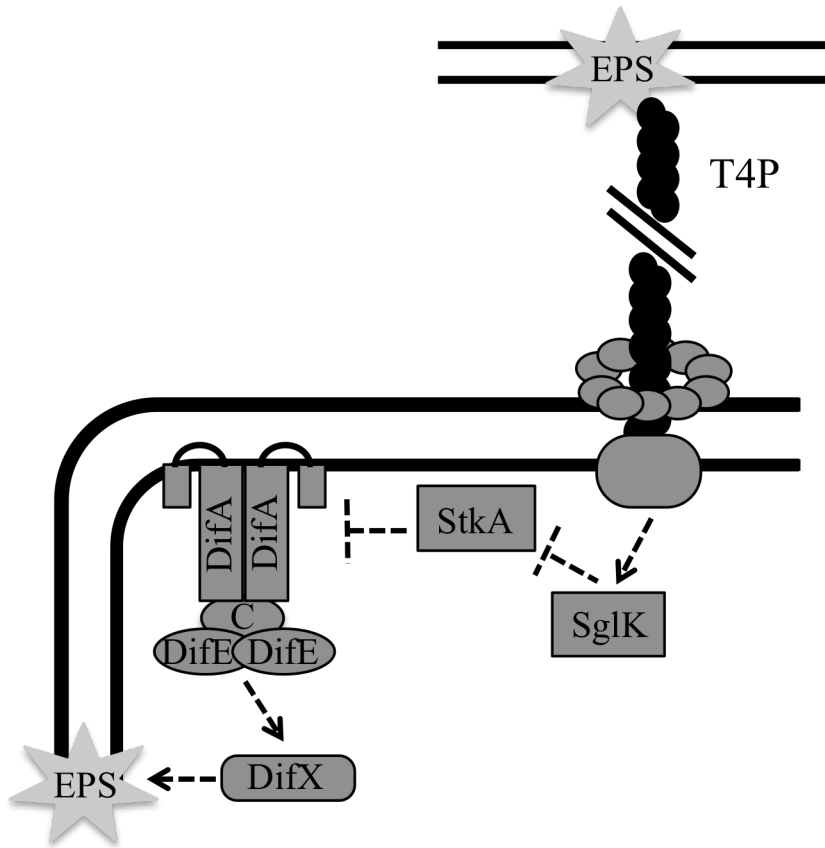


Figure 1-7: Model for the regulation of EPS production

Proposed model for the regulation of EPS production by Type IV pili, SglK, StkA, and the Dif pathway. The structure labeled C represents DifC. Dotted lines indicate proposed interactions. Figure modified from Black, *et. al.*, 2006 (10). Used under fair use, 2013.

References Cited

1. **Aklujkar, M., and D. R. Lovley.** 2010. Interference with histidyl-tRNA synthetase by a CRISPR spacer sequence as a factor in the evolution of *Pelobacter carbinolicus*. *BMC Evolutionary Biology* **10**:230.
2. **Arnold, J. W., and L. J. Shimkets.** 1988. Cell surface properties correlated with cohesion in *Myxococcus xanthus*. *Journal of Bacteriology* **170**:5771-5777.
3. **Averhoff, B.** 2009. Shuffling genes around in hot environments: the unique DNA transporter of *Thermus thermophilus*. *FEMS microbiology reviews* **33**:611-626.
4. **Ayers, M., P. L. Howell, and L. L. Burrows.** 2010. Architecture of the type II secretion and type IV pilus machineries. *Future microbiology* **5**:1203-1218.
5. **Balasingham, S. V., R. F. Collins, R. Assalkhou, H. Homberset, S. A. Frye, J. P. Derrick, and T. Tonjum.** 2007. Interactions between the lipoprotein PilP and the secretin PilQ in *Neisseria meningitidis*. *Journal of Bacteriology* **189**:5716-5727.
6. **Barrangou, R., C. Fremaux, H. Deveau, M. Richards, P. Boyaval, S. Moineau, D. A. Romero, and P. Horvath.** 2007. CRISPR provides acquired resistance against viruses in prokaryotes. *Science* **315**:1709-1712.
7. **Behmlander, R. M., and M. Dworkin.** 1994. Biochemical and structural analyses of the extracellular matrix fibrils of *Myxococcus xanthus*. *Journal of Bacteriology* **176**:6295-6303.
8. **Beloglazova, N., G. Brown, M. D. Zimmerman, M. Proudfoot, K. S. Makarova, M. Kudritska, S. Kochinyan, S. Wang, M. Chruszcz, W. Minor, E. V. Koonin, A. M. Edwards, A. Savchenko, and A. F. Yakunin.** 2008. A novel family of sequence-specific endoribonucleases associated with the clustered regularly interspaced short palindromic repeats. *The Journal of Biological Chemistry* **283**:20361-20371.
9. **Bieber, D., S. W. Ramer, C. Y. Wu, W. J. Murray, T. Tobe, R. Fernandez, and G. K. Schoolnik.** 1998. Type IV pili, transient bacterial aggregates, and virulence of enteropathogenic *Escherichia coli*. *Science* **280**:2114-2118.
10. **Black, W. P., Q. Xu, and Z. Yang.** 2006. Type IV pili function upstream of the Dif chemotaxis pathway in *Myxococcus xanthus* EPS regulation. *Molecular Microbiology* **61**:447-456.
11. **Black, W. P., and Z. Yang.** 2004. *Myxococcus xanthus* chemotaxis homologs DifD and DifG negatively regulate fibril polysaccharide production. *Journal of Bacteriology* **186**:1001-1008.

12. **Bolotin, A., B. Quinquis, A. Sorokin, and S. D. Ehrlich.** 2005. Clustered regularly interspaced short palindrome repeats (CRISPRs) have spacers of extrachromosomal origin. *Microbiology* **151**:2551-2561.
13. **Brouns, S. J. J., M. M. Jore, M. Lundgren, E. R. Westra, R. J. H. Slijkhuis, A. P. L. Snijders, M. J. Dickman, K. S. Makarova, E. V. Koonin, and J. van der Oost.** 2008. Small CRISPR RNAs guide antiviral defense in prokaryotes. *Science* **321**:960-964.
14. **Bult, C. J., O. White, G. J. Olsen, L. Zhou, R. D. Fleischmann, G. G. Sutton, J. A. Blake, L. M. FitzGerald, R. A. Clayton, J. D. Gocayne, A. R. Kerlavage, B. A. Dougherty, J. F. Tomb, M. D. Adams, C. I. Reich, R. Overbeek, E. F. Kirkness, K. G. Weinstock, J. M. Merrick, A. Glodek, J. L. Scott, N. S. Geoghagen, and J. C. Venter.** 1996. Complete genome sequence of the methanogenic archaeon, *Methanococcus jannaschii*. *Science* **273**:1058-1073.
15. **Burkhardt, J., J. Vonck, and B. Averhoff.** 2011. Structure and function of PilQ, a secretin of the DNA transporter from the thermophilic bacterium *Thermus thermophilus* HB27. *The Journal of Biological Chemistry* **286**:9977-9984.
16. **Cady, K. C., and G. A. O'Toole.** 2011. Non-identity-mediated CRISPR-bacteriophage interaction mediated via the Csy and Cas3 proteins. *Journal of Bacteriology* **193**:3433-3445.
17. **Carte, J., N. T. Pfister, M. M. Compton, R. M. Terns, and M. P. Terns.** 2010. Binding and cleavage of CRISPR RNA by Cas6. *RNA* **16**:2181-2188.
18. **Carte, J., R. Wang, H. Li, R. M. Terns, and M. P. Terns.** 2008. Cas6 is an endoribonuclease that generates guide RNAs for invader defense in prokaryotes. *Genes & Development* **22**:3489-3496.
19. **Collins, R. F., L. Davidsen, J. P. Derrick, R. C. Ford, and T. Tonjum.** 2001. Analysis of the PilQ secretin from *Neisseria meningitidis* by transmission electron microscopy reveals a dodecameric quaternary structure. *Journal of Bacteriology* **183**:3825-3832.
20. **Craig, L., M. E. Pique, and J. A. Tainer.** 2004. Type IV pilus structure and bacterial pathogenicity. *Nature reviews. Microbiology* **2**:363-378.
21. **Crowther, L. J., R. P. Anantha, and M. S. Donnenberg.** 2004. The inner membrane subassembly of the enteropathogenic *Escherichia coli* bundle-forming pilus machine. *Molecular Microbiology* **52**:67-79.
22. **Cui, Y., Y. Li, O. Gorgé, M. E. Platonov, Y. Yan, Z. Guo, C. Pourcel, S. V. Dentovskaya, S. V. Balakhonov, X. Wang, Y. Song, A. P. Anisimov, G. Vergnaud, and R. Yang.** 2008. Insight into microevolution of *Yersinia pestis* by clustered regularly interspaced short palindromic repeats. *PLoS ONE* **3**:e2652.

23. **Dana, J. R., and L. J. Shimkets.** 1993. Regulation of cohesion-dependent cell interactions in *Myxococcus xanthus*. *Journal of Bacteriology* **175**:3636-3647.
24. **Deltcheva, E., K. Chylinski, C. M. Sharma, K. Gonzales, Y. Chao, Z. A. Pirzada, M. R. Eckert, J. Vogel, and E. Charpentier.** 2011. CRISPR RNA maturation by trans-encoded small RNA and host factor RNase III. *Nature* **471**:602-607.
25. **Deveau, H., R. Barrangou, J. E. Garneau, J. Labonte, C. Fremaux, P. Boyaval, D. A. Romero, P. Horvath, and S. Moineau.** 2008. Phage response to CRISPR-encoded resistance in *Streptococcus thermophilus*. *Journal of Bacteriology* **190**:1390-1400.
26. **Deveau, H., J. E. Garneau, and S. Moineau.** 2010. CRISPR/Cas system and its role in phage-bacteria interactions. *Annual review of microbiology* **64**:475-493.
27. **Dworkin, M.** 1966. Biology of the myxobacteria. *Annual review of microbiology* **20**:75-106.
28. **Dworkin, M.** 1973. Cell-cell interactions in myxobacteria. A Symposium of the Society for General Microbiology **23**:125-142.
29. **Edgar, R., A. Rokney, M. Feeney, S. Semsey, M. Kessel, M. B. Goldberg, S. Adhya, and A. B. Oppenheim.** 2008. Bacteriophage infection is targeted to cellular poles. *Molecular Microbiology* **68**:1107-1116.
30. **Ensign, J. C., and R. S. Wolfe.** 1965. Lysis of bacterial cell walls by an enzyme isolated from a Myxobacter. *Journal of Bacteriology* **90**:395-402.
31. **Friedrich, A., C. Prust, T. Hartsch, A. Henne, and B. Averbhoff.** 2002. Molecular analyses of the natural transformation machinery and identification of pilus structures in the extremely thermophilic bacterium *Thermus thermophilus* strain HB27. *Applied and environmental microbiology* **68**:745-755.
32. **Garneau, J. E., M. E. Dupuis, M. Villion, D. A. Romero, R. Barrangou, P. Boyaval, C. Fremaux, P. Horvath, A. H. Magadan, and S. Moineau.** 2010. The CRISPR/Cas bacterial immune system cleaves bacteriophage and plasmid DNA. *Nature* **468**:67-71.
33. **Godde, J. S., and A. Bickerton.** 2006. The repetitive DNA elements called CRISPRs and their associated genes: evidence of horizontal transfer among prokaryotes. *Journal of Molecular Evolution* **62**:718-729.
34. **Grissa, I., G. Vergnaud, and C. Pourcel.** 2007. The CRISPRdb database and tools to display CRISPRs and to generate dictionaries of spacers and repeats. *BMC Bioinformatics* **8**:172.
35. **Groenen, P. M., A. E. Bunschoten, D. van Soolingen, and J. D. van Embden.** 1993. Nature of DNA polymorphism in the direct repeat cluster of *Mycobacterium tuberculosis*;

- application for strain differentiation by a novel typing method. *Molecular Microbiology* **10**:1057-1065.
36. **Haft, D. H., J. Selengut, E. F. Mongodin, and K. E. Nelson.** 2005. A guild of 45 CRISPR-associated (Cas) protein families and multiple CRISPR/Cas subtypes exist in prokaryotic genomes. *PLoS Computational Biology* **1**:e60.
 37. **Hager, A. J., D. L. Bolton, M. R. Pelletier, M. J. Brittnacher, L. A. Gallagher, R. Kaul, S. J. Skerrett, S. I. Miller, and T. Guina.** 2006. Type IV pili-mediated secretion modulates *Francisella* virulence. *Molecular Microbiology* **62**:227-237.
 38. **Hale, C., K. Kleppe, R. M. Terns, and M. P. Terns.** 2008. Prokaryotic silencing (psi)RNAs in *Pyrococcus furiosus*. *RNA* **14**:2572-2579.
 39. **Hale, C. R., P. Zhao, S. Olson, M. O. Duff, B. R. Graveley, L. Wells, R. M. Terns, and M. P. Terns.** 2009. RNA-guided RNA cleavage by a CRISPR RNA-Cas protein complex. *Cell* **139**:945-956.
 40. **Harris, B. Z., D. Kaiser, and M. Singer.** 1998. The guanosine nucleotide (p)ppGpp initiates development and A-factor production in *Myxococcus xanthus*. *Genes and Development* **12**:1022-1035.
 41. **Hart, B. A., and S. A. Zahler.** 1966. Lytic enzyme produced by *Myxococcus xanthus*. *Journal of Bacteriology* **92**:1632-1637.
 42. **Helm, R. A., M. M. Barnhart, and H. S. Seifert.** 2007. *pilQ* missense mutations have diverse effects on PilQ multimer formation, piliation, and pilus function in *Neisseria gonorrhoeae*. *Journal of Bacteriology* **189**:3198-3207.
 43. **Hodgkin, J., and D. Kaiser.** 1979. Genetics of gliding motility in *Myxococcus xanthus* (Myxobacterales): genes controlling movements of single cells. *Molecular and General Genetics* **171**:167-176.
 44. **Hodgkin, J., and D. Kaiser.** 1979. Genetics of gliding motility in *Myxococcus xanthus* (Myxobacterales): two gene systems control movement. *Molecular and General Genetics* **171**:177-191.
 45. **Ishino, Y., H. Shinagawa, K. Makino, M. Amemura, and A. Nakata.** 1987. Nucleotide sequence of the *iap* gene, responsible for alkaline phosphatase isozyme conversion in *Escherichia coli*, and identification of the gene product. *Journal of Bacteriology* **169**:5429-5433.
 46. **Jain, S., K. B. Moscicka, M. P. Bos, E. Pachulec, M. C. Stuart, W. Keegstra, E. J. Boekema, and C. van der Does.** 2011. Structural characterization of outer membrane components of the type IV pili system in pathogenic *Neisseria*. *PLoS ONE* **6**:e16624.

47. **Jansen, R., J. D. Embden, W. Gaastra, and L. M. Schouls.** 2002. Identification of genes that are associated with DNA repeats in prokaryotes. *Molecular Microbiology* **43**:1565-1575.
48. **Jinek, M., K. Chylinski, I. Fonfara, M. Hauer, J. A. Doudna, and E. Charpentier.** 2012. A programmable dual-RNA-guided DNA endonuclease in adaptive bacterial immunity. *Science* **337**:816-821.
49. **Kaiser, D.** 2003. Coupling cell movement to multicellular development in myxobacteria. *Nature reviews. Microbiology* **1**:45-54.
50. **Kaiser, D.** 2004. Signaling in myxobacteria. *Annual review of microbiology* **58**:75-98.
51. **Kaiser, D.** 1979. Social gliding is correlated with the presence of pili in *Myxococcus xanthus*. *Proceedings of the National Academy of Sciences U S A* **76**:5952-5956.
52. **Karginov, F. V., and G. J. Hannon.** 2010. The CRISPR system: small RNA-guided defense in bacteria and archaea. *Molecular cell* **37**:7-19.
53. **Karuppiyah, V., and J. P. Derrick.** 2011. Structure of the PilM-PilN inner membrane type IV pilus biogenesis complex from *Thermus thermophilus*. *The Journal of Biological Chemistry* **286**:24434-24442.
54. **Koo, J., S. Tammam, S. Y. Ku, L. M. Sampaleanu, L. L. Burrows, and P. L. Howell.** 2008. PilF is an outer membrane lipoprotein required for multimerization and localization of the *Pseudomonas aeruginosa* Type IV pilus secretin. *Journal of Bacteriology* **190**:6961-6969.
55. **Krzemieniewska, H., and S. Krzemieniewski.** 1926. Miksobakterje polski. *Acta Societatis Botanicorum Poloniae* **4**:1-54.
56. **Kuner, J. M., and D. Kaiser.** 1982. Fruiting body morphogenesis in submerged cultures of *Myxococcus xanthus*. *Journal of Bacteriology* **151**:458-461.
57. **Kunin, V., R. Sorek, and P. Hugenholtz.** 2007. Evolutionary conservation of sequence and secondary structures in CRISPR repeats. *Genome Biology* **8**:R61.
58. **Li, Y., H. Sun, X. Ma, A. Lu, R. Lux, D. Zusman, and W. Shi.** 2003. Extracellular polysaccharides mediate pilus retraction during social motility of *Myxococcus xanthus*. *Proceedings of the National Academy of Sciences U S A* **100**:5443-5448.
59. **Lillestol, R. K., P. Redder, R. A. Garrett, and K. Brugger.** 2006. A putative viral defence mechanism in archaeal cells. *Archaea* **2**:59-72.

60. **Long, C. D., D. M. Tobiason, M. P. Lazio, K. A. Kline, and H. S. Seifert.** 2003. Low-level pilin expression allows for substantial DNA transformation competence in *Neisseria gonorrhoeae*. *Infection and immunity* **71**:6279-6291.
61. **MacRae, T. H., and D. McCurdy.** 1976. Evidence for motility-related fimbriae in the gliding microorganism *Myxococcus xanthus*. *Canadian Journal of Microbiology* **22**:1589-1593.
62. **Makarova, K. S., L. Aravind, N. V. Grishin, I. B. Rogozin, and E. V. Koonin.** 2002. A DNA repair system specific for thermophilic archaea and bacteria predicted by genomic context analysis. *Nucleic acids research* **30**:482-496.
63. **Makarova, K. S., N. V. Grishin, S. A. Shabalina, Y. I. Wolf, and E. V. Koonin.** 2006. A putative RNA-interference-based immune system in prokaryotes: computational analysis of the predicted enzymatic machinery, functional analogies with eukaryotic RNAi, and hypothetical mechanisms of action. *Biology Direct* **1**:7.
64. **Makarova, K. S., D. H. Haft, R. Barrangou, S. J. Brouns, E. Charpentier, P. Horvath, S. Moineau, F. J. Mojica, Y. I. Wolf, A. F. Yakunin, J. van der Oost, and E. V. Koonin.** 2011. Evolution and classification of the CRISPR-Cas systems. *Nature reviews. Microbiology* **9**:467-477.
65. **Martin, P. R., A. A. Watson, T. F. McCaul, and J. S. Mattick.** 1995. Characterization of a five-gene cluster required for the biogenesis of type 4 fimbriae in *Pseudomonas aeruginosa*. *Molecular Microbiology* **16**:497-508.
66. **Mattick, J. S.** 2002. Type IV pili and twitching motility. *Annual review of microbiology* **56**:289-314.
67. **Mauriello, E. M., T. Mignot, Z. Yang, and D. R. Zusman.** 2010. Gliding motility revisited: how do the myxobacteria move without flagella? *Microbiology and molecular biology reviews* : MMBR **74**:229-249.
68. **Merz, A. J., M. So, and M. P. Sheetz.** 2000. Pilus retraction powers bacterial twitching motility. *Nature* **407**:98-102.
69. **Mojica, F. J., C. Diez-Villasenor, J. Garcia-Martinez, and C. Almendros.** 2009. Short motif sequences determine the targets of the prokaryotic CRISPR defence system. *Microbiology* **155**:733-740.
70. **Mojica, F. J., C. Diez-Villasenor, J. Garcia-Martinez, and E. Soria.** 2005. Intervening sequences of regularly spaced prokaryotic repeats derive from foreign genetic elements. *Journal of Molecular Evolution* **60**:174-182.

71. **Mojica, F. J., C. Diez-Villasenor, E. Soria, and G. Juez.** 2000. Biological significance of a family of regularly spaced repeats in the genomes of archaea, bacteria and mitochondria. *Molecular Microbiology* **36**:244-246.
72. **Mojica, F. J., C. Ferrer, G. Juez, and F. Rodriguez-Valera.** 1995. Long stretches of short tandem repeats are present in the largest replicons of the Archaea *Haloferax mediterranei* and *Haloferax volcanii* and could be involved in replicon partitioning. *Molecular Microbiology* **17**:85-93.
73. **Nudleman, E., and D. Kaiser.** 2004. Pulling together with type IV pili. *Journal of molecular microbiology and biotechnology* **7**:52-62.
74. **Nunn, D. N., and S. Lory.** 1991. Product of the *Pseudomonas aeruginosa* gene *pilD* is a prepilin leader peptidase. *Proceedings of the National Academy of Sciences U S A* **88**:3281-3285.
75. **O'Toole, G. A., and R. Kolter.** 1998. Flagellar and twitching motility are necessary for *Pseudomonas aeruginosa* biofilm development. *Molecular Microbiology* **30**:295-304.
76. **Parge, H. E., K. T. Forest, M. J. Hickey, D. A. Christensen, E. D. Getzoff, and J. A. Tainer.** 1995. Structure of the fibre-forming protein pilin at 2.6 Å resolution. *Nature* **378**:32-38.
77. **Peabody, C. R., Y. J. Chung, M. R. Yen, D. Vidal-Ingigliardi, A. P. Pugsley, and M. H. Saier, Jr.** 2003. Type II protein secretion and its relationship to bacterial type IV pili and archaeal flagella. *Microbiology* **149**:3051-3072.
78. **Pourcel, C., G. Salviñol, and G. Vergnaud.** 2005. CRISPR elements in *Yersinia pestis* acquire new repeats by preferential uptake of bacteriophage DNA, and provide additional tools for evolutionary studies. *Microbiology* **151**:653-663.
79. **Pul, U., R. Wurm, Z. Arslan, R. Geissen, N. Hofmann, and R. Wagner.** 2010. Identification and characterization of *E. coli* CRISPR-*cas* promoters and their silencing by H-NS. *Molecular Microbiology* **75**:1495-1512.
80. **Py, B., L. Loiseau, and F. Barras.** 2001. An inner membrane platform in the type II secretion machinery of Gram-negative bacteria. *EMBO reports* **2**:244-248.
81. **Rosenberg, E., K. H. Keller, and M. Dworkin.** 1977. Cell density-dependent growth of *Myxococcus xanthus* on casein. *Journal of Bacteriology* **129**:770-777.
82. **Ruiz, N., D. Kahne, and T. J. Silhavy.** 2006. Advances in understanding bacterial outer-membrane biogenesis. *Nature reviews. Microbiology* **4**:57-66.
83. **Semmler, A. B., C. B. Whitchurch, and J. S. Mattick.** 1999. A re-examination of twitching motility in *Pseudomonas aeruginosa*. *Microbiology* **145 (Pt 10)**:2863-2873.

84. **She, Q., R. K. Singh, F. Confalonieri, Y. Zivanovic, G. Allard, M. J. Awayez, C. C. Chan-Weiher, I. G. Clausen, B. A. Curtis, A. De Moors, G. Erauso, C. Fletcher, P. M. Gordon, I. Heikamp-de Jong, A. C. Jeffries, C. J. Kozera, N. Medina, X. Peng, H. P. Thi-Ngoc, P. Redder, M. E. Schenk, C. Theriault, N. Tolstrup, R. L. Charlebois, W. F. Doolittle, M. Duguet, T. Gaasterland, R. A. Garrett, M. A. Ragan, C. W. Sensen, and J. Van der Oost.** 2001. The complete genome of the crenarchaeon *Sulfolobus solfataricus* P2. *Proceedings of the National Academy of Sciences U S A* **98**:7835-7840.
85. **Shimkets, L. J.** 1986. Correlation of energy-dependent cell cohesion with social motility in *Myxococcus xanthus*. *Journal of Bacteriology* **166**:837-841.
86. **Sinkunas, T., G. Gasiunas, C. Fremaux, R. Barrangou, P. Horvath, and V. Siksnys.** 2011. Cas3 is a single-stranded DNA nuclease and ATP-dependent helicase in the CRISPR/Cas immune system. *The EMBO journal* **30**:1335-1342.
87. **Skerker, J. M., and H. C. Berg.** 2001. Direct observation of extension and retraction of type IV pili. *Proceedings of the National Academy of Sciences U S A* **98**:6901-6904.
88. **Stern, A., L. Keren, O. Wurtzel, G. Amitai, and R. Sorek.** 2010. Self-targeting by CRISPR: gene regulation or autoimmunity? *Trends in Genetics* **26**:335-340.
89. **Sudo, S., and M. Dworkin.** 1972. Bacteriolytic enzymes produced by *Myxococcus xanthus*. *Journal of Bacteriology* **110**:236-245.
90. **Sun, H., D. R. Zusman, and W. Shi.** 2000. Type IV pilus of *Myxococcus xanthus* is a motility apparatus controlled by the frz chemosensory system. *Current Biology* **10**:1143-1146.
91. **Tammam, S., L. M. Sampaleanu, J. Koo, P. Sundaram, M. Ayers, P. A. Chong, J. D. Forman-Kay, L. L. Burrows, and P. L. Howell.** 2011. Characterization of the PilN, PilO and PilP type IVa pilus subcomplex. *Molecular Microbiology* **82**:1496-1514.
92. **Tang, J., J. Akerboom, A. Vaziri, L. L. Looger, and C. V. Shank.** 2010. Near-isotropic 3D optical nanoscopy with photon-limited chromophores. *Proceedings of the National Academy of Sciences U S A* **107**:10068-10073.
93. **Tang, T. H., J. P. Bachelierie, T. Rozhdestvensky, M. L. Bortolin, H. Huber, M. Drungowski, T. Elge, J. Brosius, and A. Huttenhofer.** 2002. Identification of 86 candidates for small non-messenger RNAs from the archaeon *Archaeoglobus fulgidus*. *Proceedings of the National Academy of Sciences U S A* **99**:7536-7541.
94. **Tang, T. H., N. Polacek, M. Zywicki, H. Huber, K. Brugger, R. Garrett, J. P. Bachelierie, and A. Huttenhofer.** 2005. Identification of novel non-coding RNAs as potential antisense regulators in the archaeon *Sulfolobus solfataricus*. *Molecular Microbiology* **55**:469-481.

95. **Terns, M. P., and R. M. Terns.** 2011. CRISPR-based adaptive immune systems. *Current opinion in microbiology* **14**:321-327.
96. **Thony-Meyer, L., and D. Kaiser.** 1993. *devRS*, an autoregulated and essential genetic locus for fruiting body development in *Myxococcus xanthus*. *Journal of Bacteriology* **175**:7450-7462.
97. **van der Oost, J., M. M. Jore, E. R. Westra, M. Lundgren, and S. J. Brouns.** 2009. CRISPR-based adaptive and heritable immunity in prokaryotes. *Trends in Biochemical Sciences* **34**:401-407.
98. **van der Ploeg, J. R.** 2009. Analysis of CRISPR in *Streptococcus mutans* suggests frequent occurrence of acquired immunity against infection by M102-like bacteriophages. *Microbiology* **155**:1966-1976.
99. **Wiedenheft, B., K. Zhou, M. Jinek, S. M. Coyle, W. Ma, and J. A. Doudna.** 2009. Structural basis for DNase activity of a conserved protein implicated in CRISPR-mediated genome defense. *Structure* **17**:904-912.
100. **Wu, S. S., and D. Kaiser.** 1995. Genetic and functional evidence that Type IV pili are required for social gliding motility in *Myxococcus xanthus*. *Molecular Microbiology* **18**:547-558.
101. **Yang, Z., Y. Geng, D. Xu, H. B. Kaplan, and W. Shi.** 1998. A new set of chemotaxis homologues is essential for *Myxococcus xanthus* social motility. *Molecular Microbiology* **30**:1123-1130.
102. **Yang, Z., X. Ma, L. Tong, H. B. Kaplan, L. J. Shimkets, and W. Shi.** 2000. *Myxococcus xanthus dif* genes are required for biogenesis of cell surface fibrils essential for social gliding motility. *Journal of Bacteriology* **182**:5793-5798.
103. **Zegans, M. E., J. C. Wagner, K. C. Cady, D. M. Murphy, J. H. Hammond, and G. A. O'Toole.** 2009. Interaction between bacteriophage DMS3 and host CRISPR region inhibits group behaviors of *Pseudomonas aeruginosa*. *Journal of Bacteriology* **191**:210-219.

Chapter 2

Restoration of Exopolysaccharide Production to a *pilA* Mutant by CRISPR Mutations in *Myxococcus xanthus*

This chapter is a draft of a manuscript with
Wesley Black and Zhaomin Yang as co-authors

Dr. Wesley Black contributed to this work by constructing various plasmids and strains including BY802 ($\Delta pilA$ CRISPR3*). Both Dr. Black and Dr. Zhaomin Yang have been involved in conceiving and designing the experiments in this study. Dr. Yang and I, Regina A. Wallace, wrote this chapter.

Abstract

Myxococcus xanthus, a Gram-negative soil bacterium, requires Social (S) gliding motility for its complex life cycles. It has been demonstrated that the function of S motility requires two structures, Type IV pili (T4P) and exopolysaccharides (EPS). T4P is the motor that powers social movement by retraction while EPS is the proposed anchor and trigger for T4P retraction. It is known EPS production in turn requires the presence of T4P. In this study, a *pilA* mutant, which is T4P⁻ and EPS⁻, was mutagenized by a transposon for mutants with restored EPS production. A *pilA* suppressor was isolated and found to have a transposon insertion in the third Clustered Regularly Interspaced Short Palindromic Repeats (CRISPR3) in *M. xanthus*. The transposon insertion occurred in the 13th spacer of CRISPR3, 3SP13. This insertion was found to be a gain-of-function mutation and required the Repeat Associated Mysterious Proteins (RAMP) genes to suppress *pilA*. In addition, the 3SP13 insertion adversely effected fruiting body development in a RAMP-dependent manner in both the wild-type and the $\Delta pilA$ background. Analysis by RT-PCR suggested that the restoration of EPS and the detrimental effect of this mutation on development by the 3SP13 insertion could be due to an increase in the processing of CRISPR3 RNA. It has been demonstrated that CRISPR systems mediate adaptive immunity against phages and other invading genetic elements in prokaryotes. We propose here that one of the CRISPR3 spacers, once expressed and processed, may target a chromosomal gene(s) critical for EPS production and development in *M. xanthus*.

Introduction

Myxococcus xanthus, a rod-shaped Gram-negative bacterium, exhibits complex social interactions during its vegetative cycle and its developmental cycle (13, 14, 26). In the vegetative cycle, *M. xanthus*, a predatory organism, spreads out to hunt for other bacteria in its environment. Under starvation conditions, the developmental life cycle involves the coordinated effort of hundreds of thousands of cells aggregating into domed-shaped mounds, known as fruiting bodies (23, 27). In these fruiting bodies, vegetative cells differentiate into metabolically-dormant and environmentally resistant myxospores (27). In order to undergo this complex life cycle, *M. xanthus* cells must be motile. *M. xanthus* has two genetically distinct forms of motility, Adventurous (A) and Social (S) motility (19, 20, 41). A motility is the movement of a single cell while S motility involves the movement of groups of cells in close physical proximity (19, 20).

S motility has been shown to require two extracellular components: Type IV pilus (T4P) and exopolysaccharide (EPS) (23, 41). T4P is a protein filament composed of PilA monomers and the extension and retraction of this filament results in the movement of the cell. *M. xanthus* EPS are secreted polysaccharides that associate with the outer cell surface and are thought to function as the anchor and trigger for T4P retraction (28). More recently, T4P has been demonstrated to regulate the production of EPS and T4P mutants such as *pilA* deletions exhibit an EPS⁻ phenotype. In an attempt to better understand the regulation of EPS, we carried out a genetic screen to identify transposon mutations what could restore EPS production to a *pilA* deletion mutant. Here we describe a transposon insertion in CRISPR3 that suppressed the EPS defect of a *pilA* mutant.

CRISPR has recently been identified to function as an adaptive immune system in prokaryotes (2). CRISPR is a non-coding region that possesses an array of identical repeats interspaced by variable spacers (22, 31). These spacers have been found to be identical to DNA of mobile genetic elements, such as bacteriophages and transposons (7, 10, 34, 36). In order for this region to function it requires a set of CRISPR-associated (*cas*) genes that are found adjacent to the CRISPR array (22, 31). In this study, we identified that the transposon had integrated into the 13th of 52 spacers in CRISPR3. Based on our findings we conclude that the CRISPR3 transposon insertion is a gain-of-function (GOF) mutation rather than the typical loss-of-function (LOF) mutation seen in transposon insertions. We also have evidence that the Repeat Associated Mysterious Proteins (RAMP), a subfamily of Cas proteins, upstream of CRISPR3 are required for the suppression to occur. Interestingly, it was also seen that the CRISPR3 transposon mutant has detrimental effects on fruiting body development in a RAMP dependent manner. Based on our Reverse Transcription Polymerase Chain Reaction (RT-PCR) results the suppression of a *pilA* mutant may be due to an increase in processing of the pre-crRNA by the RAMP proteins. The results seen in our *in vivo* system indicates that CRISPR3, and possibly other Type III-B CRISPR arrays, function not only in defense against invading RNA, but also in the regulation of key cellular processes in a RAMP dependent manner.

Materials and Methods

Bacterial strains and growth conditions

All *M. xanthus* strains used are listed in Table 2-1. Medium for *M. xanthus* was Casitone-yeast extract (CYE) (10 g/liter casitone, 5 g/liter yeast extract, 8 mM MgSO₄ in 10 mM morpholinepropanesulfonic acid (MOPS) buffer, pH 7.6) (23). *Escherichia coli* strains used were XL1-BLUE (Stratagene) and DH5 α λ pir (25), which were grown in Luria-Bertani (LB) medium (33). *M. xanthus* and *E. coli* strains were grown at 32°C and at 37°C, respectively. 1.5% agar plates were used to grow *M. xanthus* and *E. coli*, unless otherwise indicated. Media were supplemented with kanamycin at 100 μ g/ml, and/or oxytetracycline at 15 μ g/ml when appropriate.

Isolation of *pilA* suppressor mutant

DK10407 (Δ *pilA*) (47) was mutagenized with the *mariner* transposon *magellan4* (39). This transposon contains the R6K γ *E. coli* origin of replication and *nptII*, which confers kanamycin resistance (Kan^R) (39). pMycoMar, a plasmid carrying the transposon, was transformed into DK10407 by electroporation (24). Transformants were plated on CYE plates with kanamycin and Congo Red (CR) at 30 μ g/ml (11). Mutants that appear red, potentially EPS⁺, on the CR plates were further examined using CYE plates with Calcofluor White (CW) at 50 μ g/ml (38).

To clone the transposon insertions, genomic DNA of a transposon mutant was isolated and digested with *SacII*, which does not cut within the *magellan4* transposon. The digestion mix was then used for ligation and subsequent transformation of the *E. coli* strain DH5 α λ pir by selection on kanamycin. Plasmids from the transformants were sequenced using MarR1 and MarL1 (51) and the sequence flanking the transposon was compared with the genome sequence

Table 2-1: Strains and Plasmids

Strains/ Plasmids	Relevant Genotype/ Description	Reference/ Source
Strains		
BY802	<i>ΔpilA::Tet</i> CRISPR3*	This Study
BY850	CRISPR3*	This Study
DK1622	wild-type	(23)
DK10407	<i>ΔpilA::Tet</i>	(47)
DK10416	<i>ΔpilB</i>	(49)
YZ601	<i>ΔdifA</i>	(50)
YZ603	<i>ΔdifE</i>	(6)
YZ811	<i>ΔsglK</i>	(29)
YZ1200	<i>ΔpilA::Tet ΔCRISPR3</i>	This Study
YZ1201	<i>ΔpilA::Tet ΔRAMB</i>	This Study
YZ1202	<i>ΔCRISPR3</i>	This Study
YZ1203	<i>ΔRAMB</i>	This Study
YZ1261	<i>ΔpilA::Tet ΔRAMB</i> CRISPR3*	This Study
YZ1262	<i>ΔRAMB</i> CRISPR3*	This Study
YZ1263	<i>ΔMXAN</i>	This Study
YZ1267	<i>ΔpilA::Tet ΔMXAN</i>	This Study
YZ1270	<i>ΔpilA::Tet ΔCRISPR3 att::pXY105</i>	This Study
YZ1273	<i>ΔpilA::Tet ΔMXANCRISPR3*</i>	This Study
YZ1279	<i>ΔpilB</i> CRISPR3*	This Study
YZ1280	<i>ΔsglK</i> CRISPR3*	This Study
YZ1281	<i>ΔdifA</i> CRISPR3*	This Study
YZ1282	<i>ΔdifE</i> CRISPR3*	This Study
Plasmids		
pMY7	Cloning vector, Kan ^R , <i>galK</i>	Unpublished
pMycoMar	<i>magellan4</i> mutagenesis vector	(39)
pRW100	CRISPR3 deletion in pMY7	This Study
pRW107	MXAN deletion in pMY7	This Study
pRW112	RAMB deletion in pMY7	This Study
pWB425	Expression vector, Kan ^R , intP (Mx8 attP)	(5)
pXY105	CRISPR3 in pWB425	This Study
pZErO-2	Cloning vector, Kan ^R	Invitrogen

of *M. xanthus* DK1622 (16) to identify the insertion site.

Construction of plasmids

Three plasmids were constructed for the deletion of *M. xanthus* genes, CRISPR3, MXAN_7275-7270, and RAMP genes; *cmr1*, *cas10*, *cmr3*, *cmr4*, *cmr5*, *cmr6*, and *cas6*. Primers were designed to amplify regions upstream and downstream of the genes for deletion. The fragments were then joined by overlapping PCR to generate the deletion allele and then cloned into pMY7 using *HindIII* and *XbaI*. pMY7 contains *nptII* and an *E. coli galK* gene (unpublished). The primers for the deletion of the entire CRISPR3 array were Δ CRISPR3_F1 (GCATAAGCTTGCGCTGTTACCGGAGGT) and Δ CRISPR3_R1 (TTCGCTCATGGAGGCCCTGTAGCCCATCTGAATCTCCAG) for the upstream fragment and Δ CRISPR3_F2 (ACAGGGCCTCCATGAGCGAA) and Δ CRISPR3_R2 (TAGCTCTAGAAGGCACGGAGCAACTCGGA) for the downstream fragment. The primers for the deletion of the ORFs MXAN_7275-7270 were Δ MXAN_F1 (GACCAAGCTTTCAACATATCGCCGTCGA) and Δ MXAN_R1 (GTATTCGTTCCAGAACCGGG) for the upstream fragment and Δ MXAN_F2 (CCCGGTTCTGGAACGAATACGAGAAGCCTACGGCGAGTTC) and Δ MXAN_R2 (GCTCTAGATGTTGGTTGCGTGCATGG) for the downstream fragment. The primers for the deletion of the RAMP genes *cmr1*, *cas10*, *cmr3*, *cmr4*, *cmr5*, *cmr6*, and *cas6* were Δ RAMP_F1 (GATTACAAGCTTCTCGCTCCTGGTGCGGAT) and Δ RAMP_R1 (CGGAGCGAGTGGTTGCCGAA) for the upstream fragment and Δ RAMP_F2 (ACAGGGCCTCCATGAGCGAA) and Δ RAMP_R2 (CGTCCTCTCTAGATTCCAAACCCCATGGAA) for the downstream fragment. The resulting

plasmids with Δ CRISPR3, Δ MXAN_7275-7270, and Δ RAMP alleles were pRW100, pRW107, and pRW112, respectively.

pXY105 was constructed to express CRISPR3 from the promoter of the Kan^R gene, *PnptII*. Expression constructs were created by amplifying CRISPR3 using CRISPR3_F (GCATAAGCTTGCGCTGTTCACCGGAGGT) and CRISPR3_R (AGGTCTAGATGGCCTCGCAGCTTCCAGAT) and digesting the PCR product with *HindIII* and *XbaI*. The CRISPR3 fragment was then cloned into pWB425 at the same restriction sites (5), resulting in pXY105. pWB425 contains *nptII*, a Mx8 phage attachment site and an *E. coli* origin of replication.

Construction of *M. xanthus* mutants

pRW100, pRW107, and pRW112 were used to construct Δ CRISPR3, Δ MXAN_7275-7270, and Δ RAMP mutants, respectively. These plasmids were transformed into *M. xanthus* (24) and used as a two-step homologous gene replacement method using Kan^R and *galK* as positive-negative selection (44). To construct Δ CRISPR3 strains, pRW100 was used to delete CRISPR3 from DK1622 (wild-type) and DK10407 (Δ *pilA*) to construct YZ1202 (Δ CRISPR3) and YZ1200 (Δ *pilA* Δ CRISPR3), respectively. To construct Δ MXAN_7275-7270 strains, pRW107 was used to delete Δ MXAN_7275-7270 from DK1622 and DK10407, to construct YZ1263 (Δ MXAN) and YZ1267 (Δ *pilA* Δ MXAN), respectively. To construct Δ RAMP strains, pRW112 was used to delete Δ RAMP from DK1622 and DK10407, to construct YZ1203 (Δ RAMP) and YZ1201 (Δ *pilA* Δ RAMP), respectively. Genomic DNA was isolated from Δ *pilA* suppressor mutant, BY802, and was transformed into DK1622, YZ1267, YZ1201, YZ1203, DK10416 (Δ *pilB*) (49), YZ601 (Δ *difA*) (50), YZ603 (Δ *difE*) (6), and YZ811 (Δ *sglK*) (29), to construct the following strains; BY850 (CRISPR3*), YZ1273 (Δ *pilA* Δ MXAN CRISPR3*), YZ1261 (Δ *pilA* Δ RAMP),

YZ1262 (Δ RAMP CRISPR3*), YZ1279 (Δ *pilB* CRISPR3*), YZ1280 (Δ *sglK* CRISPR3*), YZ1281 (Δ *difA* CRISPR3*), and YZ1282 (Δ *difE* CRISPR3*), respectively. To construct the CRISPR3 expression strain, pXY105 was used to transform YZ1200 (Δ *pilA* Δ CRISPR3), to construct YZ1270 (Δ *pilA* Δ CRISPR3 att::pXY105).

Examination of EPS production and fruiting body development

EPS production and fruiting body development were examined on CYE CW plates and Clone fruiting (CF) plates (10 mM MOPS, pH 7.6, 1 mM KH₂PO₄, 8 mM MgSO₄, 0.02% (NH₄)₂SO₄, 0.2% citrate, 0.2% pyruvate, and 150 mg/liter Casitone), respectively, as previously described. Briefly, an overnight culture was used to prepare a new culture at OD₆₀₀ 0.04. Cultures were allowed to incubate until a final concentration of 5x10⁸ cells/ml. Cells were harvested and re-suspended in CYE to a final concentration of 5x10⁹ cells/ml for EPS assays and in MOPS to a final concentration of 2.5x10⁹ cells/ml for fruiting body development. Five microliters of the cell suspension was spotted on CYE CW plates for EPS assays and on CF plates for fruiting body development and allowed to incubate for five days. After five days of incubation plates were documented under UV illumination at 365 nm for EPS assays. EPS⁺ colonies fluoresce under UV light while EPS⁻ colonies do not. Fruiting body development plates were documented using a Moticam 1300 at a total magnification of 12X.

Examination of CRISPR3 expression by Reverse Transcription Polymerase Chain Reaction (RT-PCR)

To perform RT-PCR, overnight cultures in CYE were used to prepare new cultures at OD₆₀₀ 0.15 and incubated for 20 hours. Cells were harvested and were re-suspended in 100 μ l CYE to a final concentration of 5x10⁸ cells/ml and spread on a 1.0% CYE plate. Plates were allowed to incubate for four days. Cells were then scraped off each plate and re-suspended in 5.0

ml of 10 mM MOPS [pH 7.6]. Five plates were used for each strain and combined to a total volume of 25 ml. The 25 mls were aliquoted out into 1.5 ml fractions and harvested. Using TriSure RNA isolation kit (Bioline), a phenol-chloroform based RNA isolation method, total RNA was isolated from one fraction and re-suspended in 100 μ l of RNase-free water. Total RNA was treated with DNaseI (Promega) to digest any contaminating genomic DNA, and further purified using TriSure RNA isolation kit, to remove DNaseI and digested nucleotides. Treated RNA was re-suspended in 25 μ l of RNase-free water. One microgram of total RNA was used for each RT-PCR. A two-step RT-PCR was performed using M-MLV Reverse Transcriptase (Promega) for the Reverse Transcription (RT) reaction and Taq DNA polymerase (New England Biolabs) for PCR. Two pairs of primers were used to examine the regions upstream and downstream of the CRISPR3*. Primers CRISPR3_UF (TGGGAGATTCAGATGGGCT) and CRISPR3_UR (TGCTCGTCGTCACGATGCTGGA) were used to examine the upstream region and CRISPR3_DF (CGTCTGGCCTTCGCCGTCGT) and CRISPR3_DR (TGGACGGGAGAAGACGTTCA) for the downstream region. The CRISPR3_UR and CRISPR3_DR primers were used in the RT reaction. The RT was optimized and performed at 44°C for one hour for both primers. The RT reaction was then heated at 85°C for 20 minutes to heat inactivate the M-MLV Reverse Transcriptase (Promega) prior to the set up of the PCR reaction. Two microliters of the RT reaction was used to set up the PCR reaction. The PCR reaction was performed in accordance with the Taq DNA polymerase (New England Biolabs) protocol using 68°C for upstream primers and 70°C for downstream primers for the primer annealing step. PCR products were resolved on a 1.4% agarose gel. After electrophoresis for 45 minutes at 120V, the gel was stained for 1 hour in a buffer solution of

ethidium bromide at 0.5 µg/ml. The gel was then visualized and documented under UV illumination. ImageJ software was used to quantify the intensities of the bands (40).

To determine the sequence of the RT-PCR products, the bands were excised from the agarose gel and a DNA extraction procedure was performed using ISOLATE kit (Bioline). Purified PCR products were then cloned into pZErO-2 (Invitrogen) at *EcoRV* restriction site. Plasmids were sequenced using the SP6 priming site and compared with the known sequence of CRISPR3.

Results

Isolation of a *pilA* suppressor in EPS production

Myxococcus xanthus pilA mutants, which do not assemble T4P due to the lack of PilA or pilin, are EPS⁻ because T4P is required for EPS production. To better understand EPS regulation in *M. xanthus*, a genetic screen was carried out to isolate suppressors of *pilA* in EPS production. Briefly, the *pilA* mutant (DK10407) was mutagenized with a *mariner* transposon and the transposon mutants were plated on agar plates supplemented with the dye Congo Red. EPS⁻ colonies appear yellowish-orange while EPS⁺ ones are red due to the binding of the dye to *M. xanthus* EPS. Using this method, two *pilA* suppressor mutants, BY801 and BY802, were isolated. The preceding paper reports the studies of BY801 and we report here the studies of BY802. The EPS⁺ phenotype of BY802 was confirmed by the binding of the fluorescent dye Calcofluor White (CW) as an alternative EPS assay. As shown in Figure 2-1A, the wild-type (DK1622) and BY802 fluoresced under UV illumination, while the *pilA* mutant did not. To verify that the EPS⁺ phenotype was linked to a single transposon insertion, the genomic DNA of BY802 was isolated and used to transform the *pilA* mutant. 16 transformants were examined and all were found to be EPS⁺ by dye binding assays (data not shown). These results show that BY802 harbors a single transposon insertion responsible for the restoration of EPS to the *pilA* mutant. This insertion is designated as CRISPR3* here after (see later section). It should be noted that the transposon insertion led to the suppression of EPS but not S motility. Consequently, the colony morphology of BY802 differs from that of the wild-type despite the suppression of the EPS defect.

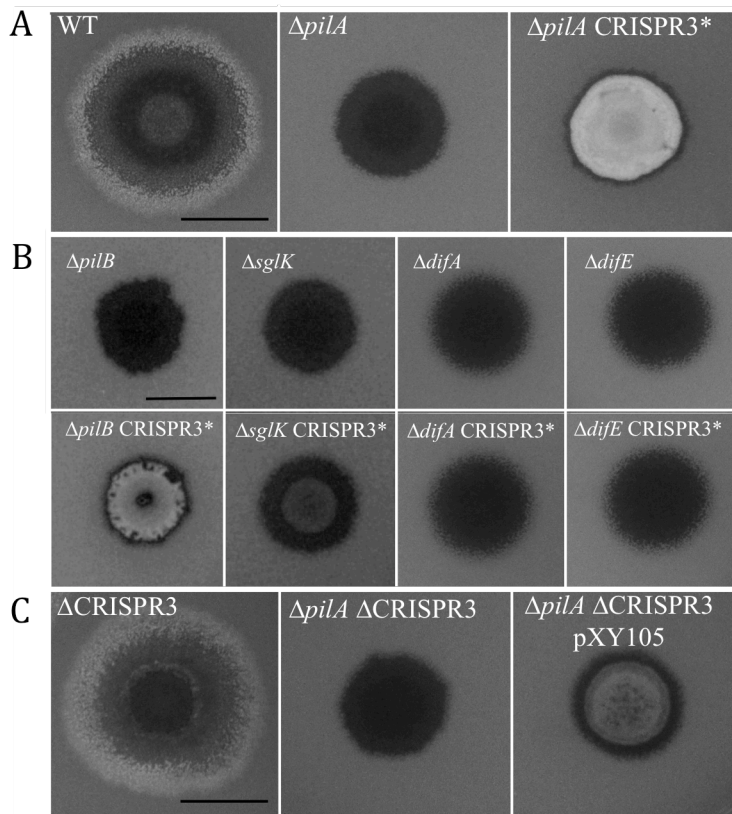


Figure 2-1: CRISPR3* is a gain-of-function mutation that suppresses $\Delta pilA$, $\Delta pilB$ and $\Delta sglK$ in EPS production

Five microliters of cell suspension of various *M. xanthus* strains at 5×10^9 cells/ml were spotted on CYE CW plates. Photographs were taken under UV illumination after five days of incubation at 32°C using a Nikon D7000. **A.** CRISPR3* suppresses a *pilA* deletion. Strains: WT (DK1622), $\Delta pilA$ (DK10407), and $\Delta pilA$ CRISPR3* (BY802). **B.** CRISPR3* suppresses *pilB* and *sglK*, but not *difA* or *difE* mutations. Strains: $\Delta pilB$ (DK10416), $\Delta pilB$ CRISPR3* (YZ1279), $\Delta sglK$ (YZ811), $\Delta sglK$ CRISPR3* (YZ1280), $\Delta difA$ (YZ601), $\Delta difA$ CRISPR3* (YZ1281), $\Delta difE$ (YZ603), and $\Delta difE$ CRISPR3* (YZ1282). **C.** Expression of CRISPR3 suppresses $\Delta pilA$. Strains: Δ CRISPR3 (YZ1202), $\Delta pilA$ Δ CRISPR3 (YZ1200), and $\Delta pilA$ Δ CRISPR3 pXY105 (YZ1270). The scale bars in all three panels represent 1 cm.

CRISPR3* suppressed $\Delta pilB$ and $\Delta sglK$, but not $\Delta difA$ or $\Delta difE$

Many genes besides *pilA* are known to play roles in EPS regulation in *M. xanthus*. These include other *pil* genes, *sglK* and *dif* genes. To examine the genetic relation of the CRISPR3* with these genes, genomic DNA of BY802 was used to transform $\Delta pilB$, $\Delta sglK$, $\Delta difA$, and $\Delta difE$ mutant strains. The resulting double mutants were examined on CW plates. As shown in Figure 2-1B, the $\Delta pilB$ CRISPR3* and $\Delta sglK$ CRISPR3* strains fluoresced while $\Delta difA$ CRISPR3* and $\Delta difE$ CRISPR3* did not. These results demonstrate that the CRISPR3* was able to restore EPS production to $\Delta pilB$ and $\Delta sglK$, but not $\Delta difA$ and $\Delta difE$ mutants. These results indicate the CRISPR3* functions downstream of *pilB* and *sglK* but upstream of *difA* and *difE* in the EPS regulatory pathway.

CRISPR3* is a transposon insertion in CRISPR3

The site of the transposon insertion in BY802 was identified by cloning and sequencing. Sequence comparisons with the *M. xanthus* genome revealed that the *mariner* transposon inserted into CRISPR3, one of the three CRISPR regions on the *M. xanthus* chromosome (Figure 2-2). The CRISPR3 array contains 53 nearly identical repeats that are 36 base pairs long and 52 variable spacers, between 33 and 40 base pairs long. The transposon inserted into its 13th spacer (3SP13), which is 38 base pairs long. The CRISPR3* transposon inserted after a TA dinucleotide at the 2nd and 3rd position in 3SP13. At the 5' end of the CRISPR array is a typical A/T rich leader sequence, which is proposed to contain the promoter for this region. Further upstream of the CRISPR3 array are seven RAMP genes: *cmr1*, *cas10*, *cmr3*, *cmr4*, *cmr5*, *cmr6*, and *cas6*, respectively. The presence of *cas10* classifies the *M. xanthus* CRISPR3 system as Type III, and *cmr5* further defines it as Type III-B. In addition, there are six predicted open-reading frames (ORFs), MXAN_7275-7270, downstream of the CRISPR3 array. These ORFs

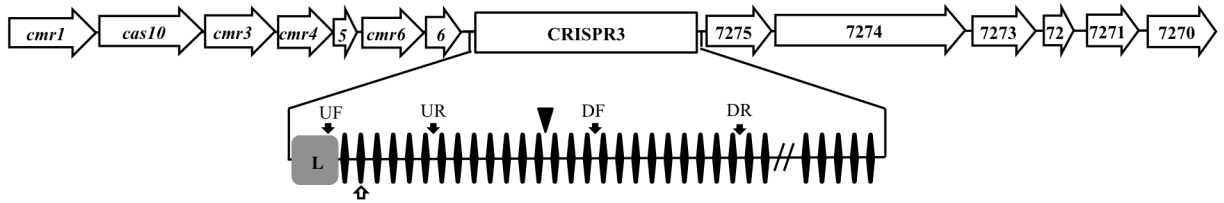


Figure 2-2: Structure of the *M. xanthus* CRISPR3 locus

A region of 20.1 kb at the CRISPR3 locus is shown on the upper-part of the figure with elements drawn to scale. Open rectangle represents CRISPR3. Open arrows represent the coding regions of the ORFs. There are seven RAMP genes upstream of CRISPR3: *cmr1*, *cas10*, *cmr3*, *cmr4*, *cmr5* (indicated by the number 5), *cmr6*, and *cas6* (indicated by the number 6). There are 6 hypothetical ORFs MXAN_7275-7270 downstream with MXAN_7272 represented by the number 72. The lower part of the figure represents a close-up of CRISPR3, which contains 53 repeats and 52 spacers after its leader sequence (L). pXY105 contains the entire CRISPR3 region including 746 bp upstream of the first repeat and 1,542 bp downstream of the last repeat. Repeats are represented by diamonds and spacers by a line in between. Not all 53 repeats and 52 spacers are represented with the two slashes indicating omissions of repeats 28 through 49. The inverted triangle represents the CRISPR3* transposon insertion in the 13th spacer. The vertical black arrows indicate where the primers used for RT-PCR hybridize. These primers are CRISPR3_UF (UF), CRISPR3_UR (UR), CRISPR3_DF (DF) and CRISPR3_DR (DR). The open arrow indicates where the CRISPR3_UR (UR) primer had hybridized during RT-PCR to produce the smaller product.

read in the same direction as the RAMP genes and CRISPR3.

CRISPR3* is likely a gain-of-function mutation

We sought to determine the genetic nature of the 3SP13 transposon insertion identified in BY802. Transposon insertions tend to result in loss-of-function (LOF) mutations more than change- or gain-of-function (GOF) mutations. The 3SP13 transposon insertion was surprising as we had expected mutations in or near protein-encoding regions. Nevertheless, this mutation should have resulted in either a LOF or a GOF mutation. We first constructed a mutation deleting all 52 spacers and 53 repeats of CRISPR3 in a $\Delta pilA$ background and this double mutant ($\Delta pilA \Delta CRISPR3$) was examined for EPS production on CW plates. As shown in Figure 2-1C, this mutant did not fluoresce, indicating the lack of EPS production. The deletion of CRISPR3 is therefore unable to suppress $\Delta pilA$. In addition, the same deletion in the wild-type background fluoresced on CW plates, indicating that CRISPR3 alone does not affect EPS production. These observations suggest that the original 3SP13 insertion in BY802 is unlikely a LOF mutation as CRISPR3 deletion failed to suppress $\Delta pilA$ or impact EPS production on its own.

We next considered the possibility that the 3SP13 insertion may have resulted in a GOF mutation. We cloned CRISPR3 into an expression vector, which drives the transcription of CRISPR3 from a kanamycin phosphotransferase promoter, *PnptII* (3). The expression plasmid (pXY105), which contains the entire CRISPR3 array and an Mx8 phage attachment site, was transformed into a $\Delta pilA \Delta CRISPR3$ strain. As shown in Figure 2-1C, the $\Delta pilA \Delta CRISPR3$ with pXY105 fluoresced on the CW plate, indicating that the expression of CRISPR3 is sufficient to suppress $\Delta pilA$. As a control, the same fragment in the opposite orientation in the expression vector was found not to cause suppression (data not shown). Based on these results, it was concluded that the *mariner* transposon in CRISPR3 is likely a GOF instead of a LOF

mutation. The *mariner* transposon insertion in BY802 is therefore designated CRISPR3* to indicate the *mariner* transposon is a GOF mutation.

RAMP genes but not the ORFs downstream are required for CRISPR3* to suppress $\Delta pilA$

Genetic elements with related functions tend to cluster in prokaryotes. To determine if the six ORFs, MXAN_7275-7270, downstream of CRISPR3 (Figure 2-2) are related to CRISPR3 function, they were deleted in the wild-type, the $\Delta pilA$ and the $\Delta pilA$ CRISPR3* backgrounds. As shown in Figure 2-3, the deletion of these genes did not alter the fluorescence of the $\Delta pilA$ CRISPR3* mutant or that of the wild-type and *pilA* mutant on CW plates. These results indicate that MXAN_7275-7270 are not required for CRISPR3* to suppress $\Delta pilA$ and their deletion had no effect on EPS production in the wild-type and the $\Delta pilA$ backgrounds.

Next, the seven RAMP genes upstream of CRISPR3 were examined. RAMP genes were previously demonstrated to be required for the function of CRISPR in other Type III-B CRISPR systems (35, 37, 48). To determine if the RAMP genes are required for CRISPR3 to function, a deletion of all seven RAMP genes (Figure 2-2) was constructed and the resulting mutants were examined for EPS production on CW plates. When the RAMP genes were deleted in the $\Delta pilA$ CRISPR3* background, the mutant was observed not to fluoresce on CW plates (Figure 2-3). The EPS⁻ phenotype of the $\Delta pilA$ Δ RAMP CRISPR3* strain indicates that the RAMP genes are required for the suppression of *pilA* by CRISPR3*. The deletion of the RAMP genes in the wild-type and the $\Delta pilA$ backgrounds did not affect EPS production, with the resulting strains behaving the same as the parent strains on CW plates (Figure 2-3). These results demonstrate that the RAMP genes are required for CRISPR3* to suppress $\Delta pilA$ in EPS production.

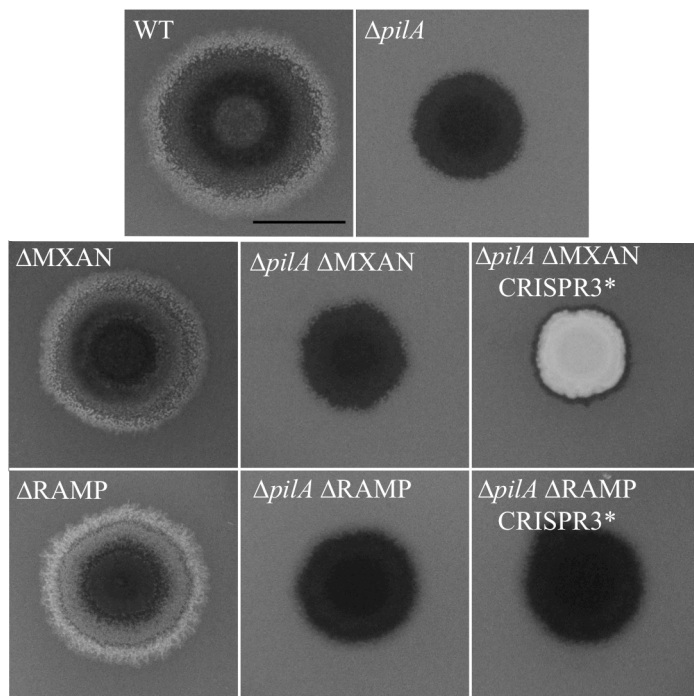


Figure 2-3: RAMP genes but not MXAN_7275-7270 are required for CRISPR3* to suppress $\Delta pilA$

Experiments were performed as in Figure 2-1. Strains: WT (DK1622), $\Delta pilA$ (DK10407), $\Delta MXAN$ (YZ1263), $\Delta pilA \Delta MXAN$ (YZ1267), $\Delta pilA \Delta MXAN$ CRISPR3* (YZ1273), $\Delta RAMP$ (YZ1203), $\Delta pilA \Delta RAMP$ (YZ1201), and $\Delta pilA \Delta RAMP$ CRISPR3* (YZ1261). $\Delta RAMP$ and $\Delta MXAN$ represent the complete deletion of *cmr1*, *cas10*, *cmr3*, *cmr4*, *cmr5*, *cmr6*, and *cas6* and MXAN_7275-7270, respectively. The scale bar represents 1 cm.

CRISPR3* affects fruiting body development in a RAMP-dependent manner

Due to EPS production being implicated in fruiting body development in *M. xanthus* (8) and the involvement of CRISPR3 in EPS regulation, the effect of the CRISPR3 mutation on development was examined. Both the wild-type and $\Delta pilA$ strains developed fruiting bodies as expected (Figure 2-4). $\Delta CRISPR3$ mutation had no impact on development in either of these two backgrounds (Figure 2-4). Surprisingly, the CRISPR3* mutation, either in the wild-type or the $\Delta pilA$ background, led to a severe defect in fruiting body formation (Figure 2-4) despite its ability to suppress EPS⁻ phenotype of $\Delta pilA$ (Figure 2-1A). The CRISPR3* GOF mutation is therefore apparently detrimental to development. Similarly, when pXY105 was introduced into the $\Delta pilA \Delta CRISPR3$ double mutant background, it abolished fruiting body development (Figure 2-4). When the RAMP genes were deleted from CRISPR3* and $\Delta pilA$ CRISPR3* strains, fruiting body development was restored in both strains (Figure 2-4). In other words, the CRISPR3* mutation is dependent on the RAMP proteins in both development (Figure 2-4) and EPS production (Figure 2-3). These observations support the conclusion that the GOF mutation CRISPR3* requires the function of the associated RAMP genes to execute its function in both fruiting body development and EPS regulation.

CRISPR3* leads to a possible increase in processing of pre-CRISPR3 RNA

How does the CRISPR3* mutation influence both EPS production and fruiting body development? One possibility is that the CRISPR3* mutation increases the transcription of CRISPR3, leading to increased production of pre-CRISPR3 RNA (pre-crRNA) and the resulting mature CRISPR RNA (crRNA) from CRISPR3. The CRISPR3 crRNA may affect both EPS production and development by regulating certain genes with function in these two processes. This possibility is consistent with the orientation of the CRISPR3* transposon insertion as the

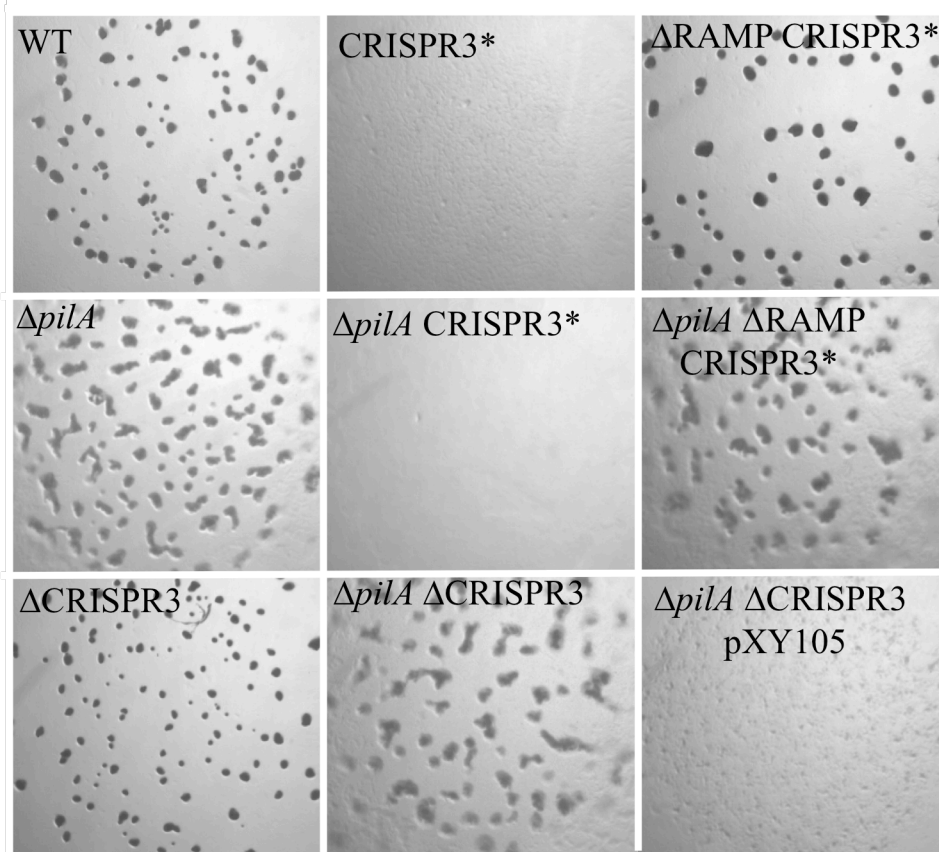


Figure 2-4: Detrimental effect of CRISPR3* on development and its dependence on RAMP genes

Five microliters of cell suspension at 2.5×10^9 cells/ml of indicated strains were plated on CF media. Photographs were taken after five days of incubation. Strains: WT (DK1622), CRISPR3* (BY850), Δ RAMP CRISPR3* (YZ1262), Δ *pilA* (DK10407), Δ *pilA* CRISPR3* (BY802), Δ *pilA* Δ RAMP CRISPR3* (YZ1261), Δ CRISPR3 (YZ1202), Δ *pilA* Δ CRISPR3 (YZ1200), Δ *pilA* Δ CRISPR3 pXY105 (YZ1270).

promoter for the *nptII* gene (*PnptII*) in the transposon reads in the same direction as the predicted CRISPR3 transcript. It is possible that there is read-through from the *PnptII* into the CRISPR3 region that is downstream of the CRISPR3* insertion. The fact that pXY105, which expresses CRISPR3 from the same promoter, restored EPS production to the $\Delta pilA$ Δ CRISPR3 strain is consistent with this possibility. Total RNA was isolated and RT-PCR was used to examine the transcripts from CRISPR3 in various strains (Figure 2-5). Two pairs of primers were used in RT-PCR (Figure 2-2). The first pair, CRISPR3_UF and CRISPR3_UR, target a region spanning from the leader sequence to the 6th spacer upstream of the CRISPR3* insertion (Figures 2-2 and 2-6). The second pair, CRISPR3_DF and CRISPR3_DR, is complementary to spacers 16 and 25 to amplify a region downstream of the CRISPR3* insertion (Figure 2-2). Surprisingly, no obvious differences were observed when the downstream primers were used in RT-PCR (data not shown) but there were obvious differences when the upstream primer pair was used (Figure 2-5). There was one band about 450 base pairs (bps) in strains without CRISPR3* as anticipated. However, in the two strains with CRISPR3* ($\Delta pilA$ CRISPR3* and $\Delta pilA$ Δ RAMP CRISPR3*), besides this 450 bp band, a smaller band around 350 bps appeared. Additionally, using ImageJ software, the intensity of the 450 bp band in the other strains were about 25% brighter in comparison with the CRISPR3* strains. These results suggested that rather than an increase in expression of the CRISPR3 region downstream of the transposon insertion, an increase in processing of CRISPR3 RNA upstream of CRISPR3* could be responsible for the effect of CRISPR3* on EPS levels and fruiting body development.

Cloning and sequencing were performed to investigate the origins of these two RT-PCR products in the CRISPR3* strains. The two bands from the $\Delta pilA$ CRISPR3* and the $\Delta pilA$ Δ RAMP CRISPR3* strains as well as the one band from the wild-type were cloned and

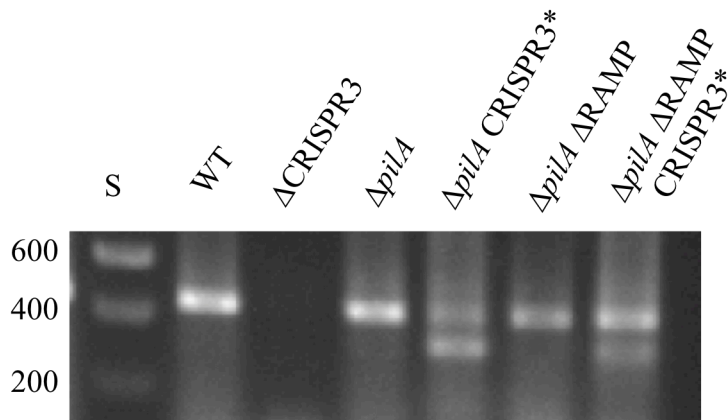


Figure 2-5: CRISPR3* may affect processing of CRISPR3 RNA transcripts upstream of the transposon insertion

RT-PCR was performed using CRISPR3_UF and CRISPR3_UR primers (Figure 2-2) as described in Materials and Methods. RT-PCR products were resolved on a 1.4% agarose gel by electrophoresis, stained with ethidium bromide and documented under UV illumination. Strains: WT (DK1622), Δ CRISPR3 (YZ1202) Δ *pilA* (DK10407), Δ *pilA* Δ RAMP (YZ1201), Δ *pilA* CRISPR3* (BY802) and Δ *pilA* Δ RAMP CRISPR3* (YZ1261). Δ CRISPR3 (YZ1202) is included here as a negative control. The DNA standard is labeled as S and the corresponding sizes are indicated in base pairs on the left of the gel.

sequenced. The upper bands from all three strains were found to be identical; they were 441 bps long as anticipated for the two upstream primers (Figures 2-2). The lower bands from $\Delta pilA$ CRISPR3* and $\Delta pilA \Delta RAMP$ CRISPR3* strains were found to be identical and they were 351 bps in length. This band was amplified by the CRISPR3_UR primer alone (Figure 2-2). Serendipitously, CRISPR3_UR, which was designed to be complementary to the 6th spacer of CRISPR3, turned out to be complementary with the CRISPR3 repeat in 15 out of 22 positions (Figure 2-6). The 5' end of the lower band was identical to the CRISPR3_UR primer, which annealed with the second repeat of CRISPR3 and the 3' end at the 6th spacer as expected, this resulted in the 351 bps fragment in the two CRISPR3* strains. Since this smaller product was seen only in the two strains with CRISPR3*, this suggests that the CRISPR3* mutation led to a decrease in CRISPR3 RNA with an intact leader sequence where CRISPR3_UF anneals and a simultaneous increase in RNA transcripts without the leader sequence (Figure 2-2). It may be concluded that the appearance of this shorter fragment in CRISPR3* strains in RT-PCR indicates that CRISPR3* results in increased processing of CRISPR3 RNA upstream of the insertion, instead of altering the expression of CRISPR3 downstream as we had suspected.

Discussion

CRISPR has been demonstrated to function as an adaptive immune system in prokaryotes (4). The mechanism by which CRISPR functions as an immune system is proposed to contain three stages, namely, Adaptation, CRISPR Expression, and Interference (45). Adaptation involves the recognition of invading elements and the integration of novel spacers originating from the foreign element into the CRISPR array (12). CRISPR Expression involves the expression of the CRISPR array as a long transcript or pre-crRNA and its processing into the crRNA (43). In the Interference stage the crRNAs are used as guides to target and cleave the foreign DNA or RNA that enters the cell (31). Together these three stages mediate CRISPR systems ability to function as an adaptive immune system.

Besides its ability to function in immunity, a CRISPR system may also regulate normal cellular functions in bacteria. Of the organisms possessing CRISPRs, 18% were found to have spacers originating from their genomes (10, 42), suggesting that certain CRISPR systems may target chromosomal genes as well. Studies of *Pseudomonas aeruginosa* provided more direct evidence that CRISPR systems may regulate chromosomal genes. A wild-type *P. aeruginosa* strain produces biofilm and displays swarming motility. However, its lysogen with the DMS3 prophage loses both biofilm and swarming motility (52). Disruption of the CRISPR2 array or five of the six *cas* genes restored biofilm formation as well as swarming motility in the lysogen (52). In addition, *devR* and *devS*, both known *cas* genes now, which are associated with CRISPR2 in *M. xanthus*, were shown to be required for fruiting body development (46). These observations provide evidence that CRISPR systems can regulate genes involved in cellular processes other than immunity in *P. aeruginosa* and *M. xanthus*.

This study provides strong evidence that a CRISPR system can regulate EPS production in *M. xanthus*. A CRISPR3 transposon insertion, CRISPR3*, restored EPS production to a *pilA* mutant in *M. xanthus* (Figure 2-1). In addition, CRISPR3* was found to suppress *pilB* and *sglK* in EPS production (Figure 2-1). CRISPR3* is likely a GOF mutation because a CRISPR3 deletion failed to suppress *pilA* in EPS production and the expression of the CRISPR3 array from a heterologous promoter resulted in *pilA* suppression (Figure 2-1). Moreover the CRISPR3* mutation itself was also found to have a detrimental effect on fruiting body development in both the *pilA* mutant and the wild-type (Figure 2-4). Our findings here clearly indicate that CRISPR3 is involved in the regulation of EPS production and fruiting body development in *M. xanthus*, both of which are processes not related to bacterial immunity directly.

We propose a molecular model to explain how CRISPR3 may regulate EPS production and fruiting body development in *M. xanthus*. We propose that CRISPR3, like CRISPR arrays in other organisms, can be transcribed as a long pre-crRNA. crRNAs are then produced from pre-crRNA processing. One or more CRISPR3 crRNAs can target mRNAs from genes involved in the regulation of EPS production and fruiting body development, possibly by cleavage or degradation. While the RAMP genes associated with CRISPR3 may not be strictly required for the initial pre-crRNA processing (Figure 2-5), one or more of the CRISPR3-RAMP genes are probably indispensable for regulation of the targeted gene(s) with a role in EPS production and development. Because EPS and fruiting are not directly related to immunity, the target genes here can be inferred to be *M. xanthus* chromosomal genes critical for these normal cellular processes.

This model is consistent with our experimental data presented here. The deletion of CRISPR3 in *M. xanthus* had no obvious phenotype (Figure 2-1), suggesting that CRISPR3 pre-

crRNA is not transcribed and/or processed at sufficient levels to affect EPS production in a wild-type background under our experimental conditions. Our data suggest that either increased transcription or processing is sufficient to affect both processes. On one hand, the expression of CRISPR3 from a heterologous promoter affected both EPS production and fruiting body development (Figures 2-1 & 2-4). On the other hand, CRISPR3*, which affected EPS production and fruiting, appeared to alter the processing of the CRISPR3 RNA but not its transcription appreciably. The deletion of RAMP genes from the CRISPR3* background did not appear to eliminate the processing of CRISPR3 RNA as indicated by the RT-PCR results (Figures 2-5). However, the RAMP genes are required for the CRISPR3* mutation to suppress *pilA* and to affect fruiting body development (Figure 2-3 and 2-4), suggesting one or more of the RAMP proteins are required for the CRISPR3 crRNA to properly target genes in *M. xanthus*. In addition, studies of other CRISPR systems support the idea that *M. xanthus* CRISPR3 may target RNA. CRISPR systems can be classified into three major types. Type I, II, and III, with each having multiple subtypes. Both Type I and Type II systems have been demonstrated to target invading DNA (15, 32). Type III has two subtypes, III-A and III-B. While Type III-A has been demonstrated to target DNA, Type III-B systems have been shown to target RNA (17, 18, 53). Because *M. xanthus* CRISPR3 is a Type III-B system, we propose in the above model that CRISPR3 crRNA targets the RNA from genes with a role in EPS production for degradation.

The lack of requirement for the RAMP genes for CRISPR3 RNA processing (Figure 2-5) was a surprise. *Pyrococcus furiosus* Cas6, a RAMP protein and a riboendonuclease, cuts the pre-crRNA in the repeat 8 nucleotides upstream of the spacer (9, 18). This cleavage product, a processing intermediate, contains the spacer flanked by part of the repeat at both the 5' end and the 3' ends (9). The 3' end of this intermediate is believed to be further processed by other

RAMP proteins to generate the crRNA. Yet in the RAMP deletion, CRISPR3 pre-crRNA appeared to be processed (Figure 2-5). We suggest that CRISPR3 pre-crRNA may be processed by the Cas6 associated with the CRISPR2 system in *M. xanthus*. Sequence alignment indicates that Cas6 from the CRISPR2 system (MXAN_7265) is 66% identical to Cas6 in CRISPR3 (MXAN_7276) (Figure 2-6). The repeats of these two arrays are nearly identical with the exception of two nucleotides (Figure 2-6). MXAN_7265 may be able to process CRISPR3 pre-crRNA albeit at a reduced level, which explains the detection of the processed CRISPR3 crRNA by RT-PCR. The absence of other CRISPR3 RAMP genes may prevent further processing and/or targeting, which explains why CRISPR3* requires the RAMP genes to suppress *pilA* and to affect development and EPS production (Figures 2-3 & 2-4). Future studies may explore our model in more detail and other possible mechanisms for CRISPR systems to regulate chromosomal genes for normal cellular processes.

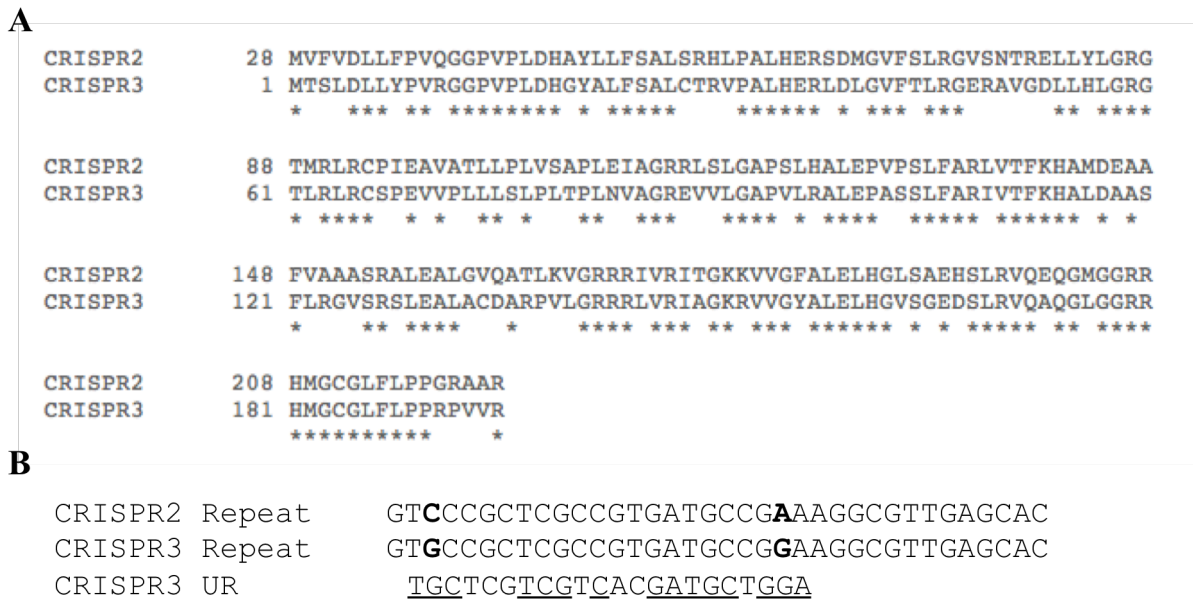


Figure 2-6: CRISPR2 and CRISPR3 Cas6 and repeat alignment

A. CRISPR2 and CRISPR3 Cas6 alignment. CRISPR2 Cas6 and CRISPR3 Cas6 are 66% identical. (*) indicates fully conserved residues. Sequence alignment was performed using SWISS-MODEL SIM- Alignment tool for protein sequences (21).

B. CRISPR2 and CRISPR3 repeat alignment. The repeat sequence for both CRISPR2 and CRISPR3 are displayed. The CRISPR3 UR primer is also aligned with the CRISPR3 repeat. The nucleotides in bold indicate mismatches between the CRISPR2 and CRISPR3 repeats. The underlined nucleotides in the CRISPR3 UR primer indicates matches with the CRISPR3 repeat.

Rational and Future Direction

M. xanthus is a Gram-negative non-pathogenic soil dwelling bacterium (13, 26). *M. xanthus* has proven to be a great organism to study due to the fact that it is easily maintained in a laboratory setting. *M. xanthus* can also be easily genetically modified to study the role genes play in *M. xanthus*. Since *M. xanthus* has these great traits it is a model organism for the study of development and Type IV pili (T4P).

In our lab we study *M. xanthus* T4P. T4P is a protein filament that facilitates the movement of *M. xanthus* cells (23, 30). There are other organisms that possess T4P that are extensively studied, including *P. aeruginosa* and *N. meningitidis* (1). The difficulty with working with these organisms is that they are pathogenic. On the other hand, *M. xanthus* is non-pathogenic making it a much better option to work with. *M. xanthus* also has better assays available to examine T4P functionality. *M. xanthus* T4P has proven to be highly similar to the T4P of *P. aeruginosa* and *N. meningitidis* making it possible to correlate the findings in *M. xanthus* to these other organisms (1).

The study of T4P in *M. xanthus* has led us to identify a *pilA* suppressor of EPS production, BY802 ($\Delta pilA$ CRISPR3*). This mutant was isolated and identified by Dr. Wesley Black. Prior to my entry into the lab some characterization of the mutant had occurred. A $\Delta pilA$ Δ CRISPR3 mutant was constructed and found to be unable to reproduce the *pilA* suppression phenotype, leading to the conclusion that CRISPR3* is not a loss-of-function mutation. The CRISPR3 over-expression plasmid, pXY105, had been constructed but had not yet been successfully screened in a $\Delta pilA$ Δ CRISPR3 background. Also, a $\Delta pilA$ Δ RAMP CRISPR3* mutant had been constructed. This mutant was shown to be EPS⁻, indicating that the RAMP genes are required for the *pilA* suppression phenotype. These results led to the early hypothesis

that one of the CRISPR3 spacers was responsible for the *pilA* suppression phenotype by targeting a gene in the EPS pathway. The mechanism by which this suppression had occurred was unclear.

Since my entering into the lab, we have determined that CRISPR3* is likely a gain-of-function mutation and that CRISPR3* is acting downstream of *sglK*, but upstream of *difA*, in the EPS regulatory pathway. We have also determined that not only does CRISPR3* effect EPS production, but that it has a detrimental effect on fruiting body development in a RAMP dependent manner. Based on our results we have proposed a molecular model. This model entails that one or more of the CRISPR3 spacers are responsible for the *pilA* suppression and the defect in fruiting body development. The CRISPR3 spacer is likely targeting the mRNA of gene(s) involved in the regulation of these cellular processes. CRISPR3 is able to exert its effect on these processes likely due to an increase in processing of the CRISPR3 pre-crRNA.

The next steps in this work entail further determining the mechanism by which CRISPR3 is able to regulate cellular processes. More specifically, we would like to address which spacer(s) is involved in the regulation. Also, we would like to determine the target(s) of the spacer(s) of interest. Mechanistically, we would like to know which RAMP proteins are involved in the regulation and in what stage of CRISPR3 function are they involved.

References Cited

1. **Ayers, M., P. L. Howell, and L. L. Burrows.** 2010. Architecture of the type II secretion and type IV pilus machineries. *Future microbiology* **5**:1203-1218.
2. **Barrangou, R., C. Fremaux, H. Deveau, M. Richards, P. Boyaval, S. Moineau, D. A. Romero, and P. Horvath.** 2007. CRISPR provides acquired resistance against viruses in prokaryotes. *Science* **315**:1709-1712.
3. **Beck, E., G. Ludwig, E. A. Auerswald, B. Reiss, and H. Schaller.** 1982. Nucleotide sequence and exact localization of the neomycin phosphotransferase gene from transposon Tn5. *Gene* **19**:327-336.
4. **Bhaya, D., M. Davison, and R. Barrangou.** 2011. CRISPR-Cas systems in bacteria and archaea: versatile small RNAs for adaptive defense and regulation. *Annual review of genetics* **45**:273-297.
5. **Black, W. P., Q. Xu, C. L. Cadieux, S.-J. Suh, W. Shi, and Z. Yang.** 2009. Isolation and characterization of a suppressor mutation that restores *Myxococcus xanthus* exopolysaccharide production. *Microbiology* **155**:3599-3610.
6. **Black, W. P., and Z. Yang.** 2004. *Myxococcus xanthus* chemotaxis homologs DifD and DifG negatively regulate fibril polysaccharide production. *Journal of Bacteriology* **186**:1001-1008.
7. **Bolotin, A., B. Quinquis, A. Sorokin, and S. D. Ehrlich.** 2005. Clustered regularly interspaced short palindrome repeats (CRISPRs) have spacers of extrachromosomal origin. *Microbiology* **151**:2551-2561.
8. **Bonner, P. J., W. P. Black, Z. Yang, and L. J. Shimkets.** 2006. FibA and PilA act cooperatively during fruiting body formation of *Myxococcus xanthus*. *Molecular Microbiology* **61**:1283-1293.
9. **Carte, J., R. Wang, H. Li, R. M. Terns, and M. P. Terns.** 2008. Cas6 is an endoribonuclease that generates guide RNAs for invader defense in prokaryotes. *Genes & Development* **22**:3489-3496.
10. **Cui, Y., Y. Li, O. Gorgé, M. E. Platonov, Y. Yan, Z. Guo, C. Pourcel, S. V. Dentovskaya, S. V. Balakhonov, X. Wang, Y. Song, A. P. Anisimov, G. Vergnaud, and R. Yang.** 2008. Insight into microevolution of *Yersinia pestis* by clustered regularly interspaced short palindromic repeats. *PLoS ONE* **3**:e2652.
11. **Dana, J. R., and L. J. Shimkets.** 1993. Regulation of cohesion-dependent cell interactions in *Myxococcus xanthus*. *Journal of Bacteriology* **175**:3636-3647.

12. **Deveau, H., R. Barrangou, J. E. Garneau, J. Labonte, C. Fremaux, P. Boyaval, D. A. Romero, P. Horvath, and S. Moineau.** 2008. Phage response to CRISPR-encoded resistance in *Streptococcus thermophilus*. *Journal of Bacteriology* **190**:1390-1400.
13. **Dworkin, M.** 1966. Biology of the myxobacteria. *Annual review of microbiology* **20**:75-106.
14. **Dworkin, M., and D. Kaiser.** 1993. *Myxobacteria II*. ASM Press, Washington, D.C.
15. **Garneau, J. E., M. E. Dupuis, M. Villion, D. A. Romero, R. Barrangou, P. Boyaval, C. Fremaux, P. Horvath, A. H. Magadan, and S. Moineau.** 2010. The CRISPR/Cas bacterial immune system cleaves bacteriophage and plasmid DNA. *Nature* **468**:67-71.
16. **Goldman, B. S., W. C. Nierman, D. Kaiser, S. C. Slater, A. S. Durkin, J. A. Eisen, C. M. Ronning, W. B. Barbazuk, M. Blanchard, C. Field, C. Halling, G. Hinkle, O. Iartchuk, H. S. Kim, C. Mackenzie, R. Madupu, N. Miller, A. Shvartsbeyn, S. A. Sullivan, M. Vaudin, R. Wiegand, and H. B. Kaplan.** 2006. Evolution of sensory complexity recorded in a myxobacterial genome. *Proceedings of the National Academy of Sciences U S A* **103**:15200-15205.
17. **Hale, C. R., S. Majumdar, J. Elmore, N. Pfister, M. Compton, S. Olson, A. M. Resch, C. V. Glover, 3rd, B. R. Graveley, R. M. Terns, and M. P. Terns.** 2012. Essential features and rational design of CRISPR RNAs that function with the Cas RAMP module complex to cleave RNAs. *Molecular cell* **45**:292-302.
18. **Hale, C. R., P. Zhao, S. Olson, M. O. Duff, B. R. Graveley, L. Wells, R. M. Terns, and M. P. Terns.** 2009. RNA-guided RNA cleavage by a CRISPR RNA-Cas protein complex. *Cell* **139**:945-956.
19. **Hodgkin, J., and D. Kaiser.** 1979. Genetics of gliding motility in *Myxococcus xanthus* (Myxobacteriales): genes controlling movements of single cells. *Molecular and General Genetics* **171**:167-176.
20. **Hodgkin, J., and D. Kaiser.** 1979. Genetics of gliding motility in *Myxococcus xanthus* (Myxobacteriales): two gene systems control movement. *Molecular and General Genetics* **171**:177-191.
21. **Huang, X. Q., and W. Miller.** 1991. A time-efficient, linear-space local similarity algorithm. *Adv Appl Math* **12**:337-357.
22. **Jansen, R., J. D. Embden, W. Gastra, and L. M. Schouls.** 2002. Identification of genes that are associated with DNA repeats in prokaryotes. *Molecular Microbiology* **43**:1565-1575.
23. **Kaiser, D.** 1979. Social gliding is correlated with the presence of pili in *Myxococcus xanthus*. *Proceedings of the National Academy of Sciences U S A* **76**:5952-5956.

24. **Kashefi, K., and P. L. Hartzell.** 1995. Genetic suppression and phenotypic masking of a *Myxococcus xanthus* *frzF*- defect. *Molecular Microbiology* **15**:483-494.
25. **Kolter, R., and D. R. Helinski.** 1978. Activity of the replication terminus of plasmid R6K in hybrid replicons in *Escherichia coli*. *Journal of molecular biology* **124**:425-441.
26. **Krzemieniewska, H., and S. Krzemieniewski.** 1926. Miksobakterje polski. *Acta Societatis Botanicorum Poloniae* **4**:1-54.
27. **Kuner, J. M., and D. Kaiser.** 1982. Fruiting body morphogenesis in submerged cultures of *Myxococcus xanthus*. *Journal of Bacteriology* **151**:458-461.
28. **Li, Y., H. Sun, X. Ma, A. Lu, R. Lux, D. Zusman, and W. Shi.** 2003. Extracellular polysaccharides mediate pilus retraction during social motility of *Myxococcus xanthus*. *Proceedings of the National Academy of Sciences U S A* **100**:5443-5448.
29. **Li, Z.** 2007. Demonstration of interactions among Dif proteins and the identification of KapB as a regulator of exopolysaccharide in *Myxococcus xanthus*. Virginia Polytechnic Institute and State University, Blacksburg.
30. **MacRae, T. H., and D. McCurdy.** 1976. Evidence for motility-related fimbriae in the gliding microorganism *Myxococcus xanthus*. *Canadian Journal of Microbiology* **22**:1589-1593.
31. **Makarova, K. S., N. V. Grishin, S. A. Shabalina, Y. I. Wolf, and E. V. Koonin.** 2006. A putative RNA-interference-based immune system in prokaryotes: computational analysis of the predicted enzymatic machinery, functional analogies with eukaryotic RNAi, and hypothetical mechanisms of action. *Biology Direct* **1**:7.
32. **Marraffini, L. A., and E. J. Sontheimer.** 2008. CRISPR interference limits horizontal gene transfer in staphylococci by targeting DNA. *Science* **322**:1843-1845.
33. **Miller, J. H.** 1972. Experiments in molecular genetics. Cold Spring Harbor Laboratory.
34. **Mojica, F. J., C. Diez-Villasenor, J. Garcia-Martinez, and E. Soria.** 2005. Intervening sequences of regularly spaced prokaryotic repeats derive from foreign genetic elements. *Journal of Molecular Evolution* **60**:174-182.
35. **Pougach, K., E. Semenova, E. Bogdanova, K. A. Datsenko, M. Djordjevic, B. L. Wanner, and K. Severinov.** 2010. Transcription, processing and function of CRISPR cassettes in *Escherichia coli*. *Molecular Microbiology* **77**:1367-1379.
36. **Pourcel, C., G. Salvignol, and G. Vergnaud.** 2005. CRISPR elements in *Yersinia pestis* acquire new repeats by preferential uptake of bacteriophage DNA, and provide additional tools for evolutionary studies. *Microbiology* **151**:653-663.

37. **Pul, U., R. Wurm, Z. Arslan, R. Geissen, N. Hofmann, and R. Wagner.** 2010. Identification and characterization of *E. coli* CRISPR-*cas* promoters and their silencing by H-NS. *Molecular Microbiology* **75**:1495-1512.
38. **Ramaswamy, S., M. Dworkin, and J. Downard.** 1997. Identification and characterization of *Myxococcus xanthus* mutants deficient in calcofluor white binding. *Journal of Bacteriology* **179**:2863-2871.
39. **Rubin, E. J., B. J. Akerley, V. N. Novik, D. J. Lampe, R. N. Husson, and J. J. Mekalanos.** 1999. In vivo transposition of mariner-based elements in enteric bacteria and mycobacteria. *Proceedings of the National Academy of Sciences U S A* **96**:1645-1650.
40. **Schneider, C. A., W. S. Rasband, and K. W. Eliceiri.** 2012. NIH Image to ImageJ: 25 years of image analysis. *Nature methods* **9**:671-675.
41. **Shimkets, L. J.** 1986. Correlation of energy-dependent cell cohesion with social motility in *Myxococcus xanthus*. *Journal of Bacteriology* **166**:837-841.
42. **Stern, A., L. Keren, O. Wurtzel, G. Amitai, and R. Sorek.** 2010. Self-targeting by CRISPR: gene regulation or autoimmunity? *Trends in Genetics* **26**:335-340.
43. **Tang, T. H., J. P. Bachelierie, T. Rozhdestvensky, M. L. Bortolin, H. Huber, M. Drungowski, T. Elge, J. Brosius, and A. Huttenhofer.** 2002. Identification of 86 candidates for small non-messenger RNAs from the archaeon *Archaeoglobus fulgidus*. *Proceedings of the National Academy of Sciences U S A* **99**:7536-7541.
44. **Ueki, T., S. Inouye, and M. Inouye.** 1996. Positive-negative KG cassettes for construction of multi-gene deletions using a single drug marker. *Gene* **183**:153-157.
45. **van der Oost, J., M. M. Jore, E. R. Westra, M. Lundgren, and S. J. Brouns.** 2009. CRISPR-based adaptive and heritable immunity in prokaryotes. *Trends in Biochemical Sciences* **34**:401-407.
46. **Viswanathan, P., K. Murphy, B. Julien, A. G. Garza, and L. Kroos.** 2007. Regulation of *dev*, an operon that includes genes essential for *Myxococcus xanthus* development and CRISPR-associated genes and repeats. *Journal of Bacteriology* **189**:3738-3750.
47. **Wall, D., S. S. Wu, and D. Kaiser.** 1998. Contact stimulation of Tgl and type IV pili in *Myxococcus xanthus*. *Journal of Bacteriology* **180**:759-761.
48. **Westra, E. R., U. Pul, N. Heidrich, M. M. Jore, M. Lundgren, T. Stratmann, R. Wurm, A. Raine, M. Mescher, L. Van Heereveld, M. Mastop, E. G. Wagner, K. Schnetz, J. Van Der Oost, R. Wagner, and S. J. Brouns.** 2010. H-NS-mediated repression of CRISPR-based immunity in *Escherichia coli* K12 can be relieved by the transcription activator LeuO. *Molecular Microbiology* **77**:1380-1393.

49. **Wu, S. S., J. Wu, and D. Kaiser.** 1997. The *Myxococcus xanthus pilT* locus is required for social gliding motility although pili are still produced. *Molecular Microbiology* **23**:109-121.
50. **Xu, Q., W. P. Black, S. M. Ward, and Z. Yang.** 2005. Nitrate-dependent activation of the Dif signaling pathway of *Myxococcus xanthus* mediated by a NarX-DifA interspecies chimera. *Journal of Bacteriology* **187**:6410-6418.
51. **Youderian, P., N. Burke, D. J. White, and P. L. Hartzell.** 2003. Identification of genes required for adventurous gliding motility in *Myxococcus xanthus* with the transposable element mariner. *Molecular Microbiology* **49**:555-570.
52. **Zegans, M. E., J. C. Wagner, K. C. Cady, D. M. Murphy, J. H. Hammond, and G. A. O'Toole.** 2009. Interaction between bacteriophage DMS3 and host CRISPR region inhibits group behaviors of *Pseudomonas aeruginosa*. *Journal of Bacteriology* **191**:210-219.
53. **Zhang, J., C. Rouillon, M. Kerou, J. Reeks, K. Brugger, S. Graham, J. Reimann, G. Cannone, H. Liu, S. V. Albers, J. H. Naismith, L. Spagnolo, and M. F. White.** 2012. Structure and mechanism of the CMR complex for CRISPR-mediated antiviral immunity. *Molecular cell* **45**:303-313.

Chapter 3

Type IV Pilus Form an Integrated Structure Extending from the Cytoplasm to the Outer Membrane

Li, C., Wallace, R. A., Black, W. P., Li, Z., Yang, Z. 2013. Type IV Pilus Form an Integrated Structure Extending from the Cytoplasm to the Outer Membrane. PLoS One 8:e70144. Authors retain ownership of copyright.

I, Regina A. Wallace, contributed to this study by designing and constructing plasmids, pRW139, pRW141-143, and pRW151, and strains YZ2214-2215, YZ2225-2226, and YZ2234.

Abstract

The bacterial type IV pilus (T4P) is the strongest biological motor known to date as its retraction can generate forces well over 100 pN. *Myxococcus xanthus*, a δ -proteobacterium, provides a good model for T4P investigations because its social (S) gliding motility is powered by T4P. In this study, the interactions among *M. xanthus* T4P proteins were investigated using genetics and the yeast two-hybrid (Y2H) system. Our genetic analysis suggests that there is an integrated T4P structure that crosses the inner membrane (IM), periplasm and the outer membrane (OM). Moreover, this structure exists in the absence of the pilus filament. A systematic Y2H survey provided evidence for direct interactions among IM and OM proteins exposed to the periplasm. For example, the IM lipoprotein PilP interacted with its cognate OM protein PilQ. In addition, interactions among T4P proteins from the thermophile *Thermus thermophilus* were investigated by Y2H. The results indicated similar protein-protein interactions in the T4P system of this non-proteobacterium despite significant sequence divergence between T4P proteins in *T. thermophilus* and *M. xanthus*. The observations here support the model of an integrated T4P structure in the absence of a pilus in diverse bacterial species.

Introduction

Myxococcus xanthus is a gram-negative δ -proteobacterium that utilizes the type IV pilus (T4P) as a motility motor to move over solid surfaces (50). Bacterial type IV pili (T4P), usually a few micrometers long and 6-7 nm in diameter, are polymeric protein filaments of the monomer pilin (14, 26, 54). The T4P-mediated motility in *M. xanthus* is known as social (S) motility (26). This is distinct from the adventurous (A) gliding motility of *M. xanthus* which is powered by an independent and different motility machinery (37). T4P in rod-shaped bacteria such as *M. xanthus* are mostly localized to one of the two cell poles (22, 26, 35). Their retraction pulls a cell forward in *M. xanthus* S motility (13, 45) and in the twitching motility of the γ -proteobacterium *Pseudomonas aeruginosa*, the β -proteobacteria *Neisseria meningitidis* and *Neisseria gonorrhoeae* among other bacterial species (35, 41). It is noteworthy that the T4P is the strongest among known biological motors as a single T4P can produce a stall force well over 100 pN when it retracts (13, 33). *M. xanthus* S motility additionally requires extracellular polysaccharides (EPS) to function because *M. xanthus* EPS⁻ mutants are defective in S motility (52, 60). The current model postulates that a T4P is triggered to retract at its cell proximal end when its distal end binds to EPS that are either associated with the *M. xanthus* cell surface or deposited on the gliding substratum (37).

About a dozen *pil* genes are required for T4P to function as a motor [see (19, 41, 50) and references therein]. *pilA* encodes prepilin which is processed to mature pilin by a peptidase. *pilM*, *pilN*, *pilO*, *pilP* and *pilQ* usually form an operon in this gene order in *M. xanthus* and essentially all bacteria with these genes. PilM is a cytoplasmic protein that is likely anchored to the membrane by binding to the cytoplasmic tail of the bitopic transmembrane (TM) protein PilN. Like PilN, PilO is predicted to have a short cytoplasmic N-terminus, a TM helix and a

periplasmic domain. PilP is an inner membrane (IM) lipoprotein exposed to the periplasm. PilQ is an outer membrane (OM) secretin which multimerizes to form a channel for the T4P to extend through the OM. PilC is predicted to be a polytopic TM protein with sizeable cytoplasmic domains. PilB and PilT are the two ATPases in the T4P system, the former responsible for T4P extension or assembly and the latter for retraction or disassembly.

In recent years, there have been various reports proposing a T4P IM complex consisting of PilM, PilN, PilO and PilP in *P. aeruginosa* and *Neisseria* (1, 17, 46, 48). Such a complex is consistent with the findings in the type II secretion system (T2SS) which is related to the T4P system evolutionarily (19, 38). For example, the T2SS protein GspL has a single TM helix with a cytoplasmic and a periplasmic domain (GspL_{cyto} and GspL_{peri}). GspL_{cyto} resembles PilM while GspL_{peri} is similar to PilN, providing evidence that PilM and PilN interactions are genuine. The lipoprotein PilP shares structural similarity with the TM protein GspC in the T2SS (21, 30). Both PilQ and the T2SS protein GspD are members of the secretin family which form channels in the OM (19, 32). How T4P proteins form a multicomponent machine for its motor function remains an active area of scientific inquiry.

This paper reports our investigation into the interactions among T4P proteins. Besides its motor function in S motility, T4P had been shown to regulate EPS production in *M. xanthus* (6). More recently, a suppressor mutation in *pilB* was discovered that was capable of restoring EPS production to a *pilA* deletion mutant (4). The analysis of genetic suppression here suggested an integrated T4P structure consisting of PilB, PilC, PilM, PilN, PilO, PilP and PilQ *in vivo*. The interactions among these proteins and the formation of this structure are likely independent of a T4P filament because these interactions were observed in a *pilA* deletion background. Using a yeast two-hybrid (Y2H) system, we demonstrate that the OM protein PilQ can be bridged inward

to the IM through interactions in the periplasm with PilP. In addition, Y2H experiments also detected similar interactions among the T4P proteins of the non-proteobacterium *Thermus thermophilus*. Our findings support an integrated T4P structure capable of extending from the cytoplasm through the IM, periplasm and OM in bacteria on diverse branches of the phylogenetic tree. At least in the proteobacterium *M. xanthus*, such a structure may form in the absence of the pilus filament.

Materials and Methods

Strains and growth conditions

M. xanthus strains used in this study are listed in Table 3-1. They were grown using CYE medium (11) at 32°C. XL-1 Blue (Stratagene) was the *Escherichia coli* strain used for plasmid construction, which was grown using Luria-Bertani (LB) medium (39) at 37°C. All plates contained 1.5% agar except CYE soft agar plates which contained 0.4% agar. When necessary, kanamycin, oxytetracycline and ampicillin were supplemented at 100, 15 and 100 µg/ml, respectively, to CYE and/or LB for selection.

Two *Saccharomyces cerevisiae* strains for the Y2H study, AH109 (*MATa*, *trp1-901*, *leu2-3*, *112*, *ura3-52*, *his3-200*, *gal4Δ*, *gal80Δ*, *LYS2::GAL1UAS-GALITATA-HIS3*, *GAL2UAS-GAL2TATA-ADE2*, *URA3::MEL1UAS-MELITATA-lacZ*) and Y187 (*MATα*, *ura3-52*, *his3-200*, *ade2-101*, *trp1-901*, *leu2-3*, *112*, *gal4Δ*, *met-*, *gal80Δ*, *URA3::GAL1UAS-GALITATA-lacZ*) (Clontech), were grown using YPDA medium [1% Yeast extract, 2% Peptone (Bacto), 2% glucose, 0.003% adenine hemisulfate (pH6.5)] (Clontech). Synthetic dropout (SD) media with specified nutrients omitted were used for selection and phenotype analysis in Y2H experiments (see later). All yeast cells were grown at 30°C.

Plasmids for *M. xanthus* strain construction

Two sets of plasmids (Table 3-2) were constructed for use in *M. xanthus*, one for deleting or replacing *M. xanthus* wild-type (WT) *pil* genes and the other for complementing *pil* deletions. All plasmids were confirmed by restriction digestions, polymerase chain reaction (PCR) and/or DNA sequencing.

The plasmids for *pil* gene deletions were pWB600 ($\Delta pilM$), pWB601 ($\Delta pilN$), pWB602 ($\Delta pilO$) and, pWB603 ($\Delta pilP$) (7, 25, 49). These plasmids were constructed using pMY7 which

Table 3-1: *Myxococcus xanthus* strains used in this study

Strains	Genotype	Reference
DK1622	Wild-type	(26)
DK8615	$\Delta pilQ$	(51)
DK10410	$\Delta pilA::tet$	(55)
DK10417	$\Delta pilC$	This study
DK10416	$\Delta pilB$	(58)
DK11122	$\Delta pilI$	(57)
DK11133	$\Delta pilH$	(57)
DK11135	$\Delta pilG$	(57)
YZ690	$\Delta pilA$	This study
YZ1181	$\Delta pilH pilB^{WA}$	This study
YZ1182	$\Delta pilC pilB^{WA}$	This study
YZ1183	$\Delta pilG pilB^{WA}$	This study
YZ1184	$\Delta pilI pilB^{WA}$	This study
YZ1185	$\Delta pilM pilB^{WA}$	This study
YZ1186	$\Delta pilN pilB^{WA}$	This study
YZ1187	$\Delta pilO pilB^{WA}$	This study
YZ1188	$\Delta pilP pilB^{WA}$	This study
YZ1189	$\Delta pilQ pilB^{WA}$	This study
YZ1190	$\Delta pilA \Delta pilQ pilB^{WA}$	This study
YZ1191	$\Delta pilA \Delta pilQ$	This study
YZ1192	$\Delta pilQ att::pilQ$	This study
YZ1573	$\Delta pilA pilB^{WA}$	This study
YZ1860	$\Delta pilM$	This study
YZ1861	$\Delta pilN$	This study
YZ1862	$\Delta pilO$	This study
YZ1863	$\Delta pilP$	This study
YZ2214	$\Delta pilC att::pilC$	This study
YZ2215	$\Delta pilN att::pilN$	This study
YZ2225	$\Delta pilM att::pilM$	This study
YZ2226	$\Delta pilO att::pilO$	This study
YZ2234	$\Delta pilP att::pilP$	This study

is pZErO (Invitrogen) containing the *Aeromonas hydrophila galk* gene (44). Deletion alleles, which were obtained using a two-step PCR procedure as described previously (5), were cloned into pMY7 digested with *Bam*HI and *Eco*RI. The $\Delta pilM$ allele deleted codons from 8 to 392, $\Delta pilN$ from 6 to 222, $\Delta pilO$ from 8 to 189 and $\Delta pilP$ from 7 to 197 of their respective genes. In addition, pCL153 ($pilB^{K327A}$ or $pilB^{WA}$) was used for the replacement of WT $pilB$ ($pilB^+$) with $pilB^{WA}$ (WA stands for Walker A), which was obtained from pWB630 (4) by digestion with *Hind*III and *Xba*I and cloned into the same sites in pBJ113.

The plasmids for complementation were pRW143 (*pilC*), pRW142 (*pilM*), pRW139 (*pilN*), pRW141 (*pilO*), pRW151 (*pilP*), and pCL179 (*pilQ*). These plasmids were constructed using the *M. xanthus* expression plasmid pWB425 as the vector (5). The target genes were PCR amplified using primers containing *Kpn*I and *Bam*HI at the 5' and 3', respectively. These fragments were cloned into the same restriction sites in pWB425. Relative to the coding regions of each gene, pRW143 contains a fragment from 19 base pairs (bp) upstream to 13 bp downstream of *pilC*, pRW142 from 17 bp upstream to 15 bp downstream of *pilM*, pRW139 from 14 bp upstream to 17 bp downstream of *pilN*, pRW141 from 60 bp upstream to 20 bp downstream of *pilO*, pRW151 from 79 bp upstream to 49 pb downstream of (*pilP*), and pCL179 from 18 bp upstream to 25 bp downstream of (*pilQ*).

***M. xanthus* strain construction**

All *M. xanthus* strains (Table 3-1) are isogenic to the laboratory WT strain DK1622 (26). The plasmids pWB600 through pWB603 (Table 3-2) with deletion alleles of *pilM* through *pilP* were used for the construction of deletion mutants using DK1622 as the parent as described previously (5). The resultant single *pil* deletion mutants are YZ1860 ($\Delta pilM$), YZ1861 ($\Delta pilN$), YZ1862 ($\Delta pilO$), and YZ1863 ($\Delta pilP$). pCL153 were then used to replace $pilB^+$ with $pilB^{WA}$ in

Table 3-2: Plasmids used in this study

Plasmids	Description	Reference
Plasmids for use in <i>M. xanthus</i>		
pBJ113	Vector, Kan ^R , <i>galK</i>	(25)
pCL153	<i>pilB</i> ^{WA} in pBJ113	This study
pCL179	<i>pilQ</i> in pWB425	This study
pMY7	Vector, Kan ^R , <i>galK</i>	Unpublished
pRW139	<i>pilN</i> in pWB425	This study
pRW141	<i>pilO</i> in pWB425	This study
pRW142	<i>pilM</i> in pWB425	This study
pRW143	<i>pilC</i> in pWB425	This study
pRW151	<i>pilP</i> in pWB425	This study
pWB425	Vector, Kan ^R , <i>att</i>	(5)
pWB600	Δ <i>pilM</i> in pMY7	This study
pWB601	Δ <i>pilN</i> in pMY7	This study
pWB602	Δ <i>pilO</i> in pMY7	This study
pWB603	Δ <i>pilP</i> in pMY7	This study
Plasmids for use in Y2H experiment		
pCL127	GAD-MxPilN	This study
pCL128	GAD-MxPilP	This study
pCL131	GAD-MxPilO	This study
pCL134	GBD-MxPilO	This study
pCL135	GBD-MxPilN	This study
pCL136	GBD-MxPilP	This study
pCL137	GAD-MxPilM	This study
pCL138	GBD-MxPilM	This study
pCL141	GAD-MxPilQc	This study
pCL142	GBD-MxPilQc	This study
pCL150	GBD-MxPilQ'	This study
pCL152	GAD-MxPilQ'	This study
pCL180	GAD-TtPilN	This study
pCL181	GBD-TtPilN	This study
pCL182	GAD-TtPilO	This study
pCL183	GBD-TtPilO	This study
pCL184	GAD-TtPilW	This study
pCL185	GBD-TtPilW	This study
pCL186	GAD-TtPilQ ₀	This study
pCL187	GBD-TtPilQ ₀	This study
pCL188	GAD-TtPilQ ₀₁	This study
pCL189	GBD-TtPilQ ₀₁	This study
pCL192	GAD-TtPilQ ₀₁₂	This study
pCL193	GBD-TtPilQ ₀₁₂	This study
pGAD	pGADT7, Amp ^R , Leu	Clontech
pGAD-T	Amp ^R , Leu	Clontech
pGBD	pGBKT7, Kan ^R , Trp	Clontech
pGBD-53	Kan ^R , Trp	Clontech

these strains to construct YZ1185 through YZ1188. In addition, pCL153 was used to replace *pilB*⁺ in DK10417 ($\Delta pilC$), DK11135 ($\Delta pilG$), DK11133 ($\Delta pilH$), DK11122 ($\Delta pilI$) and DK8615 ($\Delta pilQ$) to construct YZ1182, YZ1183, YZ1181, YZ1184 and YZ1189, respectively. To construct YZ1190 and YZ1191, genomic DNA of DK10407 ($\Delta pilA::tet$) was transformed into YZ1189 ($\Delta pilQ pilB^{WA}$) and DK8615 ($\Delta pilQ$) (51, 55-57).

For the complementation of single deletions of *pilC*, *pilM*, *pilN*, *pilO*, *pilP* and *pilQ*, the pRW series of plasmids (Table 3-2) were transformed into their corresponding deletion strains to construct YZ2214, YZ2225, YZ2215, YZ2226, YZ2234 and YZ1192, respectively.

Assays for S motility and EPS production

M. xanthus cells in exponential growth were harvested and resuspended in MOPS (morpholinepropanesulfonic acid) buffer (10 mM MOPS (pH 7.6), 2 mM MgSO₄) at 5.0×10⁹ cells/ml. For the S-motility assay, 5 μ l of the cell suspension was spotted to the center of a soft agar plate which was documented after 5 days of incubation. For EPS analysis, 5 μ l of the cell suspension was placed on a CYE plate supplemented with Calcofluor white at 50 μ g/ml. Plates were incubated for 6 days and the fluorescence was documented under ultraviolet (UV) illumination at ~365 nm (5-7).

Plasmids for Y2H experiments (Table 3-2)

The MATCHMAKER System 3 from Clontech was used for the Y2H experiments in this study. The two cloning vectors pGAD (pGADT7) and pGBD (pGBKT7) allow proteins to be fused to the C-terminus of the GAL4 transcription activation domain (GAD) and GAL4 DNA binding domain (GBD), respectively (23). A fragment with the coding region of interest of a gene from either *M. xanthus* or *T. thermophilus* was amplified by PCR and cloned into both pGAD and pGBD restricted by appropriate endonucleases. pGAD-T and pGBD-53, which

contain fusions to T-antigen and p53, are provided by Clontech as positive controls. pCL127, pCL128 and pCL131 contain *M. xanthus* (Mx) PilN, PilP and PilO fused to GAD whereas pCL135, pCL136 and pCL134 contain the same proteins fused to GBD, respectively. Note that the signal peptide of PilP and the TM helices of PilN and PilO are excluded from these constructs. pCL150 and pCL152 contain the same MxPilQ fragment truncated at the C-terminus (PilQ') in pGBD and pGAD; pCL141 and pCL142 contain the Secretin_N region at the center of MxPilQ (PilQc) in the two Y2H vectors.

Plasmids pCL180 through pCL193 contain fusions of *T. thermophilus* (Tt) Pil proteins to GAL4 in Y2H vectors (Table 3-2). pCL180, pCL182 and pCL184 contain TtPilN, TtPilO and TtPilP fused to GAD and pCL182, pCL183 and pCL185 contain the same protein fragments fused to GBD, respectively. The TtPilQ N-terminus is divided into N0, N1 and N2 subdomains. pCL186 through pCL193 contain N0 (PilQ₀), N0 and N1 (PilQ₀₁) and all three subdomains (PilQ₀₁₂) in pGAD and pGBD, respectively.

Y2H mating protocol

The plates used for the Y2H mating protocol are SD without (-) tryptophan (Trp), leucine (Leu), histidine (His), adenine (Ade) or their combinations (Clontech). The mating protocol in the manual for the MATCHMAKER system (Clontech) was followed to examine systematic protein-protein interactions in Y2H. Briefly, a pGAD-derived plasmid was transformed into Y187 by selection on SD-Leu and a pGBD-derived plasmid into AH109 by selection on SD-Trp plates. 20 µl of culture of each transformant was placed in the same well of a 96-well plate seeded with 160 µl of YPDA each. After incubation for 18 hours on a rotary shaker, 5 µl of the culture from each well was transferred onto a 150×15 mm² petri dish with SD-Trp-Leu medium in the same 96-well plate format. After 48-72 hours of incubation, cells were replica plated to

SD-Ade and SD-His plates. After 3-5 days of incubation, growth on these plates was scored for the His⁺ or His⁻ and Ade⁺ or Ade⁻ phenotypes. Note that both SD-His and SD-Ade plates were without Trp and Leu. The SD-His plates were additionally supplemented with 2.5 mM 3-Amino-1, 2, 4-triazole (3-AT) which is a competitive inhibitor of the His3 enzyme.

Y2H by co-transformation

A pair of pGAD- and pGBD-derived plasmids were co-transformed (18) into the yeast strain AH109 by selection on SD-Leu-Trp plates. Transformants were then examined for growth on SD-Ade and SD-His plates and for the expression of β -galactosidase. For the analysis of growth on SD-Ade and SD-His plates, cells in exponential growth were harvested and resuspended in SD medium. 5 μ l of cell suspensions at 4×10^6 , 8×10^5 , 1.6×10^5 and 3.2×10^4 cells per ml were placed on SD-Ade and SD-His plates in a row from left to right. The growth was documented by photographs after 3 days of incubation. The analysis of β -galactosidase activity was performed as described by the Yeast Protocols Handbook (Clontech) using ONPG (o-nitrophenyl β -D-galactopyranoside) as the substrate. 1 unit of β -galactosidase is defined as the amount that hydrolyzes 1 μ mol of ONPG per minute per cell.

Results and Discussion

Deletions of *M. xanthus pilM, pilN, pilO, pilP, pilQ* and *pilC* can be complemented

It was observed previously that individual *P. aeruginosa pilM, pilN, pilO* and *pilP* mutants could not be complemented by their respective WT genes *in trans* unless other genes in the same gene cluster or operon were provided as well (1). These observations were taken as part of the evidence to conclude that PilM, PilN, PilO and PilP formed an inner membrane (IM) complex critical for the stability of the PilQ secretin on the outer membrane (OM) (1). A similar approach was taken here to examine the complementation of *M. xanthus pil* mutations as an attempt to study interactions among *M. xanthus* T4P proteins. Because *pilM, pilN, pilO, pilP* and *pilQ* are likely in an operon in *M. xanthus* as in most other bacteria (41, 50), in-frame deletions of these *M. xanthus* genes were constructed to minimize polar effects (see Materials and Methods). A *pilC* deletion was also constructed because PilC may play a key role in organizing an IM complex since it is the only predicted polytopic TM T4P protein (41). When examined on soft agar plates (Figure 3-1), all mutants were found to be defective in S motility as anticipated since none was expected to assemble T4P (40, 50).

Next, plasmids were constructed for complementation of these deletion mutants. Six fragments containing *pilC, pilM, pilN, pilO, pilP* and *pilQ*, respectively, were cloned into an expression vector (5) which is able to integrate at the Mx8 phage attachment site (*att*) on the *M. xanthus* chromosome. The resulting plasmids were transformed into their respective deletion strains and the transformants were examined on soft agar plates for S motility (Figure 3-1) which requires fully functional T4P. Unlike the observations in *P. aeruginosa* (1), these transformants all showed S motility similar to the WT. It is noted that expression of *pil* genes *in trans* in these complemented strains are likely lower than in the WT *in situ* (4, 24). The previous observation

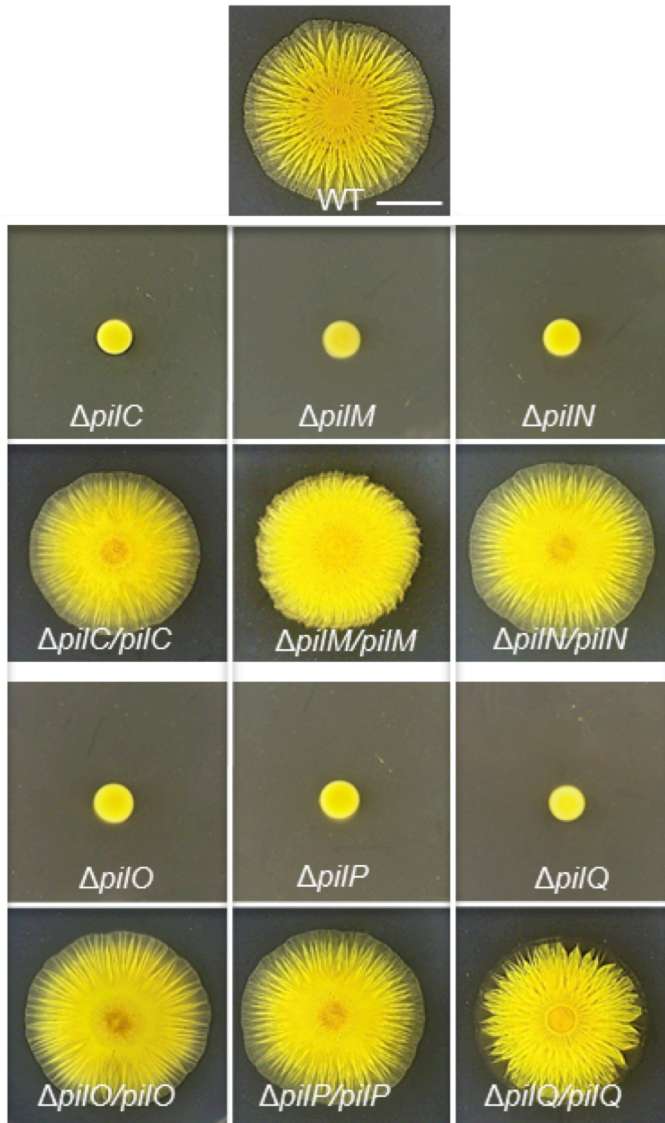


Figure 3-1: *pil* deletions can be complemented *in trans*

S motility was analyzed by colony spreading (or swarming) on soft agar plates as described in Materials and Methods. The *pil* deletion strains are DK10417 ($\Delta pilC$), YZ1860 ($\Delta pilM$), YZ1861 ($\Delta pilN$), YZ1862 ($\Delta pilO$), YZ1863 ($\Delta pilP$) and DK8615 ($\Delta pilQ$). The complemented stains are YZ2214 ($\Delta pilC/pilC$), YZ2225 ($\Delta pilM/pilM$), YZ2215 ($\Delta pilN/pilN$), YZ2226 ($\Delta pilO/pilO$), YZ2234 ($\Delta pilP/pilP$) and YZ1192 ($\Delta pilQ/pilQ$). The WT strain DK1622 was included on the top center as a control and the scale bar represents 5 mm. See Table 1 for more precise genotypes of the strains.

(1) could be explained if T4P assembly is more sensitive to an imbalance of proteins forming a complex in *P. aeruginosa* than in *M. xanthus*. Alternatively, the small insertions or scar mutations in *P. aeruginosa pil* genes (1) could be partially polar on downstream genes.

***pilB*^{WA} suppresses the EPS defect of $\Delta pilG$, $\Delta pilH$ & $\Delta pilI$, but not that of $\Delta pilC$, $\Delta pilM$, $\Delta pilN$, $\Delta pilO$, $\Delta pilP$, or $\Delta pilQ$**

Taking advantage of a newly constructed gain-of-function mutation in *pilB*, an alternative genetic approach was explored to examine if T4P proteins form an integrated structure in *M. xanthus*. PilB, a cytoplasmic ATPase in the T2SS ATPase superfamily, has been shown to function as the T4P assembly ATPase with $\Delta pilB$ mutations leading to a T4P⁻ phenotype (9, 22). Previous results indicated that $\Delta pilA$ or any other *pil* mutants that were T4P⁻ were also defective in EPS production, indicating a role for T4P in EPS regulation in *M. xanthus* (6). Recently a *pilB* mutation was found that restored EPS production to a $\Delta pilA$ mutant (4). This mutation, which is referred to as *pilB*^{WA} or *pilB*^{K327A}, resulted in the substitution of the strictly conserved lysine (K) 327 with an alanine (A) in the signature Walker A box of such ATPases. To examine if *pilB*^{WA} could suppress the EPS⁻ phenotype resulting from other T4P⁻ mutations, the *pilB*⁺ allele was replaced by *pilB*^{WA} in the deletion mutants of *pilC*, *pilM*, *pilN*, *pilO*, *pilP*, and *pilQ* as well as *pilG*, *pilH*, and *pilI*, respectively. The resulting strains were examined on plates containing Calcofluor white, a fluorescent dye that binds to *M. xanthus* EPS (Figure 3-2). As indicated by fluorescence, *pilB*^{WA} suppressed $\Delta pilG$, $\Delta pilH$ and $\Delta pilI$ in EPS production, but not $\Delta pilC$, $\Delta pilM$, $\Delta pilN$, $\Delta pilO$, $\Delta pilP$, or $\Delta pilQ$.

The lack of suppression of $\Delta pilQ$ by *pilB*^{WA} was further investigated. PilQ is the secretin that forms a multimeric channel in the OM to allow the passage of the pilus filament through the OM (40). It was previously reported that a *N. meningitidis pilQ* mutant assembled T4P in the

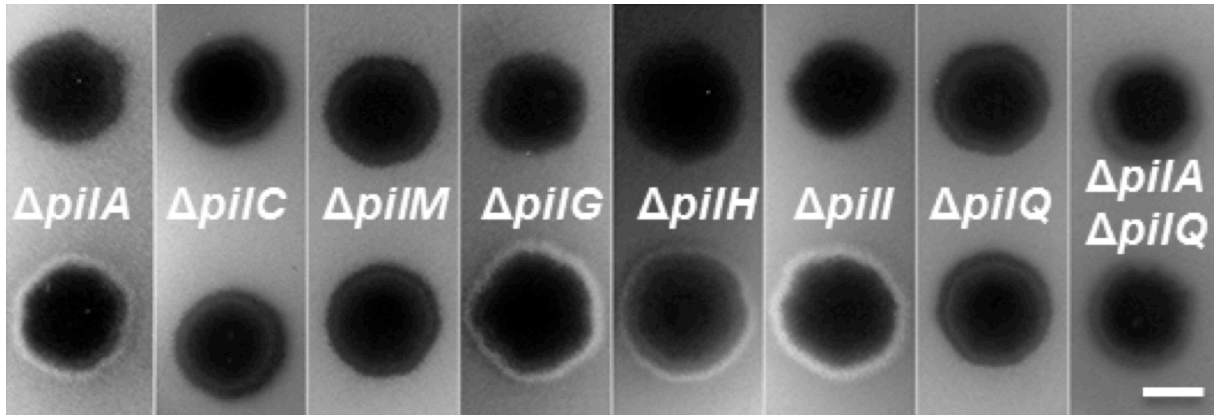


Figure 3-2: *pilB^{WA}* suppresses some but not all T4P⁻ *pil* deletions in EPS production

EPS levels were analyzed on plates with the fluorescent dye Calcofluor white (See Materials and Methods). The presence of fluorescence indicates EPS⁺ and its absence EPS⁻. Each strip shows two strains, the upper is a strain with the indicated mutation(s) in a *pilB*⁺ background and the lower in the *pilB^{WA}* background. Strains used are YZ690 ($\Delta pilA$), YZ1573 ($\Delta pilA pilB^{WA}$), DK10417 ($\Delta pilC$), YZ1182 ($\Delta pilC pilB^{WA}$), YZ1860 ($\Delta pilM$), YZ1185 ($\Delta pilM pilB^{WA}$), DK11135 ($\Delta pilG$), YZ1183 ($\Delta pilG pilB^{WA}$), DK11133 ($\Delta pilH$), YZ1181 ($\Delta pilH pilB^{WA}$), DK11132 ($\Delta pilI$), YZ1184 ($\Delta pilI pilB^{WA}$), YZ1191 ($\Delta pilA \Delta pilQ$) and YZ1190 ($\Delta pilA \Delta pilQ pilB^{WA}$). *pilB^{WA}* failed to suppress $\Delta pilN$, $\Delta pilO$, $\Delta pilP$ and $\Delta pilQ$ as it did $\Delta pilC$ and $\Delta pilM$ (data not shown).

periplasm likely because a *pilQ* mutant in an otherwise WT background can still assemble the pilus filament in the periplasm even though it fails to extend through the OM (12, 53). In addition, mutant PilA or pilins trapped in the IM may negatively influence EPS production (59). In a *pilQ* mutant, either periplasmic pili and/or an increase in unassembled pilins in the IM could down regulate EPS levels. To examine if the lack of suppression of $\Delta pilQ$ by *pilB^{WA}* was due to these reasons, we constructed a $\Delta pilA \Delta pilQ pilB^{WA}$ triple mutant. As shown in Figure 3-2, *pilB^{WA}* still failed to restore EPS production to a $\Delta pilQ \Delta pilA$ mutant. Because *pilB^{WA}* suppresses $\Delta pilA$ (Figure 3-2) (4), the results here indicate that PilB^{WA} requires PilQ to signal EPS production in *M. xanthus* in a $\Delta pilA$ background or the absence of a pilus.

What are the explanations for this pattern of suppression of *pil* mutations by *pilB^{WA}*? The suppression of $\Delta pilG$, $\Delta pilH$ and $\Delta pilI$ was perhaps not surprising. PilG, PilH and PilI are essential for the translocation of pillin across the IM (57) and their mutants in essence may resemble a $\Delta pilA$ mutant due to the lack of pilins and pili. The lack of suppression of $\Delta pilC$ and $\Delta pilM$ may also have simple explanations. PilM is a cytoplasmic protein (27) and the multi-TM protein PilC is predicted to have sizeable cytoplasmic loops (28). A frugal explanation would be that PilB^{WA} requires interactions with both PilC and PilM directly or through each other in the cytoplasm in order to signal EPS production. The suppression of $\Delta pilG$, $\Delta pilH$ and $\Delta pilI$ by *pilB^{WA}* as well as the lack of suppression of $\Delta pilC$ and $\Delta pilM$ may therefore be explained parsimoniously with little difficulty.

Without invoking multiple direct and indirect interactions, however, there would be no good explanation for the lack of suppression of $\Delta pilN$, $\Delta pilO$, $\Delta pilP$ and $\Delta pilQ$ by *pilB^{WA}*. As has been mentioned in Introduction, PilQ forms an oligomeric passage for the T4P filament on the OM. PilP is a lipoprotein anchored to the IM by a lipid moiety (16). PilO and PilN are both

predicted to have similar membrane topology, each with a cytoplasmic N-terminal tail of a dozen residues, a TM helix followed by the C-terminus in the periplasm (36, 43). It is known that the N-terminal tail of PilN interacts with PilM in the cytoplasm (27). Taking into consideration the above structural information and the suppression patterns of various *pil* mutations by *pilB^{WA}* in *M. xanthus*, a reasonable explanation assumes a multi-component complex consisting of all these proteins. To explain the requirement of PilQ for EPS production in a *pilB^{WA}* background, for example, PilQ in the OM must be connected to the cytoplasmic PilM and/or the IM spanning PilC to affect the activity of PilB^{WA}. This connection through the periplasm and the IM may involve PilP, PilO and/or PilN, but not necessarily the pilus filament. Such a model would explain how PilQ could influence the activity of PilB^{WA} in the cytoplasm and why *pilB^{WA}* suppresses none of the deletions of *pilC*, *pilM*, *pilN*, *pilO* and *pilP*. That is, PilB^{WA}, which likely represents a particular conformation of PilB *in vivo* (4), must communicate either directly or indirectly with the IM protein PilC and the cytoplasmic protein PilM anchored to the IM by PilN (28). The other proteins, PilO, PilP and PilQ, must in turn affect the activity of PilB^{WA} indirectly through their interactions with PilC, PilM and/or PilN.

Interactions among *M. xanthus* PilN, PilO, PilP and PilQ in Y2H system

The above model envisions an integrated T4P structure with extensive protein-protein interactions that were investigated more directly using the Y2H system. The Y2H mating protocol (See Materials and Methods) was utilized here since it can be used to examine interactions among large numbers of proteins and their domains. In this protocol, a protein or its domain is fused to the C-termini of both the GAL4 activation domain (GAD) and DNA binding domain (GBD) in pGAD and pGBD vectors, respectively (Table 3-2). The two fusion plasmids are then transformed into two yeast reporter strains of the opposite mating types (Y187: *MAT α*

Table 3-3: Interactions among *M. xanthus* Pil proteins detected by Y2H mating protocol

*	PilN	PilO	PilP	PilQ'	PilQ_C	p53
PilN	-	-	-	-	-	-
PilO	+	-	+	-	-	-
PilP	-	-	-	+	-	-
PilQ'	-	-	+	+	-	-
PilQ_C	-	-	+	+	-	-
T-antigen	-	-	-	-	-	+

* The first column and first row indicate proteins fused to GAD and GBD, respectively.

Diploid cells containing the indicated pair of fusions were examined for growth on SD-His and SD-Ade plates. Plus (+), growth on both plates; minus (-), growth on neither plates.

and AH109: *MATa*), respectively. The two strains are then mated with each other and with others expressing fusions to a different GAL4 domain. After mating, the diploid cells containing a pGAD- and a pGBD-derived plasmids are examined on selective plates without histidine (SD-His) or adenine (SC-Ade) for His⁺ and Ade⁺ phenotypes as indicators of the expression of two reporter genes of the Y2H system.

Table 3-3 represents results for PilN, PilO, PilP and PilQ using this mating protocol. The constructs for PilN and PilO excluded their N-terminal tails and TM domains and those for PilP excluded its predicted lipoprotein signal peptide at the N-terminus (20). PilQ constructs were designed based on primary sequence conservation (Figure 3-3A) and secondary structure predictions (8, 29) (data not shown). The PilQ' construct (Figure 3-3A and Table 3-1) excluded the C-terminal secretin region which is predicted to form β -barrels in the OM membrane (8); the PilQc construct contained the conserved Secretin_N region immediately N-terminal of the more highly conserved secretin domain (Figure 3-3A). In this experiment, seven pairs of plasmids conferred growth on selective media (Table 3-3). The results suggested the following four pairwise interactions: PilN-PilO, PilO-PilP, PilP-PilQ and PilQ-PilQ. PilP interacted with both PilQ' and PilQc (Figure 3-3A) but not with two other constructs containing the N-termini of PilQ truncated before Secretin_N (data not shown). Therefore, the Secretin_N region may solely contribute to the interaction of PilQ with PilP in *M. xanthus*. PilP and PilQ' were the only pair whose interactions were detected in both orientations in reciprocal Y2H vectors while three of the GAL4 fusions (GAD-PilN, GBD-PilO and GBD-PilQc) gave no positive interactions in this Y2H experiment (Table 3-3). It is noteworthy that the four pairs of interactions detected here (Table 3-3) are all predicted to be in the periplasm of *M. xanthus*. Various fragments of PilB,

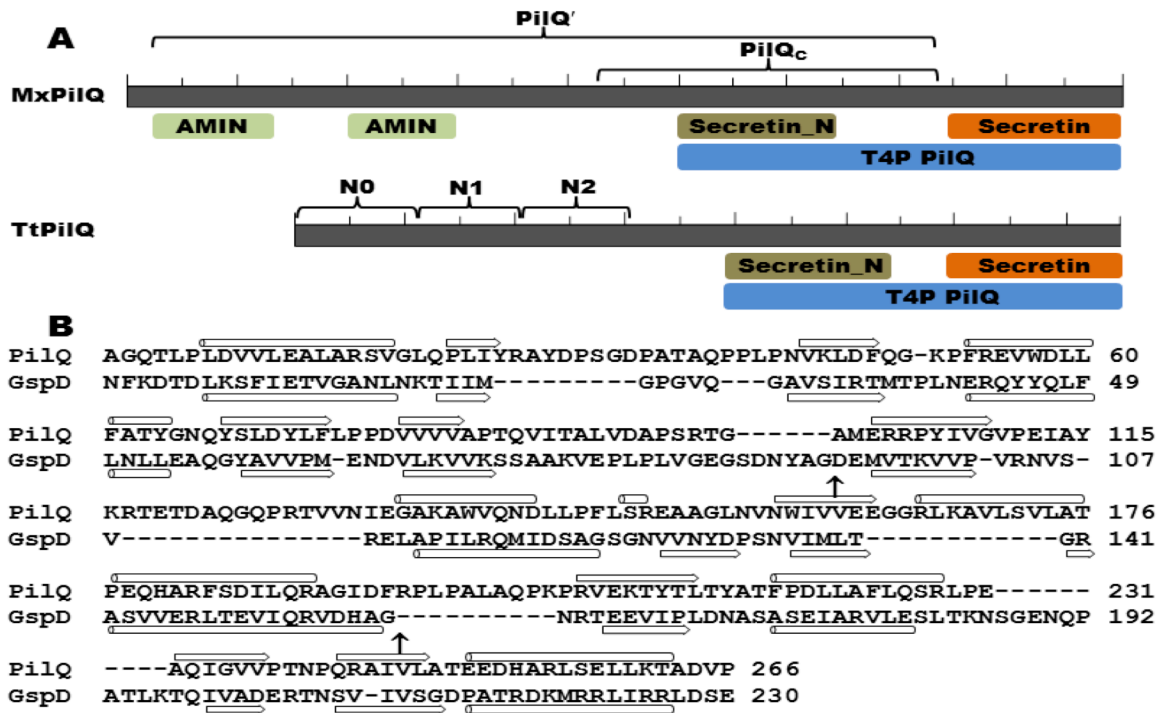


Figure 3-3: Conserved domains of PilQ

Panel **A**. Conserved domains of MxPilQ (901 residues) and TtPilQ (757 residues) (34). The conserved features are drawn to scale and are indicated by shaded letters below both proteins. Each has the PilQ region at their C-terminus consisting of the highly conserved Secretin domain and the region immediately N-terminal of secretin (Secretin_N). Two AMIN domains (15) are found at the N-terminus of MxPilQ but not TtPilQ. The brackets and the labels above indicate the different Y2H constructs and/or subdomains in each protein. Panel **B**. Structural alignment of the N-termini of TtPilQ and the T2SS secretin GspD from enterotoxigenic *E. coli* (ETEC) (29, 31). The boundaries between N0 and N1 as well as N1 and N2 subdomains in GspD are indicated by arrows (↑). The secondary structure of GspD from crystallography and that of TtPilQ predicted from modeling are indicated below and above the aligned sequences, respectively, with β strands represented by block arrows and α helices by cylinders.

PilM and PilC were also examined, but no interaction between them was detected using this Y2H mating protocol (data not shown).

The interactions detected by the mating protocol were verified by co-transformation of the yeast strain AH109 and additional analysis of the expression of reporter genes. Briefly, each of the seven pairs of plasmids that gave positive interactions (Table 3-3) was co-transformed into AH109 and the transformants were examined phenotypically. As a semi-quantitative analysis of the strength of interactions, 5-fold serial dilutions of the transformants were spotted on SD-His and SD-Ade plates as shown in Figures 3-4A and 3-4B. The pairs that showed positive interactions in the mating protocol (Table 3-2) all showed growth on these two selective plates. The expression of β -galactosidase, the third reporter of the Y2H system, confirmed these positive interactions (Figure 3-5A). When each of the plasmids was co-transformed with an empty Y2H vector, none of them led to the expression of the three reporters (Figures 3-4A, 3-4B & 3-5A), eliminating the possibility of autoactivation by any single GAL4 fusion.

In summary, the PilQ-PilQ interaction is consistent with its oligomerization in the OM. The PilQ-PilP, PilP-PilO and PilO-PilN pairwise interactions connect PilQ to PilN which interacts with PilM in the cytoplasm (27). These results are therefore supportive of a model wherein the OM secretin is connected to the cytoplasmic ATPase PilB through a series of physical interactions as proposed based on the suppression of *pil* mutations by *pilB^{WA}* in EPS production (Figure 3-2). The pilus filament is apparently not required for the formation of this integrated T4P complex as *pilB^{WA}* suppresses $\Delta pilA$ yet not a $\Delta pilA \Delta pilQ$ double mutation (Figure 3-2).

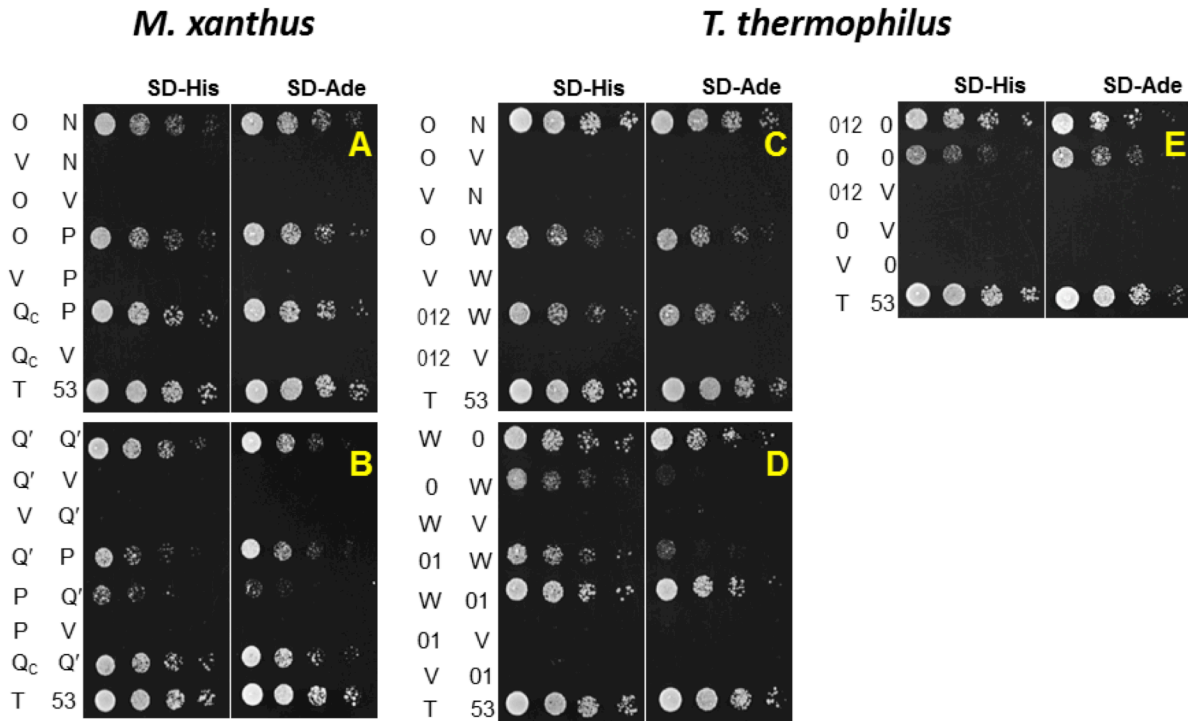


Figure 3-4: Pairwise interactions among Pil proteins in Y2H system

Panels **A** and **B**. Interactions among *M. xanthus* Pil proteins. Panels **C**, **D** and **E**. Interactions among *T. thermophilus* Pil proteins. The first and second columns on the left of each panel indicate Pil proteins or fragments fused to GAD and GBD in Y2H plasmids by their last letter, respectively. V indicates an empty Y2H vector. N0, N1, N2 and their combinations are represented by their numerals only. Last row in each panel contained the positive control with T-antigen (T) and p53 (53). The left half of each panel shows growth on SD-His and the right on SD-Ade plates, respectively. The spots in each row in a panel were inoculated by serial dilutions of the same yeast cells with the indicated Y2H plasmids. See text and Materials and Methods for details.

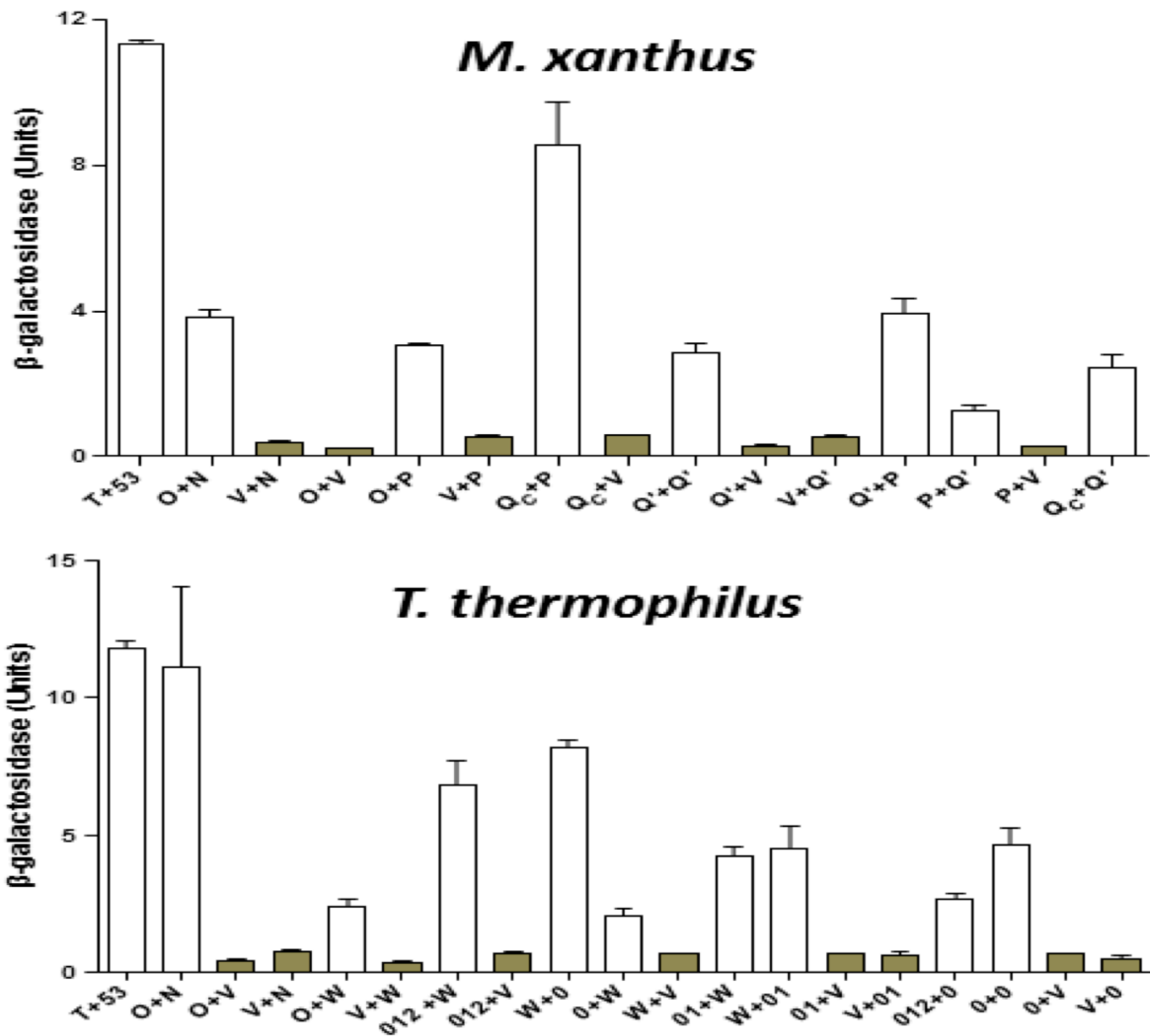


Figure 3-5: Quantification of β-galactosidase in Y2H experiment

The upper and lower panels show the β-galactosidase activity for Pil protein interactions in Y2H experiments from *M. xanthus* and *T. thermophilus*, respectively. The values for β-galactosidase activity were the average of three independent experiments and samples in each experiment were analyzed in triplicate. See Figure 3-4 for protein designations under each panel. The bars for the vector controls are shaded for comparison. See text and Materials and Methods for more details.

Similar Interactions Occur Among *T. thermophilus* T4P Proteins

T4P systems are found in diverse lineages in bacteria (35, 41), but the best experimental systems for T4P studies, which include *M. xanthus*, *P. aeruginosa*, and *Neisseria* sp., are proteobacteria (41). We used the Y2H system to investigate whether the interactions reported here for *M. xanthus* are conserved in the non-proteobacterium *T. thermophilus* (Tt), a thermophile in the deep-rooted Deinococci-Thermus phylum (2). The motivation for this choice included the prevalent use of thermophilic proteins for structural studies including *T. thermophilus* T4P proteins (10, 27, 28). The conservation of protein-protein interactions, if true, would allow the insights from structural studies of *T. thermophilus* T4P proteins to be applied to experimentally more accessible systems, and vice versa.

Most T4P proteins and their domains are well conserved in different organisms and so is the gene order in the *pilM*, *pilN*, *pilO*, *pilP* and *pilQ* gene cluster (41). There are exceptions when it comes to PilQ and PilP, however (42). As shown in Figure 3-3A, except the highly conserved secretin domain and the adjacent Secretin_N region, there is little homology between *T. thermophilus* PilQ (TtPilQ) and *M. xanthus* PilQ (MxPilQ) with the latter over 140 residues longer. Moreover, instead of the IM lipoprotein PilP, the gene between *pilO* and *pilQ* in *T. thermophilus* encodes PilW (TtPilW), which is predicted to have a single TM helix with a periplasmic region without homology to any known T4P or T2SS proteins from other bacterial lineages (42). However, because *pilW* is in the same chromosomal location as *pilP* relative to other *pil* genes, it is possible that PilW may have similar functions as PilP in bridging PilQ to the IM and to other IM T4P proteins in *T. thermophilus*. The interactions among *T. thermophilus* PilN, PilO, PilW and PilQ were therefore investigated by Y2H for comparison with *M. xanthus* T4P proteins.

We first examined the interactions among *T. thermophilus* PilW, PilO and PilN by cloning their C-termini truncated immediately after their predicted TM helices into the Y2H vectors (Table 3-2). Pairs of pGAD- and pGBD-derived fusion plasmids were then transformed into the Y2H reporter strain AH109. As shown in Figure 3-4C, transformants of PilO and PilW constructs as well as those of PilO and PilN grew on SD-His and SD-Ade plates. These observations were further validated by the expression of β -galactosidase (Figure 3-5B). The results indicate that despite sequence divergence, PilW as well as PilO and PilN interact similarly in *T. thermophilus* as PilP, PilO and PilN in *M. xanthus*.

Next, we examined the interactions between TtPilW and TtPilQ. Recall that PilP interacted with the Secretin_N region of MxPilQ in Y2H (PilQc construct in Figures 3-3A and 3-4A). Therefore, we tested the interaction of TtPilW with the Secretin_N region of TtPilQ (Figure 3-3A) using Y2H, but the relevant yeast co-transformants grew on neither SD-His nor SD-Ade (data not shown). Interestingly, while the N-terminus of TtPilQ shares no homology with *M. xanthus* PilQ (Figure 3-3A), it does have limited similarity with the periplasmic N-terminus of the T2SS secretin GspD (GspD_{peri}) (Figure 3-3B). The structure of the N-terminus of TtPilQ can in fact be modeled using the structure of GspD_{peri} as a template (29, 31). The secondary structure prediction of this modeling is shown in Figure 3-3B. Using the structures of GspD_{peri} (31) as a guide, the N-terminus of TtPilQ_{peri} can be similarly divided into N0, N1 and N2 subdomains (Figure 3-3B). While these GspD_{peri} subdomains resemble one another in structure to some degree (31), only N0 was shown to interact with GspC which is an ortholog of PilP in T2SS (30). TtPilW showed interactions with N0 and the combination of N0 and N1 of TtPilQ (TtPilQ₀ and TtPilQ₀₁) in Y2H in both orientations as indicated by growth on SD-His and SD-Ade plates (Figure 3-4D) and by expression of β -galactosidase (Figure 3-5B). TtPilW was

also detected to interact with the three subdomains combined (TtPilQ₀₁₂) in one orientation (Figure 3-4C) but not with N1 or N2 individually (data not shown). The strengths of interactions of TtPilW with TtPilQ₀ and with TtPilQ₀₁ in both orientations were similar as indicated by growth and β -galactosidase activity (Figures 3-4D & 3-5B). These observations suggest that like GspC, TtPilW interacts with the N0 subdomain of its cognate secretin despite the lack of any detectable similarity between TtPilW with GspC or PilP at the level of their primary (42) or predicted higher order structures (data not shown). Such interactions allow the bridging of PilQ to the IM in both *T. thermophilus* and *M. xanthus*.

The interaction of TtPilQ with itself was also investigated. Constructs similar to *M. xanthus* PilQ' and PilQc gave no indication of interaction using Y2H (data not shown). We additionally examined constructs containing N0, N1 and N2 in various combinations. Only two pairs among them were found to confer interactions in Y2H as shown in Figures 3-4E and 3-5B; these are TtPilQ₀ with itself and with TtPilQ₀₁₂. It is interesting to note that in the Y2H system, *M. xanthus* PilQ-PilQ interactions are mediated by Secretin_N whereas *T. thermophilus* PilQ-PilQ interactions by N0 (Figures 3-3, 3-4 and 3-5). Nevertheless, these results are consistent with the conservation of structural interactions in the periplasm and the multimerization of PilQ in both the proteobacterium *M. xanthus* and the non-proteobacterium *T. thermophilus*.

Concluding Remarks

Our analysis of genetic suppression here suggested an integrated T4P structure in *M. xanthus* (Figure 3-6). A systematic Y2H analysis detected the following pairwise interactions among *M. xanthus* Pil proteins: PilQ-PilQ, PilQ-PilP, PilP-PilO and PilO-PilN. Since PilP is an IM lipoprotein and PilN as well as PilO are integral IM proteins, these interactions allow the OM protein PilQ to communicate with the IM T4P proteins. PilM, while cytoplasmic, is likely anchored to the IM by binding to the cytoplasmic tail of PilN (27, 47). These results support a model of an integrated T4P structure in *M. xanthus* because the ability of PilB^{WA} to signal for EPS production requires all of these proteins. This integrated structure would include PilQ in the OM, the TM proteins PilN, PilO and PilC as well as the lipoprotein PilP on the IM. The cytoplasmic proteins PilM and PilB may associate with this structure dynamically as indicated by the genetic suppression patterns by *pilB*^{WA}. The interactions among these proteins in *M. xanthus* apparently occur in the absence of the pilus filament as *pilB*^{WA} suppresses $\Delta pilA$ but none of the other *pil* deletions.

Using the same Y2H system, we extended the above interactions to T4P proteins from the non-proteobacterium *T. thermophilus*. It is especially noteworthy that TtPilW shows interactions with the same T4P proteins as PilP even though they share no detectable structural similarity *in silico*. Interestingly, the more detailed interactions of TtPilW and TtPilQ resembles those of GspC and GspD in T2SS instead of *M. xanthus* PilP and PilQ. That is, both PilW and GspC interact with the N0 subdomains of their partner secretin. Similar observations were made recently between PilP and PilQ in *P. aeruginosa* and *N. meningitidis* (3, 47). The findings with *T. thermophilus* T4P proteins suggest that the interactions among T4P proteins and the formation of an integrated T4P structure are conserved across different bacterial lineages despite extensive

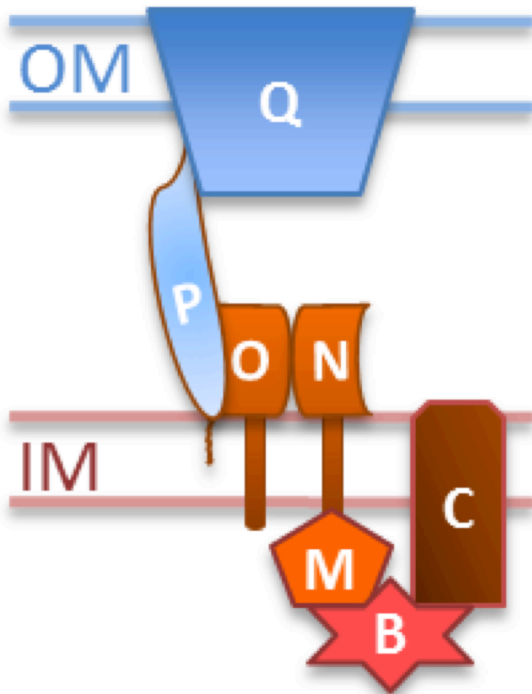


Figure 3-6: An integrated T4P structure

Pil proteins in this model are represented by their single letter designations. OM, outer membrane; IM, inner membrane. This integrated T4P structure, which consists of the indicated Pil protein at the minimum, may exist in the absence of the pilus filament. The interactions of PilB with PilC and PilM are inferred from genetic analysis and they may be either direct or indirect. See main text for details.

sequence and structural divergence. These observations suggest that a discovery in one bacterium may be applicable to related T4P systems in others even when they are evolutionarily distant. While the interactions reported here are mostly consistent with previous reports [(3, 19, 47) and references therein], they are by no means exhaustive as indicated by a recent report on *N. meningitidis* T4P protein-protein interactions using the bacterial two-hybrid (B2H) system in *E. coli* (17). Substantially more interactions were detected in the B2H system, which may require additional verification by alternative approaches because *E. coli* shares many proteins with *N. meningitidis* than does yeast with bacteria.

The results here are supportive of other reports in the literature. A very recent publication based on *in vitro* experiments concluded that *P. aeruginosa* PilM, PilN, PilO, PilP and PilQ form a transenvelope network that interact with PilA (47). The results here clearly indicate that a T4P complex can exist independently of PilA or the pilus filament. It was previously observed that certain T4P proteins localize to both cell poles in *M. xanthus* even though only one of the two poles may actively assemble and disassemble T4P at any given moment (9). The existence of a T4P complex independent of the pilus filament provides support that the T4P proteins localized to the un-piliated pole may be organized into a complex standing ready for T4P assembly for the directional reversal of T4P mediate bacterial surface motility (9, 40).

References Cited

1. **Ayers, M., L. M. Sampaleanu, S. Tammam, J. Koo, H. Harvey, P. L. Howell, and L. L. Burrows.** 2009. PilM/N/O/P proteins form an inner membrane complex that affects the stability of the *Pseudomonas aeruginosa* type IV pilus secretin. *Journal of molecular biology* **394**:128-142.
2. **Battistuzzi, F. U., and S. B. Hedges.** 2009. A major clade of prokaryotes with ancient adaptations to life on land. *Molecular biology and evolution* **26**:335-343.
3. **Berry, J. L., M. M. Phelan, R. F. Collins, T. Adomavicius, T. Tonjum, S. A. Frye, L. Bird, R. Owens, R. C. Ford, L. Y. Lian, and J. P. Derrick.** 2012. Structure and assembly of a trans-periplasmic channel for type IV pili in *Neisseria meningitidis*. *PLoS pathogens* **8**:e1002923.
4. **Black, W. P., X. Jing, F. D. Schubot, and Z. Yang.** 2013. The PilB ATPase may represent a novel class of signal transducers. submitted.
5. **Black, W. P., Q. Xu, C. L. Cadieux, S. J. Suh, W. Shi, and Z. Yang.** 2009. Isolation and characterization of a suppressor mutation that restores *Myxococcus xanthus* exopolysaccharide production. *Microbiology*.
6. **Black, W. P., Q. Xu, and Z. Yang.** 2006. Type IV pili function upstream of the Dif chemotaxis pathway in *Myxococcus xanthus* EPS regulation. *Mol Microbiol* **61**:447-456.
7. **Black, W. P., and Z. Yang.** 2004. *Myxococcus xanthus* chemotaxis homologs DifD and DifG negatively regulate fibril polysaccharide production. *J Bacteriol* **186**:1001-1008.
8. **Buchan, D. W. A., S. M. Ward, A. E. Lobley, T. C. O. Nugent, K. Bryson, and D. T. Jones.** 2010. Protein annotation and modelling servers at University College London. *Nucleic Acids Research* **38**:W563-W568.
9. **Bulyha, I., C. Schmidt, P. Lenz, V. Jakovljevic, A. Hone, B. Maier, M. Hoppert, and L. Sogaard-Andersen.** 2009. Regulation of the type IV pili molecular machine by dynamic localization of two motor proteins. *Mol Microbiol* **74**:691-706.
10. **Burkhardt, J., J. Vonck, and B. Averhoff.** 2011. Structure and function of PilQ, a secretin of the DNA transporter from the thermophilic bacterium *Thermus thermophilus* HB27. *J Biol Chem*.
11. **Campos, J. M., and D. R. Zusman.** 1975. Regulation of development in *Myxococcus xanthus*: effect of 3':5'-cyclic AMP, ADP, and nutrition. *Proc. Natl. Acad. Sci. USA* **72**:518-522.

12. **Carbonnelle, E., S. Helaine, X. Nassif, and V. Pelicic.** 2006. A systematic genetic analysis in *Neisseria meningitidis* defines the Pil proteins required for assembly, functionality, stabilization and export of type IV pili. *Mol Microbiol* **61**:1510-1522.
13. **Clausen, M., V. Jakovljevic, L. Sogaard-Andersen, and B. Maier.** 2009. High-force generation is a conserved property of type IV pilus systems. *J Bacteriol* **191**:4633-4638.
14. **Craig, L., M. E. Pique, and J. A. Tainer.** 2004. Type IV pilus structure and bacterial pathogenicity. *Nature reviews. Microbiology* **2**:363-378.
15. **de Souza, R. F., V. Anantharaman, S. J. de Souza, L. Aravind, and F. J. Gueiros-Filho.** 2008. AMIN domains have a predicted role in localization of diverse periplasmic protein complexes. *Bioinformatics* **24**:2423-2426.
16. **Drake, S. L., S. A. Sandstedt, and M. Koomey.** 1997. PilP, a pilus biogenesis lipoprotein in *Neisseria gonorrhoeae*, affects expression of PilQ as a high-molecular-mass multimer. *Molecular microbiology* **23**:657-668.
17. **Georgiadou, M., M. Castagnini, G. Karimova, D. Ladant, and V. Pelicic.** 2012. Large-scale study of the interactions between proteins involved in type IV pilus biology in *Neisseria meningitidis*: characterization of a subcomplex involved in pilus assembly. *Molecular microbiology* **84**:857-873.
18. **Gietz, R. D., and R. A. Woods.** 2002. Screening for protein-protein interactions in the yeast two-hybrid system. *Methods Mol Biol* **185**:471-486.
19. **Giltner, C. L., Y. Nguyen, and L. L. Burrows.** 2012. Type IV pilin proteins: versatile molecular modules. *Microbiology and molecular biology reviews : MMBR* **76**:740-772.
20. **Goldman, B. S., W. C. Nierman, D. Kaiser, S. C. Slater, A. S. Durkin, J. A. Eisen, C. M. Ronning, W. B. Barbazuk, M. Blanchard, C. Field, C. Halling, G. Hinkle, O. Iartchuk, H. S. Kim, C. Mackenzie, R. Madupu, N. Miller, A. Shvartsbeyn, S. A. Sullivan, M. Vaudin, R. Wiegand, and H. B. Kaplan.** 2006. Evolution of sensory complexity recorded in a myxobacterial genome. *Proc Natl Acad Sci USA* **103**:15200-15205.
21. **Golovanov, A. P., S. Balasingham, C. Tzitzilonis, B. T. Goult, L. Y. Lian, H. Homberset, T. Tonjum, and J. P. Derrick.** 2006. The solution structure of a domain from the *Neisseria meningitidis* lipoprotein PilP reveals a new beta-sandwich fold. *J Mol Biol* **364**:186-195.
22. **Jakovljevic, V., S. Leonardy, M. Hoppert, and L. Sogaard-Andersen.** 2008. PilB and PilT are ATPases acting antagonistically in type IV pilus function in *Myxococcus xanthus*. *Journal of bacteriology* **190**:2411-2421.

23. **James, P., J. Halladay, and E. A. Craig.** 1996. Genomic libraries and a host strain designed for highly efficient two-hybrid selection in yeast. *Genetics* **144**:1425-1436.
24. **Julien, B.** 2003. Characterization of the integrase gene and attachment site for the *Myxococcus xanthus* bacteriophage Mx9. *Journal of bacteriology* **185**:6325-6330.
25. **Julien, B., A. D. Kaiser, and A. Garza.** 2000. Spatial control of cell differentiation in *Myxococcus xanthus*. *Proc Natl Acad Sci USA* **97**:9098-9103.
26. **Kaiser, D.** 1979. Social gliding is correlated with the presence of pili in *Myxococcus xanthus*. *Proc. Natl. Acad. Sci. USA* **76**:5952-5956.
27. **Karuppiyah, V., and J. P. Derrick.** 2011. Structure of the PilM-PilN inner membrane type IV pilus biogenesis complex from *Thermus thermophilus*. *The Journal of biological chemistry* **286**:24434-24442.
28. **Karuppiyah, V., D. Hassan, M. Saleem, and J. P. Derrick.** 2010. Structure and oligomerization of the PilC type IV pilus biogenesis protein from *Thermus thermophilus*. *Proteins* **78**:2049-2057.
29. **Kelley, L. A., and M. J. Sternberg.** 2009. Protein structure prediction on the Web: a case study using the Phyre server. *Nature protocols* **4**:363-371.
30. **Korotkov, K. V., T. L. Johnson, M. G. Jobling, J. Pruneda, E. Pardon, A. Heroux, S. Turley, J. Steyaert, R. K. Holmes, M. Sandkvist, and W. G. Hol.** 2011. Structural and functional studies on the interaction of GspC and GspD in the type II secretion system. *PLoS pathogens* **7**:e1002228.
31. **Korotkov, K. V., E. Pardon, J. Steyaert, and W. G. Hol.** 2009. Crystal structure of the N-terminal domain of the secretin GspD from ETEC determined with the assistance of a nanobody. *Structure* **17**:255-265.
32. **Korotkov, K. V., M. Sandkvist, and W. G. Hol.** 2012. The type II secretion system: biogenesis, molecular architecture and mechanism. *Nat Rev Microbiol* **10**:336-351.
33. **Maier, B., L. Potter, M. So, C. D. Long, H. S. Seifert, and M. P. Sheetz.** 2002. Single pilus motor forces exceed 100 pN. *Proceedings of the National Academy of Sciences of the United States of America* **99**:16012-16017.
34. **Marchler-Bauer, A., S. Lu, J. B. Anderson, F. Chitsaz, M. K. Derbyshire, C. DeWeese-Scott, J. H. Fong, L. Y. Geer, R. C. Geer, N. R. Gonzales, M. Gwadz, D. I. Hurwitz, J. D. Jackson, Z. Ke, C. J. Lanczycki, F. Lu, G. H. Marchler, M. Mullokandov, M. V. Omelchenko, C. L. Robertson, J. S. Song, N. Thanki, R. A. Yamashita, D. Zhang, N. Zhang, C. Zheng, and S. H. Bryant.** 2011. CDD: a Conserved Domain Database for the functional annotation of proteins. *Nucleic acids research* **39**:D225-229.

35. **Mattick, J. S.** 2002. Type IV pili and twitching motility. *Annu Rev Microbiol* **56**:289-314.
36. **Mattick, J. S., C. B. Whitchurch, and R. A. Alm.** 1996. The molecular genetics of type-4 fimbriae in *Pseudomonas aeruginosa*--a review. *Gene* **179**:147-155.
37. **Mauriello, E. M., T. Mignot, Z. Yang, and D. R. Zusman.** 2010. Gliding motility revisited: how do the myxobacteria move without flagella? *Microbiol Mol Biol Rev* **74**:229-249.
38. **McLaughlin, L. S., R. J. Haft, and K. T. Forest.** 2012. Structural insights into the Type II secretion nanomachine. *Curr Opin Struct Biol* **22**:208-216.
39. **Miller, J. H.** 1972. Experiments in molecular genetics. Cold Spring Harbor Laboratory, Cold Spring Harbor, N.Y.
40. **Nudleman, E., D. Wall, and D. Kaiser.** 2006. Polar assembly of the type IV pilus secretin in *Myxococcus xanthus*. *Molecular microbiology* **60**:16-29.
41. **Pellicic, V.** 2008. Type IV pili: e pluribus unum? *Molecular microbiology* **68**:827-837.
42. **Rumszauer, J., C. Schwarzenlander, and B. Averhoff.** 2006. Identification, subcellular localization and functional interactions of PilMNOWQ and PilA4 involved in transformation competency and pilus biogenesis in the thermophilic bacterium *Thermus thermophilus* HB27. *The FEBS journal* **273**:3261-3272.
43. **Sampaleanu, L. M., J. B. Bonanno, M. Ayers, J. Koo, S. Tammam, S. K. Burley, S. C. Almo, L. L. Burrows, and P. L. Howell.** 2009. Periplasmic domains of *Pseudomonas aeruginosa* PilN and PilO form a stable heterodimeric complex. *Journal of molecular biology* **394**:143-159.
44. **Seshadri, R., S. W. Joseph, A. K. Chopra, J. Sha, J. Shaw, J. Graf, D. Haft, M. Wu, Q. Ren, M. J. Rosovitz, R. Madupu, L. Tallon, M. Kim, S. Jin, H. Vuong, O. C. Stine, A. Ali, A. J. Horneman, and J. F. Heidelberg.** 2006. Genome sequence of *Aeromonas hydrophila* ATCC 7966T: jack of all trades. *J Bacteriol* **188**:8272-8282.
45. **Shi, W., and H. Sun.** 2002. Type IV pilus-dependent motility and its possible role in bacterial pathogenesis. *Infect Immun* **70**:1-4.
46. **Tammam, S., L. M. Sampaleanu, J. Koo, K. Manoharan, M. Daubaras, L. L. Burrows, and P. L. Howell.** 2013. PilMNOPQ from the *Pseudomonas aeruginosa* type IV pilus system form a transenvelope protein interaction network that interacts with PilA. *Journal of bacteriology*.
47. **Tammam, S., L. M. Sampaleanu, J. Koo, K. Manoharan, M. Daubaras, L. L. Burrows, and P. L. Howell.** 2013. PilMNOPQ from the *Pseudomonas aeruginosa* Type

- IV Pilus System Form a Transenvelope Protein Interaction Network That Interacts with PilA. *J Bacteriol* **195**:2126-2135.
48. **Tammam, S., L. M. Sampaleanu, J. Koo, P. Sundaram, M. Ayers, P. A. Chong, J. D. Forman-Kay, L. L. Burrows, and P. L. Howell.** 2011. Characterization of the PilN, PilO and PilP type IVa pilus subcomplex. *Molecular microbiology* **82**:1496-1514.
 49. **Ueki, T., S. Inouye, and M. Inouye.** 1996. Positive-negative KG cassettes for construction of multi-gene deletions using a single drug marker. *Gene* **183**:153-157.
 50. **Wall, D., and D. Kaiser.** 1999. Type IV pili and cell motility. *Molecular microbiology* **32**:1-10.
 51. **Wall, D., P. E. Kolenbrander, and D. Kaiser.** 1999. The *Myxococcus xanthus pilQ* (*sglA*) gene encodes a secretin homolog required for type IV pilus biogenesis, social motility, and development. *Journal of bacteriology* **181**:24-33.
 52. **Weimer, R. M., C. Creighton, A. Stassinopoulos, P. Youderian, and P. L. Hartzell.** 1998. A chaperone in the HSP70 family controls production of extracellular fibrils in *Myxococcus xanthus*. *J. Bacteriol.* **180**:5357-5368.
 53. **Wolfgang, M., J. P. van Putten, S. F. Hayes, D. Dorward, and M. Koomey.** 2000. Components and dynamics of fiber formation define a ubiquitous biogenesis pathway for bacterial pili. *The EMBO journal* **19**:6408-6418.
 54. **Wu, S. S., and D. Kaiser.** 1995. Genetic and functional evidence that Type IV pili are required for social gliding motility in *Myxococcus xanthus*. *Molecular microbiology* **18**:547-558.
 55. **Wu, S. S., and D. Kaiser.** 1996. Markerless deletions of pil genes in *Myxococcus xanthus* generated by counterselection with the *Bacillus subtilis sacB* gene. *Journal of bacteriology* **178**:5817-5821.
 56. **Wu, S. S., and D. Kaiser.** 1997. Regulation of expression of the *pilA* gene in *Myxococcus xanthus*. *Journal of bacteriology* **179**:7748-7758.
 57. **Wu, S. S., J. Wu, Y. L. Cheng, and D. Kaiser.** 1998. The *pilH* gene encodes an ABC transporter homologue required for type IV pilus biogenesis and social gliding motility in *Myxococcus xanthus*. *Molecular microbiology* **29**:1249-1261.
 58. **Wu, S. S., J. Wu, and D. Kaiser.** 1997. The *Myxococcus xanthus pilT* locus is required for social gliding motility although pili are still produced. *Molecular microbiology* **23**:109-121.

59. **Yang, Z., R. Lux, W. Hu, C. Hu, and W. Shi.** 2010. PilA localization affects extracellular polysaccharide production and fruiting body formation in *Myxococcus xanthus*. *Molecular microbiology* **76**:1500-1513.
60. **Yang, Z., X. Ma, L. Tong, H. B. Kaplan, L. J. Shimkets, and W. Shi.** 2000. *Myxococcus xanthus dif* genes are required for biogenesis of cell surface fibrils essential for social gliding motility. *Journal of bacteriology* **182**:5793-5798.

Chapter 4
Summary of Other Experiments

CRISPR3 Related Experiments

All strains and plasmids used for CRISPR3 experiments are listed in Table 4-1 and all primers are listed in Table 4-2. The experiments outlined here were additional experiments performed that are related to the CRISPR3 study. They were included here so that future students can use the previous work to continue the project.

CRISPR3* is not able to suppress $\Delta stkA$ and $\Delta epsW$

To test the genetic relationship that the CRISPR3* mutation has with genes involved in the EPS regulation pathway, genomic DNA was isolated from BY802 ($\Delta pilA$ CRISPR3*) and transformed into YZ812 ($\Delta stkA$) and YZ1830 ($\Delta epsW$), as previously described. The resulting mutants YZ1285 ($\Delta stkA$ CRISPR3*) and YZ1286 ($\Delta epsW$ CRISPR3*) were examined on CYE CW plates. YZ1285 was seen to be fluorescing under UV light, EPS⁺ phenotype. An *stkA* mutant over-produces EPS compared to wild-type, the same was seen for YZ1285. YZ1286 was seen to not fluoresce under UV light, same as the parent strain. These results indicate that CRISPR3* has no effect on EPS production in a $\Delta stkA$ and $\Delta epsW$ background. These results indicate that CRISPR3* acts upstream of these genes in the EPS pathway.

Genes upstream of RAMP genes are not required for CRISPR3* function

The initial RAMP deletion construct involved the deletion of 12 genes, MXAN_7286-7283, *cmr1*, *cas10*, *cmr3-6*, and *cas6*, immediately upstream of CRISPR3. The deletion of all 12 genes in $\Delta pilA$ CRISPR3* background was seen to not fluoresce on CYE CW plates, EPS⁻. To verify this effect was from the RAMP genes and not from the four genes, MXAN_7286-7283, upstream of the RAMP genes, a deletion construct was made. Primers were designed to PCR amplify regions upstream and downstream of these genes. Primers Δ Upstream RAMP F1 and Δ Upstream RAMP R1 were used for the upstream region and Δ Upstream RAMP F2 and

Δ Upstream RAMP R2 for the downstream region. These two PCR fragments were joined together by overlapping PCR. The resulting fragment was digested with *HindIII* and *XbaI* and cloned into pMY7 at the same restriction sites, resulting in pRW111. pRW111 was then used to delete these four genes in wild-type and $\Delta pilA$ background, as previously described, resulting in YZ1293 ($\Delta 4$ upstream genes) and YZ1294 ($\Delta pilA \Delta 4$ upstream genes). YZ1293 and YZ1294 were then transformed with genomic DNA from BY802, resulting in YZ1295 ($\Delta 4$ upstream genes CRISPR3*) and YZ1296 ($\Delta pilA \Delta 4$ upstream genes CRISPR3*). Both strains were then examined on CYE CW plates. YZ1295 was seen to fluoresce under UV light, but YZ1296 did not. These results were expected for YZ1295, but not for YZ1296. It is possible that the deletion construct caused polar effects on the downstream RAMP genes.

To alleviate this issue a new deletion construct was made to delete the 3 upstream genes, MXAN_7286-7284, leaving most of the 4th gene, MXAN_7283, behind. To delete these three upstream genes similar methods were used as above. The primers Δ New Upstream F1 and Δ New Upstream R1 were used to amplify the upstream region and Δ New Upstream F2 and Δ New Upstream R2 for the downstream region. These PCR fragments were joined together, as previously described, and digested with *HindIII* and *XbaI* and cloned into pBJ113 at the same restriction sites, resulting in pRW113. pRW113 was then used to delete these three genes in wild-type and $\Delta pilA$ background, as previously described, resulting in YZ2201 ($\Delta 3$ upstream genes) and YZ1299 ($\Delta pilA \Delta 3$ upstream genes). YZ2201 and YZ1299 were transformed with genomic DNA from BY802 resulting in YZ2202 ($\Delta 3$ upstream genes CRISPR3*) and YZ2203 ($\Delta pilA \Delta 3$ upstream genes CRISPR3*). Both strains were examined on CYE CW plates and both were seen to fluoresce under UV light, EPS⁺. Based on these results the genes (MXAN_7286-7283) upstream of the RAMP genes were concluded to not be required for the

CRISPR3* *pilA* suppression, indicating that the RAMP genes were the only genes required for the CRISPR3* suppression phenotype.

CRISPR2 *cas* genes are not required for CRISPR3* function

CRISPR3 and CRISPR2 loci are fairly similar in that both repeat sequences are almost identical, with only two nucleotide changes, and both contain Cas6. In order to determine whether or not CRISPR2 *cas* genes were involved in the *pilA* suppressor phenotype, a deletion construct was made. If CRISPR2 proteins are required for CRISPR3* function then deleting CRISPR2 genes will prevent the suppression phenotype from occurring, resulting in EPS⁻ phenotype. To delete all CRISPR2 *cas* genes, primers Δ CRISPR2 *cas* F1 and Δ CRISPR2 *cas* R1 were used to amplify the upstream region and Δ CRISPR2 *cas* F2 and Δ CRISPR2 *cas* R2 for the downstream region. The two PCR fragments were joined together by overlapping PCR and digested by *Hind*III and *Xba*I and cloned into pMY7 at the same restriction sites, resulting in pRW108. To delete the CRISPR2 *cas* genes in the wild-type and Δ *pilA* background, pRW108 was transformed into both strains, resulting in YZ1283 (Δ CRISPR2 *cas*) and YZ1284 (Δ *pilA* Δ CRISPR2 *cas*). Genomic DNA from BY802 was transformed into YZ1283 and YZ1284, resulting in YZ1287 (Δ CRISPR2 *cas* CRISPR3*) and YZ1288 (Δ *pilA* Δ CRISPR2 *cas* CRISPR3*). YZ1287 and YZ1288 were examined on CYE CW plates and both fluoresced under UV light, EPS⁺. These results indicate that CRISPR2 *cas* genes are not required for CRISPR3* to suppress Δ *pilA*.

To determine which RAMP genes are required for CRISPR3*

Based on previous results, some or all of the RAMP genes *cmr1*, *cas10*, *cmr3*, *cmr4*, *cmr5*, *cmr6*, and *cas6*, are required for CRISPR3* phenotypes (Figure 2-3 & 2-4). To determine which RAMP genes are required more specifically, deletion constructs were designed to delete

each RAMP gene individually. Primers were designed to amplify regions upstream and downstream of each gene. For $\Delta cmr1$ primers, $\Delta cmr1$ F1 and $\Delta cmr1$ R1 were used for the upstream region and $\Delta cmr1$ F2 and $\Delta cmr1$ R2 were used for the downstream region. For $\Delta cas10$ primers, $\Delta cas10$ F1 and $\Delta cas10$ R1 were used for the upstream region and $\Delta cas10$ F2 and $\Delta cas10$ R2 were used for the downstream region. For $\Delta cmr3$ primers, $\Delta cmr3$ F1 and $\Delta cmr3$ R1 were used for the upstream region and $\Delta cmr3$ F2 and $\Delta cmr3$ R2 were used for the downstream region. For $\Delta cmr4$ primers, $\Delta cmr4$ F1 and $\Delta cmr4$ R1 were used for the upstream region and $\Delta cmr4$ F2 and $\Delta cmr4$ R2 were used for the downstream region. For $\Delta cmr5$ primers, $\Delta cmr5$ F1 and $\Delta cmr5$ R1 were used for the upstream region and $\Delta cmr5$ F2 and $\Delta cmr5$ R2 were used for the downstream region. For $\Delta cmr6$ primers, $\Delta cmr6$ F1 and $\Delta cmr6$ R1 were used for the upstream region and $\Delta cmr6$ F2 and $\Delta cmr6$ R2 were used for the downstream region. For $\Delta cas6$ primers, $\Delta cas6$ F1 and $\Delta cas6$ R1 were used for the upstream region and $\Delta cas6$ F2 and $\Delta cas6$ R2 were used for the downstream region. PCR fragments were joined together by overlapping PCR and then digested with *HindIII* and *XbaI* and cloned into pBJ113, resulting in pRW120-pRW126, respectively. All plasmids were transformed into $\Delta pilA$, resulting in YZ2205-YZ2211. The deletions were never screened so there are intermediate strains stored at -80°C . Once these strains are screened to verify the appropriate genes are deleted, genomic DNA from BY802 will be transformed into each deletion background. The resulting mutants will then be screened on CYE CW plates to determine if they are able to fluoresce under UV light. If the mutants are fluorescing, EPS^+ phenotype, then this indicates that the respective genes are not required for CRISPR3* function. If the mutants are not fluorescing, EPS^- phenotype, then this indicates that the respective genes are required for CRISPR3* function. These results will allow us to further specify our proposed model for the regulation of chromosomal genes by CRISPR3*.

To determine which spacer(s) are required for *pilA* suppression

We have hypothesized in our molecular model that one or more of the spacers in CRISPR3 is responsible for the EPS suppression phenotype, as well as, the detrimental effect seen in fruiting body development in a CRISPR3* background. To try to determine which spacer(s) is required for the *pilA* suppression, expression constructs were designed to express various regions of CRISPR3 under the control of a heterologous promoter. In order to do this pXY105 was digested with *XhoI*. *XhoI* cuts upstream of CRISPR3 as well as in CRISPR3 and on the vector resulting in 2 fragments containing CRISPR3, a 2.2 kb and a 3.3 kb fragment. The 2.2 kb fragment contains some of the leader sequence and spacers 1-21, while the 3.3 kb fragment contains spacers 22-52 (Figure 4-1). These two fragments were then cloned into pWB425 at *XhoI* restriction site, resulting in pRW101 (2.2 kb, Orientation I), pRW102 (2.2 kb, Orientation II), pRW103 (3.3 kb, Orientation I), and pRW104 (3.3 kb, Orientation II). Orientation I fragments are in the same direction as the Kan^R gene, while Orientation II fragments are in the opposite direction of the Kan^R gene. Based on results seen from pXY105 and pXY108, pRW101 and pRW103 were transformed into Δ CRISPR3 and Δ *pilA* Δ CRISPR3 backgrounds, resulting in YZ1274 (Δ CRISPR3 att::pRW101), YZ1275 (Δ CRISPR3 att::pRW103), YZ1276 (Δ *pilA* Δ CRISPR3 att::pRW101), and YZ1277 (Δ *pilA* Δ CRISPR3 att::pRW103). These strains were all screened on CYE CW plates. YZ1274 and YZ1275 were both fluorescing under UV light, EPS⁺, while YZ1277 was seen to not fluoresce, EPS⁻. YZ1276 displayed partial weak fluorescence on the CYE CW plates. To try to verify these phenotypes genomic DNA was isolated from YZ1276 and YZ1277 and transformed back into Δ *pilA* Δ CRISPR3 background, resulting in YZ1290 and YZ1291, respectively. When these two strains were examined on CYE CW plates both were seen to not be fluorescing, EPS⁻. These results

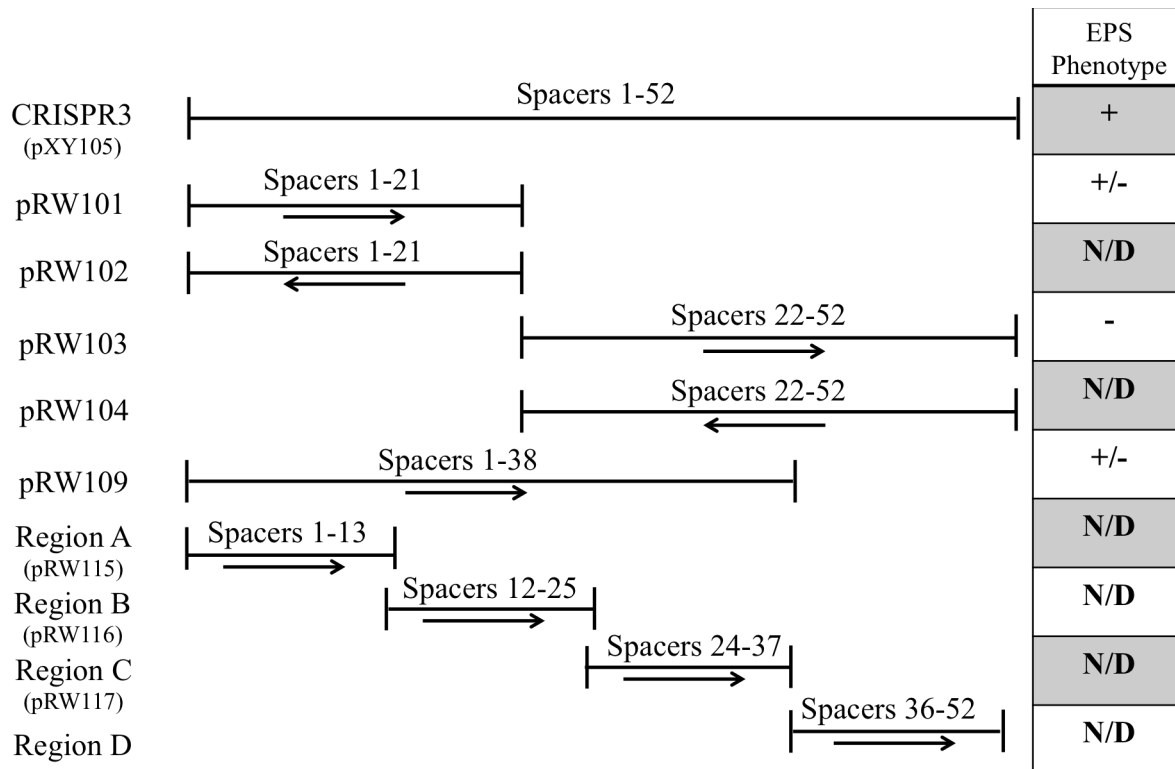


Figure 4-1: CRISPR3 regions for various expression constructs

This figure depicts the respective sizes of CRISPR3 for various expression constructs. The arrow underneath each fragment represents the orientation of the CRISPR3 fragment. The EPS phenotype for each construct is indicated on the right. + represents EPS+ phenotype, - represents EPS- phenotype, +/- represents a partial EPS+ phenotype, and N/D represents Not Determined.

raised some questions regarding the design of our plasmids. One question was is the entire leader sequence provided in our constructs? In order to alleviate this concern another expression construct was designed to include more of the region immediately upstream of CRISPR3 to ensure the entire leader sequence was present. Since partial EPS⁺ phenotype was seen from the expression construct that contained spacers 1-21 only, this construct was designed to include the spacers 1-38. To obtain this construct pXY105 was digested with *Hind*III and *Sau*3AI. *Hind*III cuts on the vector while *Sau*3AI cuts in the 39th spacer of CRISPR3. This fragment was then cloned into pWB425 at *Hind*III and *Bam*HI, resulting in pRW109. pRW109 was transformed into Δ *pilA* Δ CRISPR3, resulting in YZ1289 (Δ *pilA* Δ CRISPR3 att:pRW109). YZ1289 was examined on CYE CW plates and was seen to be partially fluorescing, EPS⁺, similar to YZ1276. To further determine if this phenotype was accurate, genomic DNA from YZ1289 was isolated and transformed into Δ *pilA* Δ CRISPR3, resulting in YZ1292. YZ1292 was examined on CYE CW plates and was seen to be partially fluorescing, EPS⁺. Based on these results it is likely that the spacer(s) of interest is one of the 1st 38 spacers of CRISPR3. The weak fluoresce observed here could be due to the plasmid integrating at the Mx8 attachment site on the *M. xanthus* chromosome, which has previously been seen to result in weaker expression.

To further examine the CRISPR3 spacers, new expression constructs were designed to express smaller regions of CRISPR3. Primers were designed to amplify CRISPR3 in four segments; region A includes spacers 1-13, region B includes spacers 12-25, region C includes spacers 24-37, and region D includes spacers 36-52 (Figure 4-1). Primers for region A were CRISPR3 1-13 F and CRISPR3 1-13 R. Primers for region B were CRISPR3 12-25 F and CRISPR3 12-25 R. Primers for region C were CRISPR3 24-37 F and CRISPR3 24-37 R. Primers for region D were CRISPR3 38-52 F and CRISPR3 38-52 R. Each PCR fragment was

digested with *Bam*HI and *Xba*I and cloned into pRW110, pZErO-2 with a P_{kan} promoter cloned in at *Hind*III and *Kpn*I. Region A, B and C were successfully cloned into pRW110, resulting in pRW115-117, respectively. Region D still needs to be cloned into pRW110. All four plasmids also need to be transformed into *M. xanthus*. Once the resulting mutants are obtained they will need to be screened for their ability to reproduce the *pilA* suppression phenotype. If one of the four regions is able to reproduce the *pilA* suppression phenotype this will indicate that the spacer responsible for the *pilA* suppression is located in that region. This method can then be used to analyze smaller and smaller regions until the responsible spacer(s) is identified. Identifying the spacer(s) required for the *pilA* suppression would also help to possibly identify the target of the suppression.

Table 4-1: Strains and plasmids used in CRISPR3 related experiments

Strains	Genotype	Reference
BY802	$\Delta pilA::Tet^R$ CRISPR3* (Kan ^R)	This Study
DK1622	Wild-type (WT)	(3)
DK10407	$\Delta pilA::Tet^R$	(5)
YZ812	$\Delta stkA$	Unpublished (Zhuo Li)
YZ1200	$\Delta pilA::Tet^R \Delta CRISPR3$	This Study
YZ1202	$\Delta CRISPR3$	This Study
YZ1274	$\Delta CRISPR3$ att::pRW101 (Kan ^R)	This Study
YZ1275	$\Delta CRISPR3$ att::pRW103 (Kan ^R)	This Study
YZ1276	$\Delta pilA::Tet^R \Delta CRISPR3$ att::pRW101 (Kan ^R)	This Study
YZ1277	$\Delta pilA::Tet^R \Delta CRISPR3$ att::pRW103 (Kan ^R)	This Study
YZ1283	$\Delta casII$	This Study
YZ1284	$\Delta pilA::Tet^R \Delta casII$	This Study
YZ1285	$\Delta stkA$ CRISPR3* (Kan ^R)	This Study
YZ1286	$\Delta epsW$ CRISPR3*	This Study
YZ1287	$\Delta casII$ CRISPR3* (Kan ^R)	This Study
YZ1288	$\Delta pilA::Tet^R \Delta casII$ CRISPR3* (Kan ^R)	This Study
YZ1289	$\Delta pilA::Tet^R \Delta CRISPR3$ att::pRW109 (Kan ^R)	This Study
YZ1290	$\Delta pilA::Tet^R \Delta CRISPR3$ + gYZ1276 ($\Delta pilA::Tet^R \Delta CRISPR3$ att::pRW101)	This Study
YZ1291	$\Delta pilA::Tet^R \Delta CRISPR3$ + gYZ1277 ($\Delta pilA::Tet^R \Delta CRISPR3$ att::pRW103)	This Study
YZ1292	$\Delta pilA::Tet^R \Delta CRISPR3$ + gYZ1289 ($\Delta pilA::Tet^R \Delta CRISPR3$ att::pRW109)	This Study
YZ1293	$\Delta 4$ genes Upstream of RAMP	This Study
YZ1294	$\Delta pilA::Tet^R \Delta 4$ genes Upstream of RAMP	This Study
YZ1295	$\Delta 4$ genes Upstream of RAMP CRISPR3* (Kan ^R)	This Study
YZ1296	$\Delta pilA::Tet^R \Delta 4$ genes Upstream of RAMP CRISPR3* (Kan ^R)	This Study
YZ1299	$\Delta pilA::Tet^R \Delta 3$ New Upstream RAMP genes	This Study
YZ1830	$\Delta epsW$	Unpublished (Wesley Black)
YZ2201	$\Delta 3$ New Upstream RAMP genes	This Study
YZ2202	$\Delta 3$ New Upstream RAMP genes CRISPR3*	This Study
YZ2203	$\Delta pilA::Tet^R \Delta 3$ New Upstream RAMP genes CRISPR3*	This Study
YZ2205	$\Delta pilA::Tet^R \Delta cmr1$ Intermediate	This Study
YZ2206	$\Delta pilA::Tet^R \Delta cas10$ Intermediate	This Study
YZ2207	$\Delta pilA::Tet^R \Delta cmr3$ Intermediate	This Study
YZ2208	$\Delta pilA::Tet^R \Delta cmr4$	This Study
YZ2209	$\Delta pilA::Tet^R \Delta cmr5$ Intermediate	This Study
YZ2210	$\Delta pilA::Tet^R \Delta cmr6$ Intermediate	This Study
YZ2211	$\Delta pilA::Tet^R \Delta cas6$ Intermediate	This Study
Plasmid	Description	Reference
pBJ113	Allelic Exchange vector, Kan ^R , <i>galK</i>	(2)
pMY7	Allelic Exchange vector, Pretty much same as pBJ113	Unpublished (Manli Yang)
pRW101	2.0 kb CRISPR3 <i>XhoI</i> fragment from pXY105 cloned into pWB425 at <i>XhoI</i> site, orientation I, Kan ^R	This Study
pRW102	2.0 kb CRISPR3 <i>XhoI</i> fragment from pXY105 cloned into pWB425 at <i>XhoI</i> site, orientation II, Kan ^R	This Study
pRW103	3.3 kb CRISPR3 <i>XhoI</i> fragment from pXY105 cloned into pWB425 at <i>XhoI</i> site, orientation I, Kan ^R	This Study
pRW104	3.3 kb CRISPR3 <i>XhoI</i> fragment from pXY105 cloned into pWB425	This Study

	at <i>XhoI</i> site, orientation II, Kan ^R	
pRW108	$\Delta casII$ PCR fragment cloned into pMY7 at <i>HindIII/XbaI</i> sites, Kan ^R , <i>galK</i>	This Study
pRW109	CRISPR3 <i>HindIII-Sau3AI</i> fragment from pXY105 cloned into pWB425 at <i>HindIII-BamHI</i> sites, Kan ^R	This Study
pRW110	Pkan promoter PCR fragment cloned into pZero at <i>HindIII/KpnI</i> sites, Kan ^R	This Study
pRW111	$\Delta 4$ genes Upstream of RAMP PCR fragments cloned into pMY7 at <i>HindIII/XbaI</i> sites, Kan ^R , <i>galK</i>	This Study
pRW113	ΔNew Upstream (3 genes upstream of RAMP) PCR fragment cloned into pBJ113 at <i>HindIII/XbaI</i> sites, Kan ^R , <i>galK</i>	This Study
pRW115	CRISPR3 region A (Spacers 1-13) PCR fragment cloned into pRW110 at <i>BamHI/XbaI</i> sites, Kan ^R	This Study
pRW116	CRISPR3 region B (Spacers 12-25) PCR fragment cloned into pRW110 at <i>BamHI/XbaI</i> sites, Kan ^R	This Study
pRW117	CRISPR3 region C (Spacers 24-37) PCR fragment cloned into pRW110 at <i>BamHI/XbaI</i> sites, Kan ^R	This Study
pRW120	$\Delta cmr1$ PCR fragment cloned into pBJ113 at <i>HindIII/XbaI</i> sites, Kan ^R , <i>galK</i>	This Study
pRW121	$\Delta cas10$ PCR fragment cloned into pBJ113 at <i>HindIII/XbaI</i> sites, Kan ^R , <i>galK</i>	This Study
pRW122	$\Delta cmr3$ PCR fragment cloned into pBJ113 at <i>HindIII/XbaI</i> sites, Kan ^R , <i>galK</i>	This Study
pRW123	$\Delta cmr4$ PCR fragment cloned into pBJ113 at <i>HindIII/XbaI</i> sites, Kan ^R , <i>galK</i>	This Study
pRW124	$\Delta cmr5$ PCR fragment cloned into pBJ113 at <i>HindIII/XbaI</i> sites, Kan ^R , <i>galK</i>	This Study
pRW125	$\Delta cmr6$ PCR fragment cloned into pBJ113 at <i>HindIII/XbaI</i> sites, Kan ^R , <i>galK</i>	This Study
pRW126	$\Delta cas6$ PCR fragment cloned into pBJ113 at <i>HindIII/XbaI</i> sites, Kan ^R , <i>galK</i>	This Study
pWB425	Expression vector with phage attachment site, MCS, Kan ^R with a strong promoter	(1)
pXY105	pWB425 + CRISPR3 (<i>HindIII-XbaI</i>)	This Study

Table 4-2: Primers used to examine CRISPR

Primers	Primer Sequence (5' to 3')	Restriction Sites
ΔUpstream RAMP F1	GATTACA <u>AAGCTT</u> CTCGCTCCTGGTGCGGAT	<i>HindIII</i>
ΔUpstream RAMP R1	CGGAGCGAGTGGTTGCCGAA	None
ΔUpstream RAMP F2	TTCGGCAACCACTCGCTCCGAACCATTCCCGTTTCAAGAGATGA	None
ΔUpstream RAMP R2	CGTCCT <u>CTAGAC</u> CGCCCTTCAGCAGGAGAAAGGATT	<i>XbaI</i>
ΔNew Upstream F1	GATTACA <u>AAGCTT</u> TGCTCTTCAGCTTGAGC	<i>HindIII</i>
ΔNew Upstream R1	GAAATAGGTGGGAAGTGGAAG	None
ΔNew Upstream F2	CTTCCAATTCCCACCTATTTTCGAATCCATATGTAATTTCCA	None
ΔNew Upstream R2	CGTCCT <u>CTAGAC</u> CGCCCTTCAGCAGGAGAAAGGATT	<i>XbaI</i>
ΔCRISPR2 <i>cas</i> F1	GACCA <u>AAGCTT</u> GTGGCGCTCGGACGCGAA	<i>HindIII</i>
ΔCRISPR2 <i>cas</i> R1	CGCCTCGCAGCATCACAGCA	None
ΔCRISPR2 <i>cas</i> F2	TGCTGTGATGCTGCGAGGCGGACGGACGACAATCAAGCAC	None
ΔCRISPR2 <i>cas</i> R2	GCTCTAGACACACAGCCCTTGTCCTG	<i>XbaI</i>
Δ <i>cmr1</i> F1	TTACA <u>AAGCTT</u> GGAACGTGCCGATGACG	<i>HindIII</i>
Δ <i>cmr1</i> R1	TGAAGGTGGGTACAGGCAGAA	None
Δ <i>cmr1</i> F2	TTCTGCCTGACCCACCTTCATTCTTCTGGTGGCTGGAGGA	None
Δ <i>cmr1</i> R2	CCTCT <u>CTAGAC</u> GGGCACGGGCACGAACTG	<i>XbaI</i>
Δ <i>cas10</i> F1	TTACA <u>AAGCTT</u> GATCGCGCTCAAGTGGCT	<i>HindIII</i>
Δ <i>cas10</i> R1	CACCGGCCCTCTTTGAGAA	None
Δ <i>cas10</i> F2	TTCTCAAAGAGGGGCGGTGGCCAGCGGAAAGCTCATTCC	None
Δ <i>cas10</i> R2	CCTCTAGAGTCCCAGCGCCCACTCCTC	<i>XbaI</i>
Δ <i>cmr3</i> F1	TTACA <u>AAGCTT</u> CGTCACGCCATGGACG	<i>HindIII</i>
Δ <i>cmr3</i> R1	GTACCAACCTCGCCCGTCCT	None
Δ <i>cmr3</i> F2	AGGACGGGCGAGGTTGGTACCAACCGCCCGTCACGGACA	None
Δ <i>cmr3</i> R2	CCTCT <u>CTAGAC</u> CCTGTGTGGCTGTCTCCA	<i>XbaI</i>
Δ <i>cmr4</i> F1	TTACA <u>AAGCTT</u> CCTCCGAGACACCGGATGC	<i>HindIII</i>
Δ <i>cmr4</i> R1	GGACAGCGCGTGAAGAAGAT	None
Δ <i>cmr4</i> F2	TCTTCTCACGCGCTGTCCCTGGCCTGGATGGCTCCGGA	None
Δ <i>cmr4</i> R2	CCTCT <u>CTAGAC</u> CGTGTGGTGCAGCGTCAGC	<i>XbaI</i>
Δ <i>cmr5</i> F1	TTACA <u>AAGCTT</u> CGTGGGCACCTTCGCGC	<i>HindIII</i>
Δ <i>cmr5</i> R1	AACCCGCGCATAGACATCCA	None
Δ <i>cmr5</i> F2	TGGATGTCTATGCGCGGTTTCAGGCCACCTTCCCCCTGGA	None
Δ <i>cmr5</i> R2	CCTCT <u>CTAGAC</u> CGCCTCTGCCTGTGCAT	<i>XbaI</i>
Δ <i>cmr6</i> F1	TTACA <u>AAGCTT</u> CCTCTGGGAGACAGCCA	<i>HindIII</i>
Δ <i>cmr6</i> R1	GGCATACCGCTCGTACACCA	None
Δ <i>cmr6</i> F2	TGGTGTACGAGCGGTATGCCGAGTTGCTCGCGAGGATGGG	None
Δ <i>cmr6</i> R2	CCTCT <u>CTAGAA</u> TGTCACGCACCGCACAG	<i>XbaI</i>
Δ <i>cas6</i> F1	TTACA <u>AAGCTT</u> TTCATGATGCGCAGTGGG	<i>HindIII</i>
Δ <i>cas6</i> R1	GAGCGCATACCCATGGTCCA	None
Δ <i>cas6</i> F2	TGGACCATGGGTATGCGCTCGTCCGCAGCTCGGGGAACT	None

$\Delta cas6$ R2	CCTCTCTAGATGCACGCGCAGGTTGTCCG	<i>Xba</i> I
CRISPR3 1-13 F	GATCGGATCCTGGGAGATTCAGATGGGCT	<i>Bam</i> HI
CRISPR3 1-13 R	GATCTAGAGGGTCAGCAAAGCGTTGT	<i>Xba</i> I
CRISPR3 12-25 F	GATGGATCCATTTGCATTTGCGTCCTCCG	<i>Bam</i> HI
CRISPR3 12-25 R	GATCTAGATGGACGGGAGAAGACGTTCA	<i>Xba</i> I
CRISPR3 24-37 F	GATGGATCCAACCCGGCCCGCGCCA	<i>Bam</i> HI
CRISPR3 24-37 R	GATCTAGAGTCAATTTCTGGCGCATCG	<i>Xba</i> I
CRISPR3 38-52 F	GATGGATCCGGCCGGATTGAGCGGAT	<i>Bam</i> HI
CRISPR3 38-52 R	GATCTAGATGGCCTCGCAGCTTCCAG	<i>Xba</i> I

***M. xanthus* Pil Related Experiments**

All strains and plasmids used for *M. xanthus* experiments are listed in Table 4-3 and all primers are listed in Table 4-4. *M. xanthus* experiments outlined here are experiments that were performed to try to facilitate the start of new potential projects in the lab.

Construction of HA- and c-myc- *pilC* complementation constructs

At this point, the function of PilC is not known. It has been hypothesized that PilCs two cytoplasmic domains may have two different functions. To test this hypothesis PilC will be divided into its two domains and determined if the respective domain is able to complement EPS production or T4P biogenesis in a $\Delta pilC$ background. To verify that the PilC domain is present in the cell the domains will be tagged with Human influenza hemagglutinin (HA) epitope tag or c-Myc epitope tag. Prior to performing this experiment it is necessary to determine whether full length PilC is functional when HA and c-Myc epitope tags are fused to the N- and C- termini of PilC, respectively. To test this complementation constructs were designed. Three constructs were prepared; one with HA fused to the N-terminus of PilC, one with c-Myc fused to the C-terminus of PilC and another with HA fused to the N-terminus and c-Myc fused to the C-terminus of PilC. To make these complementation constructs primers were designed to amplify *pilC* and the epitope tags. For HA-PilC the primers were HA-PilC F1, HA-PilC F2 and *pilC* R. For PilC-myc the primers were *pilC* F, PilC-myc R1, and PilC-myc R2. After two rounds of PCR each PCR fragment was digested and cloned into pWB425. HA-PilC was digested with *HindIII* and *EcoRI*, PilC-myc was digested with *KpnI* and *XbaI*, and HA-PilC-myc was digested with *HindIII* and *XbaI*. The resulting plasmids were pRW148 (pWB425 + HA-PilC), pRW149 (pWB425 + PilC-myc) and pRW150 (pWB425 + HA-PilC-myc). pRW148, pRW149, and pRW150 were all transformed into $\Delta pilC$ resulting in YZ2221, YZ2235, and YZ2236,

respectively. YZ2221, YZ2235, and YZ2236 were examined on 0.4% soft agar plates for their ability to complement the $\Delta pilC$ S motility defect. YZ2221 was able to partially complement $\Delta pilC$, while YZ2235 and YZ2236 were not. The soft agar plates, for all strains, were allowed to incubate for extended period of time to try to isolate any flares. After 10 days of incubation, flares for all strains were observed. Four flares (YZ2241-YZ2244) were isolated from YZ2221 ($\Delta pilC$ + HA-PilC). Two flares (YZ2245-YZ2246) were isolated from YZ2235 ($\Delta pilC$ + PilC-myc). One flare (YZ2247) was isolated from YZ2236 ($\Delta pilC$ + HA-PilC-myc). Genomic DNA was isolated from YZ2242, YZ2243, YZ2246, and YZ2247 and transformed into the $\Delta pilC$ background resulting in YZ2248-YZ2251, respectively. The resulting mutants were examined on 0.4% agar plates and found to complement the $\Delta pilC$ S motility defect. The results indicate these mutations occurred in the tagged PilCs. At this point the exact site of the mutations are unknown. Further work will be needed to determine where the mutation occurs, whether the mutation is in PilC or in the corresponding epitope tag.

Construction of *M. xanthus-Candidatus* Hybrid PilB

M. xanthus PilB has proven to be difficult to purify in previous experiments. To alleviate this problem we wanted to construct a hybrid PilB that was easily purifiable and functional in *M. xanthus*. *Candidatus Chloracidobacterium thermophilum B* PilB is a great candidate because *Candidatus*' PilB is highly similar to *M. xanthus* PilB. Also *Candidatus* is a thermophilic bacterium. Proteins from thermophilic organisms tend to be easier to purify due to their ability to tolerate high heat. Two *M. xanthus-Candidatus Chloracidobacterium thermophilum B* Hybrid PilBs were constructed in order to find an easily purifiable PilB that was also functional in *M. xanthus*. For both of these hybrids *M. xanthus* N-terminus of PilB was used while the C-terminus of *Candidatus* PilB was used. Hybrid 1 contains amino acids 1-213 of *M. xanthus* PilB

and amino acids 254-615 of *Candidatus* PilB. Hybrid 2 contains amino acids 1-329 of *M. xanthus* PilB and amino acids 373-615 of *Candidatus* PilB. In order to obtain these hybrids primers were designed to amplify *M. xanthus pilB* and *Candidatus pilB* separately and then join the two fragments together by overlapping PCR. Primers used to amplify *M. xanthus pilB* were *M. xanthus* PilB F primer and MxPilB Hyb1 R for Hybrid 1 and MxPilB Hyb2 R for Hybrid 2. Primers used to amplify *Candidatus pilB* were *Candidatus* PilB R primer and CdPilB Hyb1 F for Hybrid 1 and CdHyb2 F for Hybrid 2. PCR fragments were digested with *KpnI* and *EcoRI* and cloned into pWB425 at the same restriction sites, resulting in pRW146 (Hybrid1) and pRW147 (Hybrid2). pRW146 and pRW147 were both transformed into $\Delta pilB$, resulting in YZ2223 and YZ2224, respectively. Both strains were examined on soft agar plates for their ability to complement the S motility defect in $\Delta pilB$. Initially neither hybrid was motile, but after 10 days of incubation flares were observed. Two flares were isolated for Hybrid 1 (YZ2227 and YZ2228) and five flares were isolated for Hybrid 2 (YZ2229-YZ2233). The flares were further examined and found to have mutations in the hybrid PilBs. YZ2227 and YZ2228 were found to have the same mutations, deletion of amino acid 296I and 297K and an amino acid change C436K. Of the five flares isolated for Hybrid 2, YZ2229 and YZ2231 were the only ones found to have mutations. YZ2229 had three amino acid changes A173T, N372T and C436R. YZ2231 had three mutations as well N372T, C436R and the addition of 915C.

Construction of *M. xanthus-T. thermophilus* Hybrid PilB

Two *M. xanthus-Thermus thermophilus* Hybrid PilBs were constructed in order to find an easily purifiable PilB that was also functional in *M. xanthus*. For both of these hybrids *M. xanthus* N-terminus of PilB was used while the C-terminus of *T. thermophilus* PilB was used. Hybrid 1 contains amino acids 1-213 of *M. xanthus* PilB and amino acids 217-565 of *T.*

thermophilus PilB. Hybrid 2 contains amino acids 1-329 of *M. xanthus* PilB and amino acids 331-565 of *T. thermophilus* PilB. In order to obtain these hybrids primers were designed to amplify *M. xanthus pilB* and *T. thermophilus pilB* separately and then join the two fragments together by overlapping PCR. Primers used to amplify *M. xanthus pilB* were *M. xanthus* PilB F primer and MxPilB Hyb1 R primer for Hybrid 1 and MxPilB Hyb2 R primer for Hybrid 2. Primers used to amplify *T. thermophilus pilB* were *T. thermophilus* PilB R primer and Tth PilB1 F primer for Hybrid 1 and Tth PilB2 F primer for Hybrid 2. For Hybrid 2 a mutant version was also prepared using genomic DNA from YZ2229 as template for the *M. xanthus pilB*, which was determined to have an A173T mutation in the *M. xanthus* portion of PilB. PCR fragments were digested with *KpnI* and *XbaI* and cloned into pWB425 at the same restriction sites, resulting in pAY101 (Hybrid1), pAY102 (wild-type Hybrid2) and pAY103 (mutant Hybrid2). pAY101, pAY102, and pAY103 were transformed into $\Delta pilB$, resulting in YZ2252, YZ2253, and YZ2254, respectively. All strains were examined on soft agar plates for their ability to complement the S motility defect in $\Delta pilB$. None of the hybrids were seen to be motile based on the initial examination on soft agar plates. These hybrids will need to further examined to try to isolate flares.

Construction of an autonomously replicating vector for *M. xanthus*

A novel vector containing a strong constitutive promoter that is capable of autonomously replicating in *M. xanthus* was constructed, so that genes can be over-expressed to examine their effects in the wild-type background. In order for a vector to autonomously replicate in *M. xanthus* an origin of replication is required that is compatible with *M. xanthus*. Only one autonomously replicating plasmid has been identified in myxobacteria, pMF1, from *Myxococcus fulvus* (6). The origin of replication, pMF1 ori, has been tested in *M. xanthus* and has proven to

be functional, but the plasmids were not stably maintained by the cells (6). In order to increase the stability, the partitioning (*par*) system found on pMF1 was investigated and shown to increase the stability of the plasmid in *M. xanthus* (4). Using this information we have constructed a vector containing the pMF1 ori and a large region of the *par* loci, *parCAB*. The construction of this vector will be outlined below. pZErO-2 was digested using restriction enzymes *Afl*III and *Hind*III. These restriction enzymes cut out the Lac promoter upstream of the Multiple Cloning Site (MCS). In order to re-ligate the vector, primers, *Afl*III-M13R (CATGTAGCGGATAACAATTCACACAGGATCGATA) and M13R-*Hind*III (AGCTTATCGATCCTGTGTGAAATTGTTATCCGCTA), were designed. The two primers were annealed together and then ligated into pZErO-2 to restore the *Afl*III and *Hind*III restriction sites, resulting in pNC101. Next pWB800 was digested with restriction enzymes *Xba*I and *Bsp*HI to cut out pMF1 ori. The appropriate fragment containing pMF1 ori was then cloned into pNC101 at the same restriction sites, resulting in pNC106. Lastly, pXS11 was digested with *Bsp*HI to cut out *parCAB*. The corresponding fragment for *parCAB* was ligated into pNC106 at *Bsp*HI, resulting in pNC107 (Orientation I) and pNC108 (Orientation II). Orientation I has the *parCAB* genes in the same direction as the Kan^R gene, while Orientation II has the *parCAB* genes in the opposite orientation as the Kan^R gene. pNC107 is depicted in Figure 4-2.

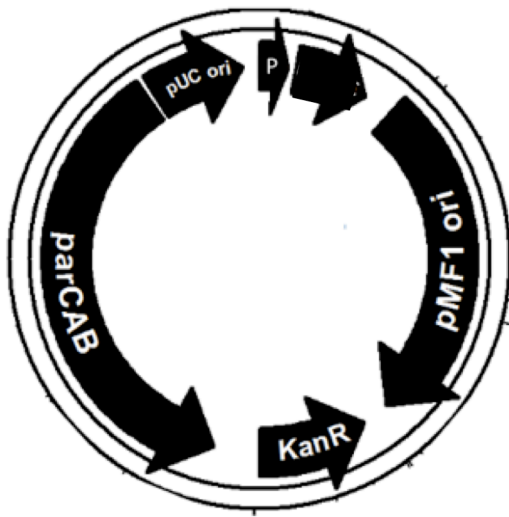


Figure 4-2: Plasmid map of over expression vector pNC107

The pNC107 vector contains pMF1 origin of replication, pMF1 ori, partitioning genes, *parCAB*, and a Kanamycin resistance gene, Kan^R. A strong constitutive promoter, P, will eventually be cloned into the vector. Any gene can be cloned into the vector downstream of the promoter to lead to expression of that gene.

Table 4-3: Strains and plasmids used in *M. xanthus* Pil related experiments

Strains	Genotype	Reference
YZ2221	$\Delta pilC$ + HA-PilC	This Study
YZ2223	$\Delta pilB$ + <i>M. xanthus</i> - <i>Cab. Thermophilum</i> PilB Hybrid 1	This Study
YZ2224	$\Delta pilB$ + <i>M. xanthus</i> - <i>Cab. Thermophilum</i> PilB Hybrid 2	This Study
YZ2227	$\Delta pilB$ + <i>M. xanthus</i> - <i>Candidatus</i> PilB Hybrid 1 Flare #1	This Study
YZ2228	Δpil + <i>M. xanthus</i> - <i>Candidatus</i> PilB Hybrid 1 Flare #2	This Study
YZ2229	$\Delta pilB$ + <i>M. xanthus</i> - <i>Candidatus</i> PilB Hybrid 2 Flare #1	This Study
YZ2230	$\Delta pilB$ + <i>M. xanthus</i> - <i>Candidatus</i> PilB Hybrid 2 Flare #2	This Study
YZ2231	$\Delta pilB$ + <i>M. xanthus</i> - <i>Candidatus</i> PilB Hybrid 2 Flare #3	This Study
YZ2232	$\Delta pilB$ + <i>M. xanthus</i> - <i>Candidatus</i> PilB Hybrid 2 Flare #4	This Study
YZ2233	$\Delta pilB$ + <i>M. xanthus</i> - <i>Candidatus</i> PilB Hybrid 2 #2 Flare #1	This Study
YZ2235	$\Delta pilC$ + PilC-Myc	This Study
YZ2236	$\Delta pilC$ + HA-PilC-Myc	This Study
YZ2241	$\Delta pilC$ + HA-PilC Flare #1	This Study
YZ2242	$\Delta pilC$ + HA-PilC Flare #9	This Study
YZ2243	$\Delta pilC$ + HA-PilC Flare #10	This Study
YZ2244	$\Delta pilC$ + HA-PilC Flare #2	This Study
YZ2245	$\Delta pilC$ + PilC-Myc Flare #2	This Study
YZ2246	$\Delta pilC$ + PilC-Myc Flare #6	This Study
YZ2247	$\Delta pilC$ + HA-PilC-Myc Flare #2	This Study
YZ2248	$\Delta pilC$ + gYZ2241	This Study
YZ2249	$\Delta pilC$ + gYZ2243	This Study
YZ2250	$\Delta pilC$ + gYZ2246	This Study
YZ2251	$\Delta pilC$ + gYZ2247	This Study
YZ2252	$\Delta pilB$ + <i>Myxo-Tth pilB</i> Hybrid 1	This Study
YZ2253	$\Delta pilB$ + <i>Myxo-Tth pilB</i> Hybrid 2	This Study
YZ2254	$\Delta pilB$ + <i>Myxo-Tth pilB</i> mutant Hybrid 2	This Study
Plasmids	Description	References
pAY101	<i>Myxo-Tth pilB</i> Hybrid 1 PCR fragment cloned at <i>KpnI/EcoRV</i> sites of pWB425, Kan ^R	This Study
pAY102	<i>Myxo-Tth pilB</i> Hybrid 2 PCR fragment cloned at <i>KpnI/EcoRV</i> sites of pWB425, Kan ^R	This Study
pAY103	<i>Myxo-Tth pilB</i> mutant Hybrid 2 PCR fragment cloned at <i>KpnI/EcoRV</i> sites of pWB425, Kan ^R	This Study
pNC101	pZErO-2 with <i>lac</i> promoter removed, Kan ^R	This Study
pNC106	4.4-kb pMF1 <i>ori</i> (bp 124 to 4484) <i>XbaI-BspHI</i> fragment of pWB800 cloned into pNC101, Kan ^R	This Study
pNC107	3.2 kb <i>parCAB BspHI</i> fragment from pXS11 cloned into pNC106, orientation I, Kan ^R	This Study
pNC108	3.2 kb <i>parCAB BspHI</i> fragment from pXS11 cloned into pNC106, orientation II, Kan ^R	This Study
pRW146	<i>M. xanthus</i> - <i>Cab. Thermophilum</i> PilB Hybrid 1 PCR fragment cloned into pWB425 at <i>KpnI/EcoRI</i> sites, Kan ^R	This Study
pRW147	<i>M. xanthus</i> - <i>Cab. Thermophilum</i> PilB Hybrid 2 PCR fragment cloned into pWB425 at <i>KpnI/EcoRI</i> sites, Kan ^R	This Study
pRW148	HA-PilC PCR fragment cloned into pWB425 at <i>HindIII/EcoRI</i> sites, Kan ^R	This Study
pRW149	PilC-Myc PCR fragment cloned into pWB425 at <i>KpnI/XbaI</i> sites, Kan ^R	This Study
pRW150	HA-PilC-Myc PCR fragment cloned into pWB425 at <i>HindIII/XbaI</i> sites, Kan ^R	This Study
pWB425	Expression vector with phage attachment site, MCS, Kan ^R with a strong promoter	(1)

pWB800	pMF1 ori fragment cloned into pZErO-2 at <i>ApoI</i> and <i>BglIII</i> (T4 pol treated) PCR fragment cleaved with <i>ApoI</i> and <i>SmaI</i> .	Unpublished (Wesley Black)
pXS11	Shuttle vector with a 2.5-kb fragment from pMF1 (17242-50)	(4)
pZErO-2	Cloning vector (Kan ^R)	Invitrogen

Table 4-4: Primers used for *M. xanthus* Pil experiments

Primer	Primer Sequence	Restriction site
HA-PilC F1	CCGTACGACGTGCCCCGACTACGCG <u>GGTACCG</u> CAGCCCCAGCAGTGAAG TC	<i>Bam</i> HI
HA-PilC F2	CAG <u>AAGCTTC</u> GGAGGTCCAGCTCATGTACCGTACGACGTGCCCCGACTA	<i>Hind</i> III
PilC-myc R1	GGAGATCAGCTTCTGCTC <u>GAA</u> TTCCTGGATGGCGCCGGCAAGCG	<i>Eco</i> RI
PilC-myc R2	GTCT <u>CTAGA</u> TCACAGGTCCTCCTCGGAGATCAGTTCTGCTCGA	<i>Xba</i> I
MxPilB F	AG <u>GGTACCTT</u> CAAGGAAGAGGCATCAA	<i>Kpn</i> I
MxPilB Hyb1 R	GATGCGGAAGCGGACGCGGA	None
MxPilB Hyb2 R	CGTCGTCTTGCCCCGAGCCCCG	None
CdPilB R	CAG <u>GAA</u> TTCGGGTGGTCACAGAACCGT	<i>Eco</i> RI
CdPilB Hyb1 F	TCCGCGTCCGCTTCCGCATCGATGGTCTGTTGCGGGAAGT	None
CdHyb2 F	CGGGCTCGGGCAAGACGACGACGCTCTACTCGGGCACTGGC	None
pQE-SPF	GTTCTGAGGTCATTACTG	None
MyxoTth PilB1 F	CCGCGTCCGCTTCCGCATCGACGGCGCCCTGCGGCCGTA	None
MyxoTth PilB2 F	CGGGCTCGGGCAAGACGACGACCACCTTTTCCATCCTCAA	None

References Cited

1. **Black, W. P., Q. Xu, C. L. Cadieux, S.-J. Suh, W. Shi, and Z. Yang.** 2009. Isolation and characterization of a suppressor mutation that restores *Myxococcus xanthus* exopolysaccharide production. *Microbiology* **155**:3599-3610.
2. **Julien, B., A. D. Kaiser, and A. Garza.** 2000. Spatial control of cell differentiation in *Myxococcus xanthus*. *Proceedings of the National Academy of Sciences U S A* **97**:9098-9103.
3. **Kaiser, D.** 1979. Social gliding is correlated with the presence of pili in *Myxococcus xanthus*. *Proceedings of the National Academy of Sciences U S A* **76**:5952-5956.
4. **Sun, X., X. J. Chen, J. Feng, J. Y. Zhao, and Y. Z. Li.** 2011. Characterization of the partitioning system of *Myxococcus* plasmid pMF1. *PLoS ONE* **6**:e28122.
5. **Wall, D., S. S. Wu, and D. Kaiser.** 1998. Contact stimulation of Tgl and type IV pili in *Myxococcus xanthus*. *Journal of Bacteriology* **180**:759-761.
6. **Zhao, J. Y., L. Zhong, M. J. Shen, Z. J. Xia, Q. X. Cheng, X. Sun, G. P. Zhao, Y. Z. Li, and Z. J. Qin.** 2008. Discovery of the autonomously replicating plasmid pMF1 from *Myxococcus fulvus* and development of a gene cloning system in *Myxococcus xanthus*. *Applied and environmental microbiology* **74**:1980-1987.